2-1-2012

Carbon nanotubes/low density polyethylene composite films for strain sensing

Radwa Raafat Abdel Chafy

The American University in Cairo

School of Sciences and Engineering

Carbon Nanotubes/Low Density Polyethylene Composite Films for Strain Sensing

By

Radwa Raafat Abdel Chafy

A thesis submitted in partial fulfillment of the requirements for the degree

Of

Master of Science in Mechanical Engineering

Under the supervision of:

Dr. Amal Esawi

Professor, Mechanical Engineering Department

American University in Cairo

Dr. Mustafa Arafa

Associate Professor, Mechanical Engineering Department

American University in Cairo

Fall 2011

The American University in Cairo

Carbon Nanotubes/Low Density Polyethylene Composite Films for Strain Sensing

A Thesis Submitted by Radwa Raafat Abdel Chafy

To Department of Mechanical Engineering

January/2012

In partial fulfillment of the requirements for the degree of Masters of Science in Engineering

Has been approved by

Dr. Amal M. K. Esawi

Thesis Committee Chair / Adviser _____

Affiliation _____

Dr. Mustafa Arafa

Thesis Committee Chair / Adviser _____

Affiliation _____

Dr. Asaad Mazen

Thesis Committee Reader / examiner _____

Affiliation _____

Dr. Adham Ramadan

Thesis Committee Reader / examiner _____

Affiliation _____

_____ _____ _____ ____

Department Chair/ Program Director Date Dean Date

ACKNOWLEDGMENT

It is a pleasure to thank those who made this thesis possible. I especially want to thank my advisors Dr. Amal Esawi and Dr. Mustafa Arafa for their help and guidance during the research. Special thanks to Eng. Rami Wasfi, Eng. Ehab Salama, Eng. Hanady Hussein, Eng. Ahmed Abdel Gawad, and Mr. Essam Aziz for their help with different samples testing and analyses at the different stages of this research. Also, thanks are due to Dr. Hosny Omar, Professor at the Physics department, for his helpful advice and fruitful discussions.

I would like as well to thank the Science and Technology Research Center (STRC) for the financial help and support. In addition, I want to express my gratitude for my colleagues in the Mechanical department for their help and cooperation**.** Lastly, and most importantly, I wish to thank my family for their continuous support.

ABSTRACT

Carbon nanotubes (CNTs) are known to have remarkable mechanical and electrical properties. One of those properties is piezoresistance which makes them suitable to be used in the field of strain sensing. Multi-walled nanotubes (MWNTs) were incorporated in low-density polyethylene (LDPE) matrix to form composite film sensors with different concentrations of 1, 2, 3.5, 5, 6.5, and 8 weight%. The fabrication of such composite was carried out using solid-state mixing, followed by melt blending process. Both extrusion and compression molding processes were used where compression showed more promising results in terms of electrical conductivity. Two types of molds were examined in compression molding, namely flash type mold and a positive type mold. The positive type mold showed better control over process parameters.

Furthermore two types of multi-walled carbon nanotubes of different aspect ratios were investigated using the positive type mold to examine their effect on the composite conductivity. The ones with the higher aspect ratio showed much higher conductivity. Strain sensitivity measurements were carried out on composite film samples at percolation threshold and beyond and gauge factors were obtained which showed significantly higher sensitivity than that of conventional strain gauges.

TABLE OF CONTENTS

LIST OF TABLES

LIST OF FIGURES

ACRONYMS

ASTM	American Society for Testing Materials
BPR	Ball-to-Powder Ratio
CNTs	Carbon Nanotubes
CVD	Chemical Vapor Deposition
DSC	Differential Scanning Calorimetry
FESEM	Field Emission Scanning Electron Microscope
GF	Gauge Factor
HDPE	High Density Polyethylene
HEBM	High Energy Ball Milling
LLDPE	Linear Low Density Polyethylene
LDPE	Low Density Polyethylene
MWNTs	Multi-Walled Nanotubes
PE	Polyethylene
PLLA	Poly(L-lactide)
PMMA	polymethyl methacrylate
SWNTs	Single-Walled Nanotubes
SHM	Structural Health Monitoring

NOMENCLATURE

ΔH_f	Enthalpy of melting
ΔH^o_f	Enthalpy for a 100% crystalline polymer
R_o	Initial Resistance (at no load condition)
R^*	Normalized resistance
T_m	Melting temperature
T_p	Crystallization temperature
wt%	Weight percent
X_c	Degree of crystallinity
ρ	Electrical Resistivity
σ	Electrical Conductivity

φ	Filler weight fraction
Φ_c	Percolation Threshold
ε	Strain

CHAPTER 1

INTRODUCTION and OBJECTIVES

1.1 Introduction

Strain gauges are commonly used devices that measure the strain of an object. They are used in many applications mainly in the field of Structural Health Monitoring (SHM). Their working principle is based on the theory of piezoresistance which is a phenomenon that describes the ability of a material to change its electrical resistance with respect to the applied strain on it. The change in resistance is correlated to the amount of applied strain by the gauge factor (GF) which is a measure of the gauge's sensitivity.

The most frequently used gauge is the metallic foil gauge, which is also known as the conventional strain gauge. The metallic foil gauge mainly consists of an insulating backing that supports a metallic foil pattern. The gauge factor of the metallic foil gauge normally ranges between 2 and 3.2 [1]. This is a restrictive sensing ability as it means that only a small change of resistance occurs for a certain amount of strain. In order for a material to detect small strains, a higher change in resistance is required. Another limitation of the conventional strain gauges is their low ductility which usually causes their fracture before finishing the testing process.

Carbon nanotubes (CNTs), first discovered by Iijima in 1991, have been the subject of research due to their remarkable mechanical, chemical, and physical properties [2]. Various methods have been used to synthesize carbon nanotubes such

as chemical vapor deposition (CVD), laser ablation, and arc discharge [3]. Two main types of carbon nanotubes have been produced, namely single-walled carbon nanotubes (SWNTs) and multi-walled carbon nanotubes (MWNTs). One of the very interesting properties of CNTs is their electrical properties where it was found that they have a very high conductivity equivalent to 1000 times that of copper [4]. In the research conducted by Dharap *et al.* [5] in 2004, SWNTs showed good piezoresistive properties where their electrical resistance changed proportionally with applied strain. This finding paved the way to research the possibility of using carbon nanotubes in strain sensing.

The challenge of harvesting the good properties of carbon nanotubes for strain sensing is the difficulty of them producing a proper film sample as Van der Waals forces that bond the nanotubes together is not strong enough to keep them bound under strain [6]. Therefore the idea of adding a polymer material to pristine nanotubes has emerged to improve interfacial adhesion of the CNTs [6]. Carbon nanotubes were used as filler material embedded in polymer matrix to produce composite films that can be used in strain sensing. The degree of dispersion of carbon nanotubes in the polymer matrix is an essential factor that affects the produced composite properties.

Different factors were shown to have an effect on the composite film sensing properties. Some of these factors are the processing method, type of polymer – thermoplastic or thermoset –, type of carbon nanotubes, and the amount of carbon nanotubes embedded in the polymer composite. Various methods were carried out to fabricate a CNT/polymer composite in order to obtain a composite film with a good degree of CNT dispersion. The two most common techniques were solution method

and melt-processing. The type of polymer material plays a role in determining which processing method to be used.

Other factors expected to have an effect on the composite film sensitivity include the type of adhesion used to glue the film sample onto the structure undergoing testing to ensure good strain transfer, and also the strain range investigated.

Several studies have been done to investigate CNT/polymer composites mechanical properties but not much work has studied their electrical properties. And even much less research has been conducted on the possibility of using such composites in strain sensing. In most work, MWNTs have been favoured due to their lower price in comparison with SWNTs [1]. So far the studies done showed promising results in the field of using CNT/polymer composites in strain sensing, yet the research is only in its early beginning as some challenges still exist.

1.2 Objectives

The aim of this research is to fabricate carbon nanotube/ polymer composite films for strain-sensing applications. In addition, the current research aims to study the effect of several factors on the electrical properties and strain sensing capability, namely the mixing method, processing technique, carbon nanotubes morphology and amount, and composite crystallinity. Multi-walled carbon nanotubes and low density polyethylene (LDPE) polymer have been selected for this study.

CHAPTER 2

BACKGROUND

2.1 Strain Gauge

The strain gauge is a measurement device used to determine the strain in a structure. Due to the difficulty of directly measuring the stress sustained by an object, the idea of measuring strain and then converting it to the equivalent stress value emerged [7]. The basic principle of a strain gauge is that it changes its electrical resistance as a result of the mechanical strain applied on it. Figure 2.1 represents the most common type of strain gauge named the metallic foil strain gauge (also known as the conventional strain gauge).

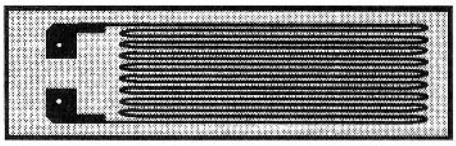

Figure 2.1: Metallic foil strain gauge (metal foil pattern –serpentine shaped- bonded on an insulating backing) [8]

When the strain gauge is under tensile strain, its gauge length as well as its electrical resistance will experience a change. The relation between the amount of change in resistance and the change in gauge length is defined as the strain sensitivity or the gauge factor (GF). This factor is calculated as demonstrated in equation (2.1):

$$GF = (\Delta R/R_o) / (\Delta L/L_o) = (\Delta R/R_o) / \varepsilon \quad \textbf{(2.1)}$$

Where ΔR is the change in resistance, R_o is the initial strain gauge resistance prior to loading, ΔL is the change in gauge length, L_o is the initial gauge length, and ε

is the strain applied which is equivalent to ($\Delta L/L_o$) [7]. The gauge factor of the conventional strain gauge ranges from 2 to 3.2 [1].

2.2 Carbon NanoTubes (CNTs)

Carbon Nanotubes (CNTs) have attracted great attention since their discovery by Iijima in 1991 [2]. CNTs are simply rolled sheets of graphite built up on the nanoscale that are fabricated via several routes such as arc discharge, chemical vapor deposition (CVD), and laser ablation. They have remarkable physical, mechanical, thermal, electrical, and raman active properties [9, 10]. These properties of CNT endow them as an ideal filler material in composites [11].

CNTs are known to possess high flexibility, low density (1.3-2.4 g/cm^3), and large aspect ratio (typically >1000 – indicating a large surface area) [12-14]. Also, they demonstrated thermal conductivity about double that of diamond and electric-current-carrying capacity up to 1000 times higher than copper wire [4, 11, 13]. However, the atomic structure of nanotubes affects their electronic properties. The atomic structure of CNTs is described by the chirality vector (C_h) that depends on how the graphite sheet is rolled as shown in Figure 2.2. The three forms of chirality are the zigzag, chiral, and armchair configurations. Equation (2.2) expresses how the chiral vector is calculated:

$$C_h = n\vec{a}_1 + m\vec{a}_2 \qquad \textbf{(2.2)}$$

Where a1 and a2 are the unit vectors as indicated in Figure 2.2, the integers n and m represent the number of steps along the two unit vectors $\vec{a}_1$ and $\vec{a}_2$ respectively [15].

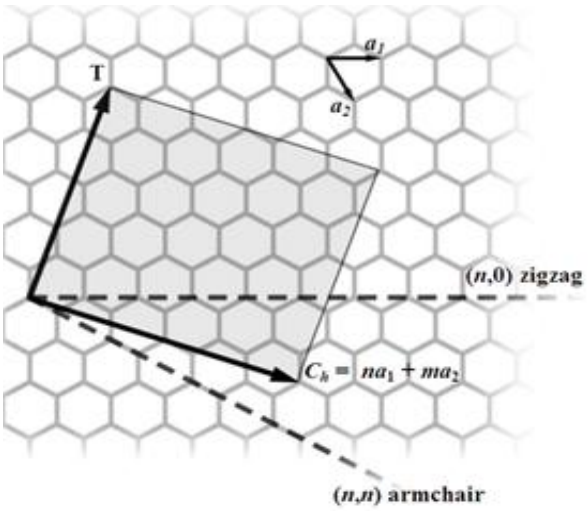

Figure 2.2: Chirality of nanotubes described by the chiral vector (C_h) [16]

Recently, a great attention has been focused on CNTs in the field of composite materials mainly for two purposes, mechanical reinforcement and electrical conductivity [13]. One of the most significant characteristics of CNTs is piezoresistivity, where change in the electrical properties is induced by strain, which make them a promising smart sensor material [10]. Their small size allows them to be used as extremely small sensors that are sensitive to mechanical deformations [6]. Due to their capability to change electronic properties when subjected to strain, CNTs have been considered a potential candidate for strain sensors. Both, individual SWNTs and MWNTs were found to exhibit a repeatable load–unload relationship between their mechanical deformation and the electrical conductance [1, 2].

2.2.1 Types of Carbon NanoTubes

The performance of CNTs as a filler material in composites depends on many factors, such as, the type of CNTs (SWNTs or MWNTs), their morphology and structure, their processing method as well as other factors related to the matrix used [11]. Figure 2.3 presents the two main types of carbon nanotubes.

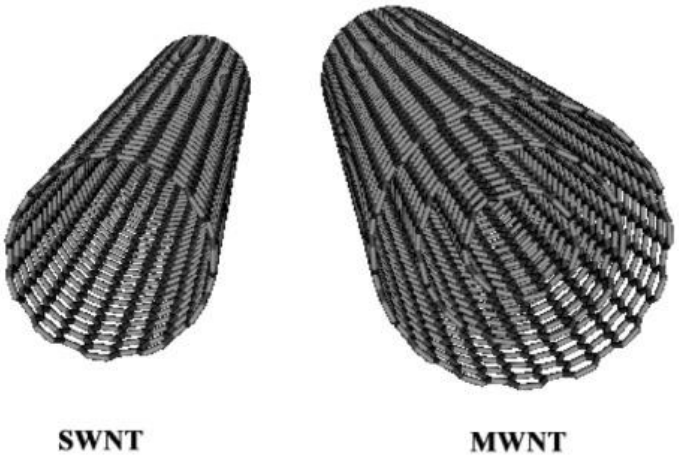

Figure 2.3: Types of Carbon Nanotubes, SWNTs and MWNTs [17]

2.2.1.1 Single-Walled NanoTubes (SWNTs)

Single-walled carbon nanotubes as their name indicates consist of a wrapped one-atomic-thick layer of graphite sheet. SWNTs exhibit superior mechanical and electrical properties [5] yet they are challenging to produce thus they are more expensive than MWNTs [1].

2.2.1.2 Multi-Walled NanoTubes (MWNTs)

Multi-walled carbon nanotubes are in the form of concentric cylinders rolled around a common central hollow with a certain separation between the layers close to the graphite interlayer spacing of 0.34 nm [18]. MWNTs are commonly used and favoured due to some advantages when compared with SWNTs, such as their cost advantage [1, 2, 13], and their ease of production [19]. In addition, they are always conductive and have a relatively high conductivity, 1.85×10^3 S/m, when compared to other nano or micro fillers such as carbon black [1]. There are two forms of MWNTs, entangled and non-entangled as shown in Figure 2.4. The non-entangled MWNTs give electrical conductivities 50 times higher than the usual entangled MWNTs resulting from industrial mass production, probably for the reason that straight

MWNTs have less defects [20]. Another reason for the difference in conductivity might be due to the interference of magnetic fields associated with passing electric currents in conductors, where in the case of entangled MWNTs these fields can result in higher current impedance.

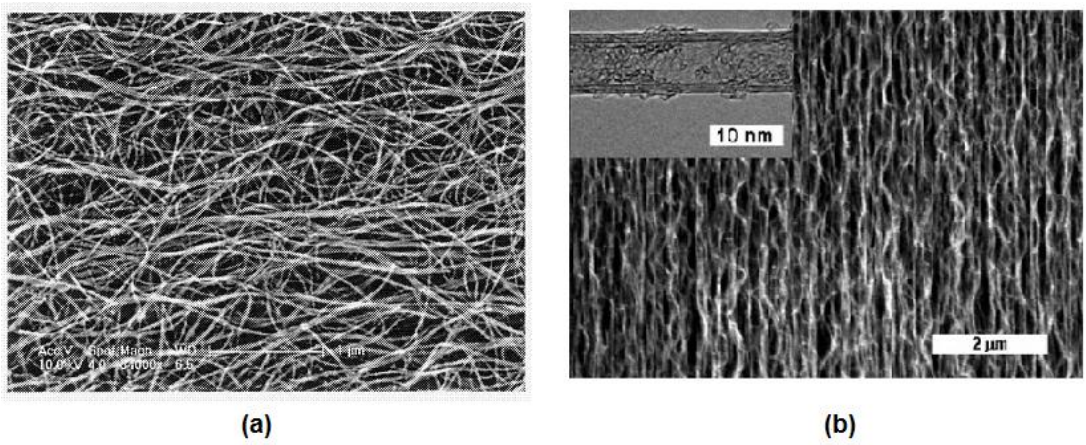

Figure 2.4: Photos showing examples of (a) entangled CNTs [21], and (b) non-entangled CNTs with an inset of a single MWNT seen on the upper left corner [22]

2.3 Low-Density Polyethylene (LDPE) polymer

Various types of polymer matrices have been used in research whether thermoplastics or thermosets in order to produce a CNT/Polymer composite. Some main properties are looked for when choosing polymer matrix: ease of production, good flexibility, good chemical resistance, and low density.

Polyethylene (PE) is a thermoplastic polymer and is one of the most widely used polymeric materials for its good characteristics such as, lightweight, and superior molding. These qualities render PE a good candidate as matrix of polymer-based electrically conductive composites [19]. Low Density Polyethylene (LDPE) is a grade of polyethylene that has the chemical structure of $(C_2\text{-}H_4)_n$. It is a highly branched structure that has a low crystalline content as well as low density [23]. LDPE exhibits

excellent flexibility, excellent chemical resistance, low coefficient of friction, and moderate stiffness that make it a proper candidate for composites that can be used in different applications [18].

2.4 Solid-State Mixing Methods

Good dispersion of CNTs throughout the polymer matrix is essential as it affects the final composite properties [14]. Mechanical mixing of the nanotubes with the polymer powder prior to processing is a favoured step in order to promote good CNTs dispersion. In addition, it helps in disentangling the nanotubes thus breaking large agglomerates into smaller ones.

2.4.1 Turbula Mixing

Turbula mixer is a low energy mixing device used to provide homogenous mixing of powders. It has a maximum speed of 101 rpm [24]. The mixer works by moving the mixing container in a three dimensional motion of rotation, translation, and inversion. Figure 2.5 shows an example of a turbula mixer.

Figure 2.5: An example for a turbula mixer [24]

2.4.2 Ball Milling

Ball milling is a high energy mixing method that uses a grinding tool, usually steel balls, that leads to local generation of high pressure as a result of collisions throughout the grinding jar [9, 14]. It is also referred to as High Energy Ball Milling (HEBM). The main parameters in the ball milling process are the rotation speed, the milling time, and the ball-to-powder ratio (BPR). Figure 2.6 shows a planetary ball mill, which is one of the most common types of ball mills, with a demonstration of how the milling process takes place.

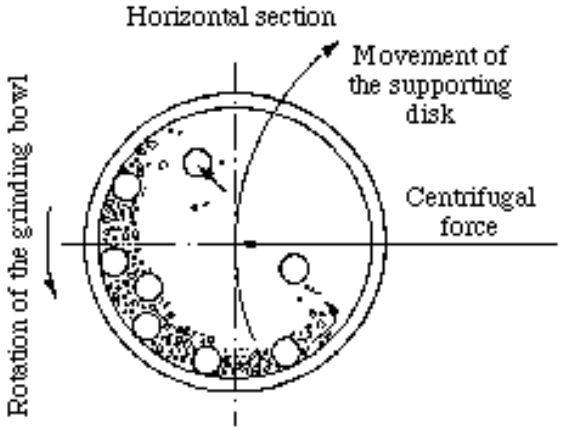

Figure 2.6: A horizontal section of the ball milling jar for a planetary ball mill demonstrating the milling process [25]

2.5 Composite Processing Techniques

The simple processing of polymers using conventional methods can be carried out without damaging the CNTs, and thus reducing the manufacturing cost [11]. However, an important challenge lies in transmitting the unique properties of CNT to the polymer matrix when fabricating the composite [4, 9]. Some critical issues should be taken into consideration, choosing the appropriate processing method [9], uniform

dispersion of the nanotubes throughout the polymer matrix [6, 12, 13], and enhanced interfacial interaction between the polymer and the nanotubes [4, 6, 13].

One of the simplest and fastest methods used to fabricate CNT/polymer composites is melt blending which makes it suitable to be scaled up in production [1, 26]. Melt processing indicates the blending of CNTs with the melted polymer by the application of shear forces [14]. Two of the most common techniques of melt processing are extrusion and compression molding.

2.5.1 Extrusion

Extrusion is the process where solid material, usually in the form of pellets, is continuously fed to a heated chamber and carried along with the aid of a feedscrew. Single-screw extruder is commonly used in polymer production. An example of a single-screw extruder is shown in Figure 2.7. The configuration of the die, through which the produced extrudate exists, decides the shape of the final product. The main advantage of extrusion lies in its ability to promote shear mixing by the screw rotation that helps in dispersing the filler material within the polymer matrix. It has also been reported to cause some alignment of the nanotubes at the outmost surface [26].

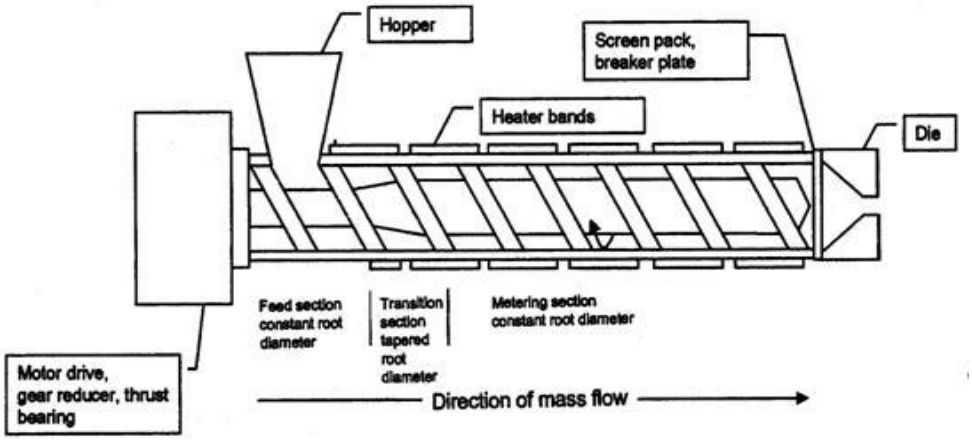

Figure 2.7: An example of single-screw extruder [27]

2.5.2 Compression Molding

Another technique of melt blending is compression molding. This process is mainly adding a molding charge into a preheated mold and by applying heat and pressure, the molding material takes the shape of the mold cavity. Pressure is applied on the mold using the heated platens of a hydraulic press. The mold consists of two parts, usually an upper and a lower part. The molding charge can vary from powder particles to pre-formed sheets. Figure 2.8 represents the molding process.

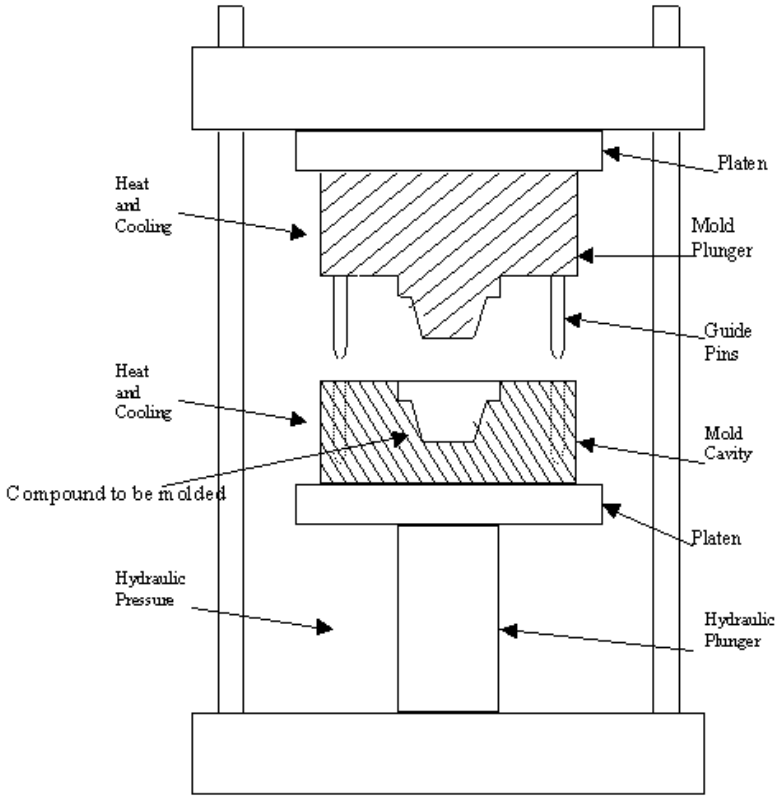

Figure 2.8: An example of compression molding process [28]

2.6 CNT/Polymer Composite Electrical properties

CNT/polymer composites have attracted much attention as they offer electrically conductive polymer materials at much lower filler contents as compared to conventionally used conductive fillers, such as carbon black [18]. A number of possible applications were suggested for the electrically conductive composites, such as sensing applications, electrostatic discharge, photovoltaic cells, and electromagnetic interference materials [1, 29]. There are a number of factors that affect the degree of conductivity of the composite material which are volume fraction of the filler, filler aspect ratio, and the degree of filler dispersion [19, 30]. This is in addition to the intrinsic conductivity of the filler material itself [19].

CNT/polymer composite conductivity is determined by the CNTs network formation that is limited by the carrier transport within the polymer matrix [19]. The

resistance between neighboring nanotubes that are not in contact is called “tunneling resistance” where electrons hop from one nanotube to the other in order to allow current flow. A description of this hopping mechanism is illustrated in Figure 2.9 [31].

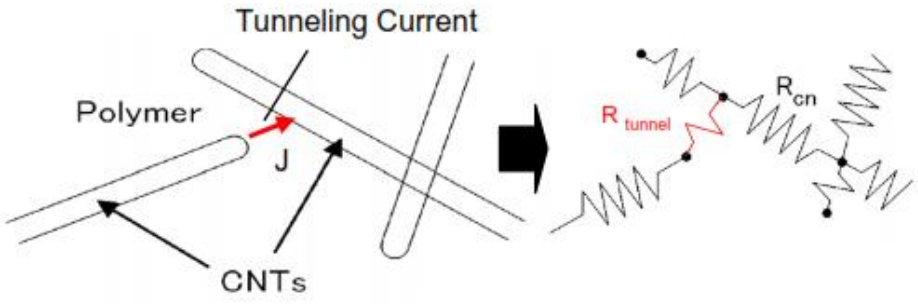

Figure 2.9: The tunneling resistance between neighboring nanotubes [31]

2.6.1 Percolation Behavior

Percolation threshold (Φ_c) is defined as “the critical point corresponding to the onset of long-range, global connectivity of the minor constituent” [32]. This value is easily detected as a sudden increase in the composite properties, equivalent to some orders of magnitude. An example for the phenomenon of percolation threshold is presented in Figure 2.10 showing the nonlinear change in composite properties upon reaching the percolation threshold. Insets at three different stages of geometrical structures are also presented in Figure 2.10 demonstrating the change in filler phase, where in first inset (1) the filler particles are observed to be scattered with large distances in between. In the second one (2), upon reaching the percolation threshold, distance between filler particles greatly decreased and even some filler particles are in contact allowing a filler network formation. In the third inset (3) most filler particles are found to be in contact leading to development of filler agglomerations.

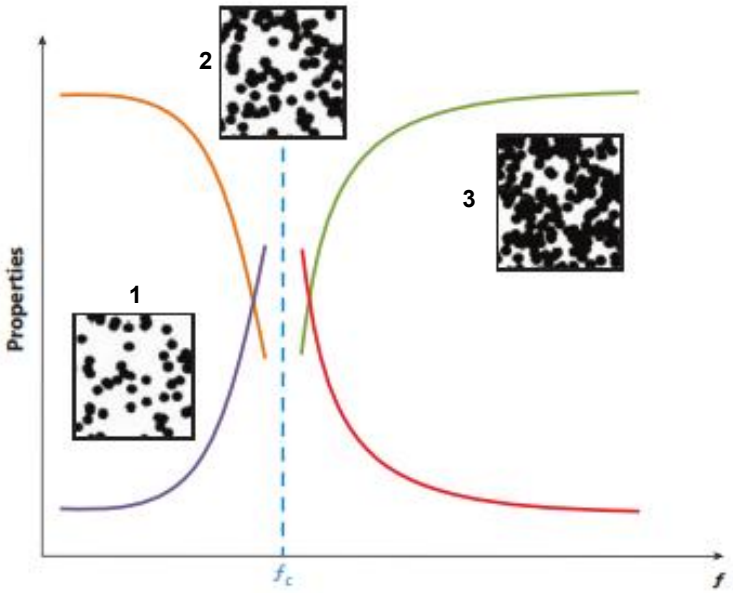

Figure 2.10: Schematic diagram of composite system properties versus filler content (f) showing the abrupt change in material properties upon the onset of reaching percolation threshold (f_c) [32]

2.6.2 Composite Strain Sensing

As mentioned previously, the piezoresistance is the ability of changing resistance with respect to the applied strain. This property of CNT/Polymer composite makes it suitable to be used in the field of strain measurement. The strain sensitivity of the composite sensor is measured same way as that used for strain gauge which is by calculating the gauge factor. In order to observe a direct relation between the applied strain and the change in resistance, normalized resistance (R^*) as described in equation (2.3) is used by researchers [1].

$$R^* = \Delta R / R_o \qquad \textbf{(2.3)}$$

CHAPTER 3

LITERATURE REVIEW

Different fabrication techniques have been used to produce CNT/polymer composite strain sensors and were reported in previous work. The effect of the fabrication process on the electrical properties of the produced composite films was investigated as well as the effect of other factors such as the type of polymer used and the type and morphology of CNT. In this chapter, the fabrication processes used in various studies are demonstrated. Moreover, the factors that affect the percolation threshold, the strain sensitivity of CNT/polymer composite strain sensors, and the effect of CNTs addition on polymer crystallinity are discussed.

3.1 CNT/Polymer Composite Fabrication

It was reported that poor dispersion of CNTs leads to high electrical resistivity which in turn increases the percolation threshold [4]. Many methods were attempted to separate the CNTs into tiny bundles by using mechanical, chemical or combined methods. However, the tendency of CNTs, whether SWNTs or MWNTs, to agglomerate makes homogeneous dispersion within the polymer matrix a challenge mainly due to high intermolecular Van der Waals interactions between the nanotubes [6, 9, 11, 18, 33, 34]. Moreover, the existence of synthesis induced entangled CNTs agglomeration makes dispersion a difficult task [18]. On the other hand, Bauhofer *et al.* [20] reported that perfect dispersion does not necessarily lead to high electrical conductivity, since this usually implies the formation of a polymer layer around each

CNT, which in turn impedes the flow of electric current from one nanotube to another.

In order to obtain CNT/polymer composite films with good dispersion of CNTs within the polymer matrix, researchers have used two consecutive steps, namely mixing and processing.

3.1.1 Mixing Methods

Different methods have been attempted in order to reach an efficient dispersion of CNTs in polymer matrices. In-situ polymerization, solution method and melt processing are examples of these methods [9, 11, 14, 18]. The type of polymer matrix, whether thermoplastic or thermosetting, plays an important role in deciding the processing method to be used for fabricating CNT/polymer composites [14].

The two most widely used methods are solution method and dry blending [1]. The dry blending process, at near room temperature, is favored for its simplicity, and also as it can readily be scaled up in production [1] unlike other methods, such as high power ultrasonic mixers, solution mixing and in situ polymerization which may not be commercially viable and are environmentally controversial [4]. Attempts have been done to mix CNTs with polymer powder by utilizing HEBM, which showed a satisfactory level of dispersion of CNTs into the polymer matrix, resulting in an improvement of the physical properties of the composites [9, 14].

Other studies used the solution mixing method to mix the CNTs with the polymer matrix, which is more commonly used in fabricating CNTs/polymer composites [1, 18, 34-36]. For instance, Liu *et al.* [34] used a solvent (Dichlochmethane), that readily evaporates, to disentangle the MWNTs and then

added PLLA polymer and sonication of the mixture took place for 6 hrs to achieve good degree of CNTs dispersion. It was reported that the solvent used only took 24 hours to evaporate while other solvents, such as chloroform, can take up to 1 week to fully evaporate. Meanwhile, Knite *et al.* [35] used chloroform as a solvent to dissolve polyisoprene polymer with MWNTs and the mixture was left to dry for 24 hours only. The temperature at which the mixture is left to dry, plays an important role in determining the time needed for complete evaporation to take place.

The use of solution method raises some concerns that any solvent remnants in the composite may degrade its mechanical properties which means it will negatively affect the stress transfer from the polymer matrix to the CNTs [26]. Esawi *et al.* [26] used both the dry mixing and the solution mixing method to investigate and compare their effect on the MWNTs dispersion within Polypropylene matrix. Although FESEM analysis showed that the solvent-mixed samples suffered from some porosity, uniform dispersion was obtained for samples up to 5 wt% MWNTs. Moreover, with regards to the conductivity of the nanocomposites, it was reported that the curing temperature and the mixing conditions are key factors in the solution mixing method, which in turn influence the formation of the conducting network significantly [29]. The results show that the bulk conductivity of the nanocomposites is affected by the curing temperature, the mixing speed and the mixing time carried out in the fabrication process, which ranges from the order of 10^{-6} S/m to the order of 1.0 S/m depending on the different process conditions used [29].

In a research conducted by Pham *et al.* [1] both the dry mixing and solution mixing methods were used to fabricate MWNTs/PMMA composite films for strain sensing. According to the study [1], it was observed that the solution mixed samples

showed better CNTs dispersion within the polymer matrix than the dry mixing method. In addition, Bauhofer *et al.* [20] stated that solvent processing techniques occasionally prevent an overall sheathing of CNT which in turn improves the electrical performance of composites.

Other methods, such as chemical treatment using surfactants in order to disperse CNTs, were also reported [19, 36]. Yu *et al.* [36] used dispersion-assistant surfactants to distribute the CNTs within the polymer matrix but it was indicated that surfactants could block the contacts among carbon nanotubes, which in turn weaken the piezoresistive response of the composite. Another novel method in dispersing CNTs within the polymer matrix was reported by using organo-clay as a co-filler [37]. The organo-clay co-filler, which was introduced along with MWNTs, enhanced the dispersion of MWNTs in the polymer matrix irrespective of the MWNTs filler content.

In the work conducted by Hu *et al.* [29], the effect of the fabrication process on the electrical properties of CNT/polymer composites have been investigated, where epoxy was chosen as the polymer matrix. One of the findings was that a mixing process with moderate shear forces and short mixing time is good enough since no significant aggregates of MWNTs were identified in the produced specimens. Too high shear forces and too long mixing time may cause breakage of the MWNTs networks. This indicates that an optimal mixing does exist to avoid both over-dispersion and serious aggregation of CNTs in order to enhance the electrical conductivity of composites at only low volume fractions of CNTs.

3.1.2 Processing Techniques

Melt processing – such as extrusion, compression molding, injection molding, etc. – is the most common fabrication method to produce polymer composites. The reasons behind its being a favored method lie in its simplicity, availability of such common techniques and its suitability for mass production.

Extrusion process was used in several studies as it was reported that shear forces during the melt mixing help in disentangling the CNT aggregates thus enhance the CNTs dispersion within the polymer matrix [26]. In the study carried out by Valentino *et al.* [12], shear mixing by the twin-screw extruder was relied on to promote CNTs dispersion within the polymer matrix, hence no additional mixing step took place prior to extrusion. Similarly, in McNally *et al.* [4] study, no mixing step took place before processing, instead two combined methods to produce CNT/PE composite were used by means of twin-screw extrusion to induce CNTs dispersion followed by melt blending using compression molding. Same methodology was carried out by Barus *et al.* [13].

A novel fabrication method was used to fabricate CNT-composite thin films by creating a systematic Layer-by-Layer (LbL) assembly technique [38]. This technique demands the sequential dipping of a charged substrate (i.e. glass, silicon, among others) in oppositely charged polyanion and polycation solutions to deposit a variety of species one monolayer at a time. Each additional monolayer to be deposited is based on opposite charge electrostatic and Van der Waals force interactions. Homogeneous multiphase carbon nanotube–polyelectrolyte composite thin films were fabricated via this technique. Although it was stated that such method promotes specific tailoring of macro-scale sensor properties, it was indicated that sensor

performance was negatively affected by an exponential decay in film resistivity and light sensitivity.

3.2 Polymer Matrix

Different types of polymer matrices were used in the literature in the process of producing CNT/polymer composite. It was reported that the use of different matrices can cause variation in composite conductivity by 10 or more orders of magnitude [20]. The reason for this large variation was justified by the extreme distance dependency of tunneling through polymer barriers between CNTs. Thus, in addition to the method of dispersion, the polymer type also has an important effect on the percolation threshold and maximum conductivity of composites [20].

3.3 Percolation Behavior for Composite Films

As previously mentioned in chapter 2, upon increasing the amount of CNTs the electrical resistivity is reduced as the average distance between neighboring nanotubes decreases. Electron transport is then facilitated through tunneling (or hopping mechanism) which can be recognized when the volume fractions of CNTs are near the percolation threshold, at which a great increase in the electrical conductivity is observed [4, 31]. The tunneling effect disappears gradually with increasing additions of CNTs which implies that high strain sensitivity can be achieved in the composite if the CNTs loading is maintained close to the percolation threshold [1, 31].

Depending on the polymer matrix and processing technique as well as the type of carbon nanotubes used, percolation thresholds ranging from less than 1.0 wt% to over 10.0 wt% of CNT loading have been observed experimentally [29, 30].

Percolation behavior was considered when a large rise in conductivity value is obtained [9]. An example of percolation behavior is shown in Figure 3.1 where percolation threshold was observed around 2 wt% MWNTs as the conductivity increased by 6 orders of magnitude in the range of 1 to 3 wt% [9].

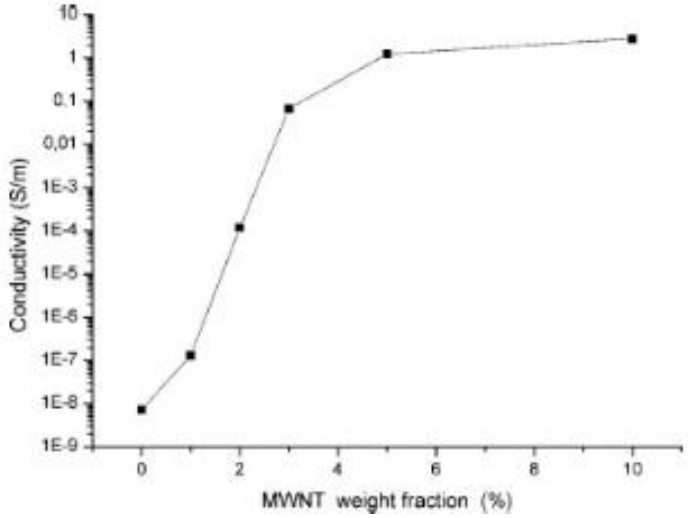

Figure 3.1: Percolation threshold obtained in the range of 1-3 wt% MWNTs [9]

Table 3.1 demonstrates some of the percolation threshold results reported. A large variation in percolation thresholds (Φ_c) can be seen ranging from 0.1 wt% for SWNT/PMMA composite [6] to 12.5 wt% (as observed in the range of 10 – 15 wt%) for MWNT/LDPE composite [18]. For instance, though Zhao *et al.* [18] and Valentino *et al.* [12] used same polymer (LDPE) and same type of CNTs (MWNTs), there is a large difference between their percolation thresholds showing that the processing method had a great effect on the electrical properties of the produced composite samples. Furthermore, McNally *et al.* [4] and Valentino *et al.* [12] used MWNTs and extrusion process using a twin-screw extruder, but the resulting percolations varied in values revealing that the polymer used have an impact as well.

Table 3.1: Different examples of reported ranges of percolation thresholds

Polymer used	CNTs type	Processing method	Φ_c	Reference
LDPE	MWNTs	Solution method followed by hot pressing	10 – 15 wt%	[18]
PE (Linear medium density type)	MWNTs	Extrusion (using twin-screw extruder)	7.5 wt%	[4]
LLDPE	MWNTs	HEBM followed by compression molding	1 – 3 wt%	[9]
PMMA	MWNTs	Solution mixing followed by compression molding	1 – 3 wt%	[1]
LDPE	MWNTs	Melt blending process (using twin-screw extruder)	1 – 2.5 wt%	[12]
HDPE	MWNTs	Melt blending process (using twin-screw extruder)	1 – 2.5 wt%	[12]
PMMA	SWNTs	Solution method followed by molding	0.1 wt%	[6]

Although Pham *et al.* [1] fabricated 2 sets of samples, one with solution mixing and the other with dry mixing, only the percolation behavior of the solution mixed set was reported. It was stated that percolation behavior for dry blended films could not be detected as the resistance values of films below 6 wt% MWNTs exceeded the capacity of the measuring equipment used. Bauhofer *et al.* [20] reported that the unusual results of high percolation threshold indicates that the filler particles (CNTs) were not homogeneously dispersed.

Some factors should be taken into consideration when assessing the percolation threshold such as CNTs type, CNTs aspect ratio, electrodes type, sample dimensions, and resistance-time dependency. These factors are discussed below.

3.3.1 CNTs type and morphology

Several works preferred using MWNTs over SWNTs due to their lower cost and also it was reported that unlike SWNTs, MWNTs are always conductive [1]. However, it was stated that the effect of CNTs type as well as the method of treatment (purification, oxidation) did not show an apparent impact on the maximum conductivity of composite films [20].

Moreover, a study was carried out comparing two different kinds of MWNTs morphology, purchased from two different manufacturers, each embedded in epoxy polymer composite and analyzed their effect on the composite piezoresistivity behavior [39]. The first kind was small in diameter and curvy, while the second was larger in diameter and straight. It was found that each of the two kinds of MWNTs have different piezoresistivity characteristics and working mechanisms. The results showed that the type of CNTs differs in working mechanisms of sensing, where piezoresistivity in the first type was revealed to be caused by deformation of MWNTs while the second type behavior was a result of the tunneling effect caused by the change in distances between neighboring carbon nanotubes due to the applied tensile strain as presented in Figure 3.2.

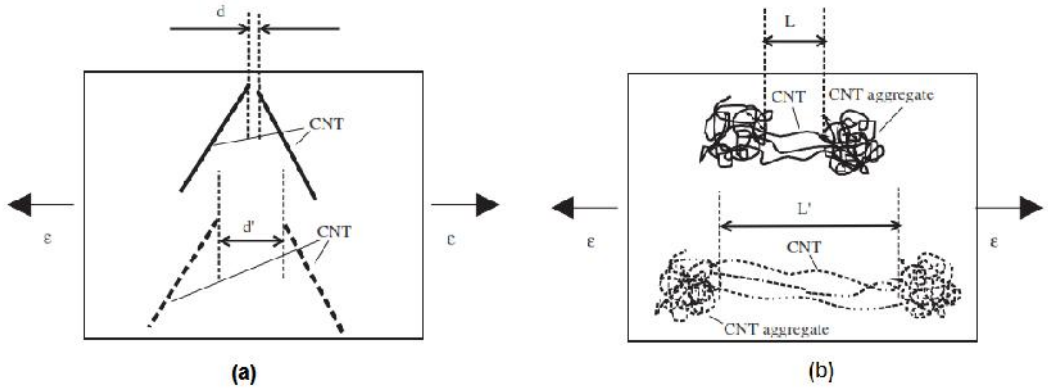

Figure 3.2: (a) Schematic diagram showing the working mechanism of the larger diameter straight MWNTs, while (b) Schematic diagram showing the working mechanism of the smaller diameter curvy MWNTs [39]

CNTs morphology was further emphasized in literature. In Bauhofer *et al.* [20] review of literature, it was observed that the CNTs entanglement state has a high effect on composite conductivity as it was reported that non-entangled MWNTs give electrical conductivity 50 times higher than the usual entangled MWNTs. The advantage that was emphasized for entangled nanotubes is their ability to better attachment in the polymer matrix when compared with straight nanotubes [9].

3.3.2 CNTs Aspect Ratio

Several studies have reported that a high aspect ratio of the filler material results in lower percolation threshold of the composite material and thus causing a higher electrical conductivity [20, 30]. This in turn implies that less volume fraction of filler particles would be needed to reach a certain targeted conductivity [30]. It is important to indicate that this finding is related to the statistical percolation threshold as most theoretical analyses carried out ignore the possible movement of filler particles when predicting the percolation behavior [20].

3.3.3 Electrode Types

Different types of electrodes were used when measuring the electrical conductivity of CNT/polymer composite according to availability of electrode material. The most common type is silver paste or paint as shown in Figure 3.3 [6, 31, 34, 38-41]. Another type is gold electrodes using gold sputtering [4, 12]. Other types used by researchers include copper foil [35], aluminum paint deposition [18], clamping film between conductive materials such as brass [1], or a combination of different materials such as copper wire with the aid of silver paste [29] and silver conductive epoxy encapsulated by copper film [34].

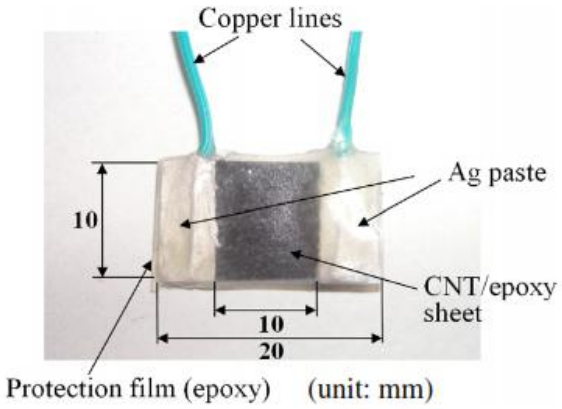

Figure 3.3: Silver paste electrodes used for CNT/epoxy sheet with copper lines used to connect with resistance measurement device [31]

In the work conducted by Kwok *et al.* [41], the effect of electrodes type on composite electrical resistance was investigated in order to decrease contact resistance that leads to localized heating around the electrode. Comparison was carried out between bare composite film surface with no electrodes, single-sided adhesive copper tape, double-sided adhesive carbon tape, narrow silver paint line, wide silver paint line, a combination of small conducting rubber pad with silver paint and copper sheet pressed together by miniature C-clamp, and another one with the same combination

but with large conducting rubber pad. In all cases, resistance was measured using two-point probe method using alligator clips. When resistance was measured directly from bare composite film, high contact resistance was observed especially that alligator clips have very small contact area. Moreover, the irregularity of the surface of composite film as well as its low conductivity represented a challenge for resistance measurement. It was clear that an intermediate material (electrode) would be beneficial.

Furthermore, the results showed that the following electrode types gave lowest contact resistance in descending order: wide silver paint, narrow silver paint, combination of small contact electrode, and combination of large contact electrode respectively [41]. The largest contact resistance was detected for the double-sided adhesive carbon tape followed by that of the bare composite. As for the single-sided copper tape, the contact resistance obtained lied as an average between the rest of the results [41].

3.3.4 Film Dimensions

In most research carried out for CNT/polymer composites, the samples used were in the form of rectangular film specimens. Li *et al.* [2] investigated the strain sensing of pure MWNTs films and the effect of using different film dimensions on the stability of the initial resistance values was studied. The films used were all of the same thickness of 0.13 mm. According to the findings, the optimal aspect ratio of a film sample, which is the ratio of the width to the length, is 7 where this conclusion was based on the stability of measurements. However, it was mentioned that there may be an upper limit for the optimal aspect ratio of the film as the resistance will

increase when the aspect ratio increases which might decrease the strain sensitivity [2].

Although no research study investigated the effect of film thickness on the composite conductivity, the thickness values reported in literature varied from one study to another. For instance, McNally *et al.* [4] used CNT/PE films of 0.35mm in thickness which is in the same range as reported in [6, 9], while Zhao *et al.* [18] used CNT/LDPE films of 2mm in thickness which is close to what Knite *et al.* [35] used. In Valentino *et al.* [12] work, the investigated films of MWNT/LDPE and MWNT/HDPE had a thickness of 0.8 (±0.1) mm.

3.3.5 Initial Resistance Time Dependence

The phenomenon of the electrical resistance decay with respect to time at no load condition was observed in several studies [1, 2, 18, 38]. Li *et al.* [2] investigated MWNT film stability at zero load condition for a period of 30 minutes. Three different behaviors were obtained which were categorized as an unstable group, a gradually stable group, and a stable group. It was suggested that probable reasons for the instability at zero loading are defects and breakdown of the MWNT shell structure as defects in the CNTs can significantly change the resistance values under an electrical field by a decreasing trend.

The effect of temperature on resistance was addressed in other work conducted by Loh *et al.* [38]. It was stated that the nature of the resistivity decay was not clear however, it was observed that the CNT/Polyelectrolyte film samples were influenced by temperature. The film samples did exhibit a decrease in resistance with increasing temperature. The cause of the rise in temperature was the constant current

supplied by the multimeter while measuring the resistance. The direct current supplied, though of small value of 5 μA, caused an increase in the overall temperature of the film samples by activating the electrons at the nanotube-to-nanotube junctions which increased the conductivity of the samples.

Other studies did report only fluctuation of resistance readings for a certain period of time at no-load condition [1, 42]. Pham *et al.* [1] recorded resistance measurements for a period of 500s, fluctuations in resistance readings were obtained in the range of 0.07% of the initial resistance reading which were considered of negligible effect. However, it was decided for the sake of the accuracy of measurements that a 60s delay in data recording would give enough time for readings stability. Another study gave an account of initial resistance time dependence yet it stated that consistency of measurements was obtained when the system reached equilibrium [42].

3.4 Composite Films Strain Sensitivity

Measurement of strain sensitivity is carried out by testing the film sample change in resistance with respect to the applied strain. A piezoresistive effect was attained for pure CNTs and CNT/polymer composite films [1, 2, 5, 6, 31, 34-36, 38-40, 42]. Figure 3.4 presents an example of strain sensitivity for MWNT/PMMA composite films for three different MWNTs concentrations of 6, 8, and 10 wt% produced via melt processing for strains up to 0.6% [1], while Figure 3.5 shows the strain sensitivity of SWNT/PMMA composite films of 0.5, 1, 3, 5, and 10 wt% for strains up to 0.15% [6].

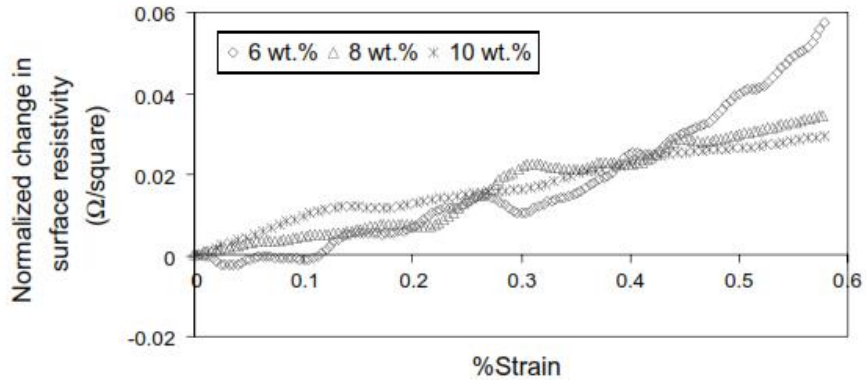

Figure 3.4: Normalized resistivity versus applied strain for MWNTs concentrations of 6, 8, and 10 wt% for MWNT/PMMA composite films [1]

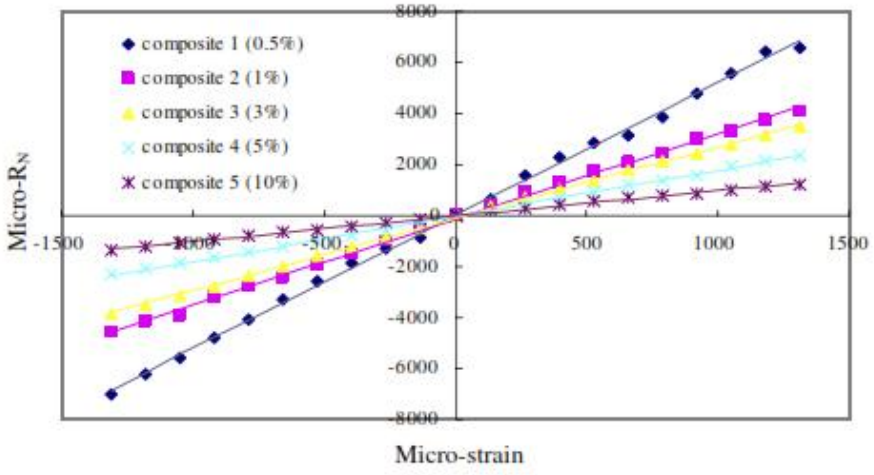

Figure 3.5: Micro Normalized Resistance versus Micro-strain of 5 different composites of 0.5, 1, 3, 5, and 10 wt% SWNTs for SWNT/PMMA composite films [6]

Some pioneering investigations were conducted by Dharap *et al.* [5] on pure SWNTs films, also known as buckypaper, which showed a nearly direct relation between film resistance and applied strain as load was applied incrementally and held for several seconds to leave time for readings to stabilize [5]. Similarly, Li *et al.* [2] observed a linear correlation between the MWNTs film resistance and the applied strain up to 1800 με which is the maximum value in the tested range in case of tension and compression. On the other hand, Kang *et al.* [6] reported nonlinear behavior for SWNTs buckypaper films under tension for strain beyond the value of 500με. The non-linearity was attributed to the possible separation and slippage of SWNTs, which

are intertwined with simple mechanical bonding in the buckypaper i.e. weak van der Waals forces. Hence, nanocomposites are preferred as they provide a method to improve the load transfer capability by using CNTs as filler in a polymer matrix [34]. SWNT/PMMA composite films were used instead of SWNT buckypapers to improve strain transfer across film sensors by means of stronger polymer interfacial bonding [6]. Although the composite films showed lower strain sensitivity than the buckypaper sensor, it possessed a moderately linear symmetric strain response under static and dynamic strain [6]. Yu *et al.* [36] reported that they investigated the sensing capability of the CNT/polymer composite films shows strain sensitivity 3.5 times the conventional strain gauge.

In general, the composite films piezoresistivity behavior obtained is mainly attributed to change in CNTs network conductivity – due to the loss of contact among CNTs –, change in tunneling resistance due to a variation in the distance between neighboring CNTs, and the piezoresistivity of the CNTs themselves caused by their deformation under applied strain [39].

3.4.1 Gauge Factor

The gauge factor (GF), which represents the sensitivity of strain sensors, showed great variation in values from one study to another. It was observed that low values of electrical resistances lead to low values of gauge factors [1, 2, 6, 20]. For instance, Li *et al.* [2] worked on pure MWNTs films where gauge factor in the range of (2 – 3.76) was obtained as the films initial resistances ranged from 30 to 300 Ω. Also, in the study conducted by Loh *et al.* [38] on MWNT/Polyelectrolyte film samples, which underwent cyclic loading, the highest gauge factor obtained was only

0.208 yet a linear behavior was attained for strains up to 10,000μm/m. Similarly, Vemuru *et al.* [40] reported a low gauge factor of 0.3482 for the fabricated MWNTs films where the correlation between change in voltage and applied strain remained linear until 1000 με. On the other hand, a gauge factor of 7 was achieved for SWNTs buckypaper samples; however, a nonlinear behavior was detected when applying strains beyond 500μm/m [6].

As discussed earlier, the CNTs morphology does affect the percolation behavior of composite films and also it affects their gauge factors. Two forms of MWNTs, purchased from different manufacturers, were used. Different weight percentages were embedded in the epoxy matrix. Their strain sensitivities were investigated [39]. Table 3.2 shows the resulting gauge factors for testing range up to 6000με under tensile loading. By comparing the results at 5 wt%, it can be observed that MWNT-7 (with the high aspect ratio) gave a gauge factor of 1.5 times that of the LMWNT-10 (with the low aspect ratio).

Table 3.2: Gauge Factors for two different forms of MWNTs embedded in Epoxy Matrices [39]

Form of MWNTs	MWNTs (wt %)	GF
LMWNT-10 (type 1: of low aspect ratio)	5	3.8
	7	4.1
	10	4.3
	15	3.2
MWNT-7 (type 2: of high aspect ratio)	1	22.4
	4	7.6
	5	6.2
	7	4.8
	10	3.2

Moreover, it was reported that CNT/polymer composite strain sensors are more strain sensitive when using low concentrations of CNTs, which means larger values of gauge factors [1]. Table 3.3 demonstrates an example of this phenomenon, according to CNTs loading percentage and mixing method used, where a decreasing trend in gauge factors is observed with the increase in the MWNTs wt% for both the dry blended and the solution based samples.

Table 3.3: Gauge Factor values for MWNT/PMMA composite films according to MWNTs loading % and processing method [1]

MWNT wt%	1 wt%	3 wt%	5 wt%	6 wt%	8 wt%	10 wt%
Dry blended	N/A	N/A	N/A	8.44	7.45	5.66
Solution based	15.32	4.59	4.26	3.27	1.9	1.44

It is clear from the gauge factor values of the solution mixing method that a great difference lies between the sensitivity of the 1 wt% MWNT and the 10 wt%. This variation in gauge factor values is also observed for the dry mixed powder for the 6, 8 and 10 wt%. However, it must be noted here that for the dry mixed powder results, unavailable gauge factors at low weight percent of MWNTs were observed which was explained by less efficient dispersion, when compared with the solution method, and thus loss in carbon nanotubes network [1].

The theory of higher tunneling resistance or higher ratio of the tunneling resistance to the total resistance leads to higher sensing sensitivity was as well indicated by Hu *et al.* [43] experimentally and numerically.

3.4.2 Conductivity Theorems

The first formal study on the concept of percolation thresholds was conducted by Broadbent and Hammersley in 1957 [44]. Later, a statistical percolation theory was developed to describe the dependence of composite materials conductivity on the filler volume fraction. It is called the percolation theory and is represented as follows:

$$\sigma_{com} = \sigma_0 (\varphi - \varphi_c)^t \qquad \text{for } \varphi > \varphi_c \tag{3.1}$$

Where σ_{com} is the composite conductivity, σ_0 is a parameter that depends on the electrical conductivity of the filler, φ is the filler volume fraction, φ_c is the percolation threshold, and t is the critical exponent that reflects the dimensionality of the composite system [9, 19, 20, 29, 30]. According to Hu *et al.* [29] and Bauhofer *et al.* [20], the critical exponent "t" is a universal value that is expected to have a value of 2 for a 3D system. Likewise, Pham *et al.* [1] used the same equation to deduce a semi-empirical GF model. Experimental investigations carried out by Hu *et al.* [31, 43, 45] on CNT/Polymer nanocomposites have shown same pattern of percolation behavior as the conventional electronic properties presented by the percolation-like power law.

As some work uses weight fractions instead of volume fractions, a relation was suggested based on the type of CNTs used. For SWNT, it was considered that vol% is equal to the wt%, while for MWNT the vol% is regarded as double the wt% independent of the polymer matrix used [20]. It is stated that any resulting inaccuracies are not expected to have any significant effect on the experimental results interpretation.

As for the stepwise change or transition observed in composite conductivity, it is expected to be near the percolation threshold. At this threshold, the formation of a 3D network of interconnected CNTs starts to form that facilitates the movement of electrons by creating a low resistance path thus greatly reducing the overall conductivity of the composite system [9, 35].

3.5 Effect of composite crystallinity on electrical properties

It was reported that the polymer crystallinity have shown to influence the degree of CNTs dispersion [46]. Jeon *et al*. studied [46] the effect of polymer crystallinity using SWNTs with different polymer matrices of homopolymer iPP and polypropylene-ethylene copolymer. They observed that with the decrease in polymer crystallinity, SWNTs became less connected and their morphology changed to be more curly which in turn decreased the composite electrical conductivity. This effect was clearly visible at percolation threshold where a loss in CNTs network would be most felt, but in higher CNTs concentrations the conductivity was less sensitive to polymer crystalline state.

Studies carried out on analyzing the effect of adding CNTs to neat polymer were done using differential scanning calorimetry (DSC) to examine the changes in melting temperature (T_m), crystallization temperature (T_p), and degree of crystallinity (X_c) [46, 47]. No significant change was observed for the melting temperature upon adding CNTs to the pristine polymer. However, the increase in CNTs content caused a reduction in the degree of crystallinity which was reasoned due to the reduction in polymer content [46, 47].

Most research carried out was investigating and examining the CNT/polymer composite electrical conductivity and percolation threshold, but very few concentrated on studying the piezoresistance property of such composites. The gauge factors of studied composite materials did not reach high values as expected, except for few values. Moreover, no focus was given on using simple processing methods and easily fabricated polymeric material.

CHAPTER 4

EXPERIMENTAL PROCEDURE

4.1 Materials

4.1.1 Carbon Nanotubes (CNTs)

Two types of CNTs were purchased from different suppliers. Both of them are Multi-Walled Nanotubes (MWNTs), the main difference lies in their aspect ratio. The CNTs were used as is, no prior treatments took place.

- **Large MWNTs**

Large MWNTs type was purchased from MER Corporation – Arizona, USA [48]. They are produced by Catalytic Chemical Vapor Deposition (CCVD) with 140 (± 30) nm in average diameter and 7 (± 2) micron length giving an aspect ratio around 50, with >90% purity. Figure 4.1 shows SEM image for the Large MWNTs.

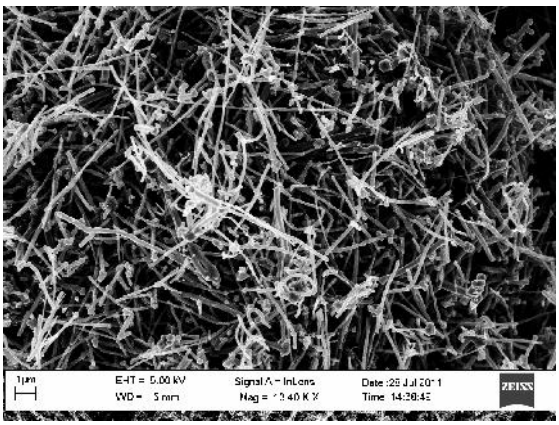

Figure 4.1: SEM photo of Large MWNTs

- **Elicarb MWNTs**

Elicarb MWNTs were supplied by Thomas Swan & Co. Ltd – County Durham, UK [49]. They are produced by Chemical Vapor Deposition (CVD) process. They have an average outer diameter of 10–12 nm, length of tens of microns, aspect ratio of 2000 approximately and purity in the range of 70 - 90%. Figure 4.2 presents SEM for this type of MWNTs.

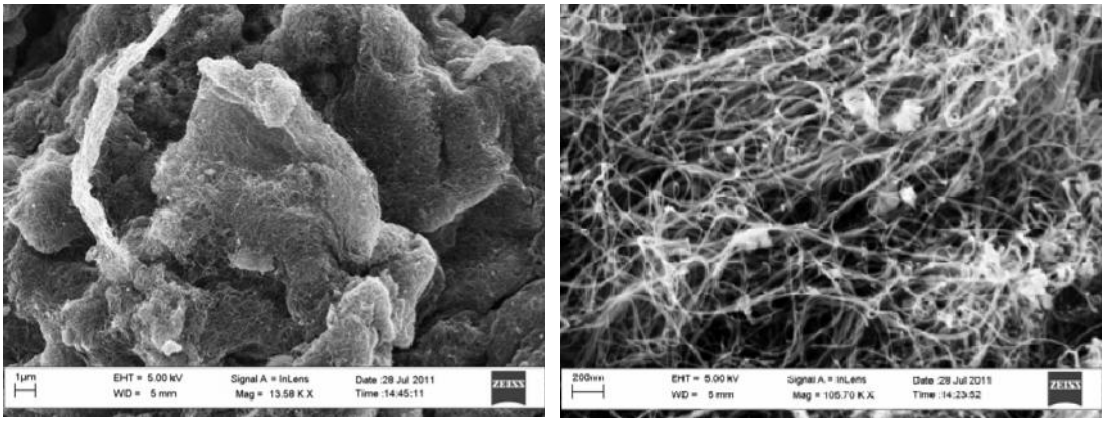

Figure 4.2: SEM photos of Elicarb MWNTs

4.1.2 Low Density Polyethylene (LDPE)

LDPE polymer was supplied by Westlake Chemical Corporation – Texas, USA, in the form of powder with density of 0.923 g/cm^3, and melt index of 2 g/10min.

4.2 Experimental Outline

Figure 4.3 shows the sequence of stages of the experimental procedure.

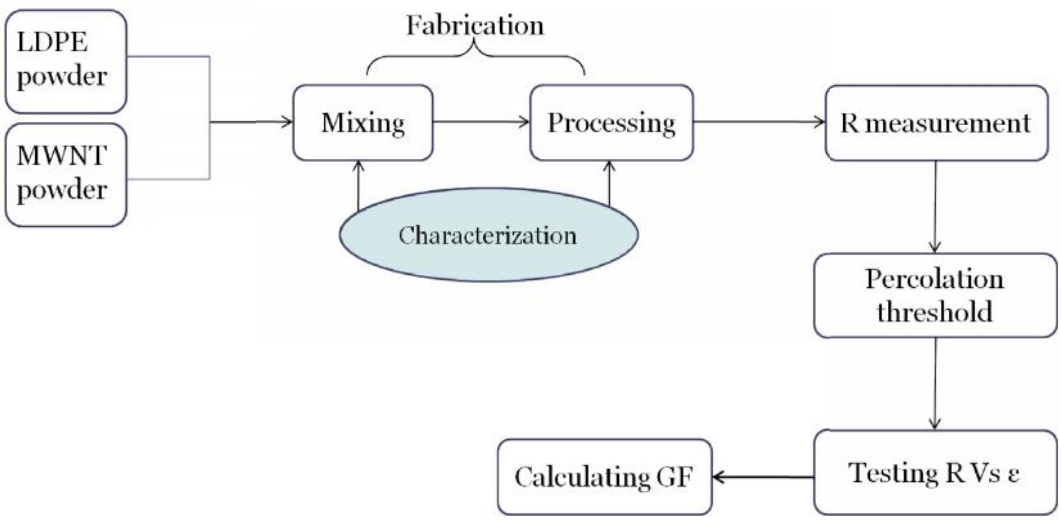

Figure 4.3: Flow diagram representing experimental work carried out

4.3 Fabrication

As presented in Figure 4.3 the fabrication stage consists of two steps, namely mixing and processing. Different methods were tried in each of these steps to produce consistent CNT/LDPE composite films.

4.3.1 Mixing

The mixing step is carried out prior to processing in order to disperse the CNTs within the LDPE polymer matrix. Mechanical solid-state mixing was selected as it is considered an efficient technique to produce novel composites [9]. Two types of mechanical mixing were examined.

- **Low Energy Mixing**

The CNT/LDPE powder mix was agitated in a turbula mixer (Turbula T2F, Switzerland), shown in Figure 4.4, for 2 hours at a speed of 46 rpm [26].

Figure 4.4: Turbula Mixer used

- **High energy mixing**

High energy ball milling (HEBM) technique was also used. The samples were prepared using a Planetary Retsch Ball Mill (PM 400) shown in Figure 4.5. Jars used were 125 mL in size, and powder mass was 25g. A rotational speed of 400 rpm was used with the aid of steel balls of 10mm in diameter. A ball-to-powder ratio of 5:1 was used in order to avoid damage to the CNTs. The mixed powders were examined by the SEM to make sure no nanotubes breakage occurred. The balls helped in disentangling the CNTs agglomerates and forcing the dispersion of CNTs within the polymer particles. Earlier work using ball milling for mixing polymer composites was reported as Gorrasi *et al.* [9] used the ball milling method to mix LLDPE with MWNTs at a speed of 580 rpm with the aid of only 5 steel balls for a period of 45 minutes.

Three time intervals were investigated in order to get the suitable milling time that allows CNTs to disperse within the polymer particles and yet to keep interconnection between CNTs. The milling times inspected were 15, 30 and 60 minutes.

Figure 4.5: Retsch Ball Mill (PM 400 – MA-Type)

4.3.2 Processing

The second step of the fabrication stage is processing in order to produce film specimens. Extrusion and compression molding processing methods were investigated.

- **Extrusion**

Various attempts were carried out in order to obtain the optimal extrusion conditions to be used. One major factor that controlled the produced film thickness is the chill roller speed. Figure 4.6 shows the Randcastle single screw micro-extruder (Randcastle Extrusion Systems Inc.) used. The temperatures of the four zones of the extruder were maintained constant according to the values recommended for pure LDPE polymer. This implies that temperatures of the upper, middle and bottom parts of the barrel, and the die were kept at 177°, 205°, 232°, and 232°C respectively. Two

specimens were produced using this processing technique, each using one of the two mixing methods, which contained 8 wt% Large MWNTs.

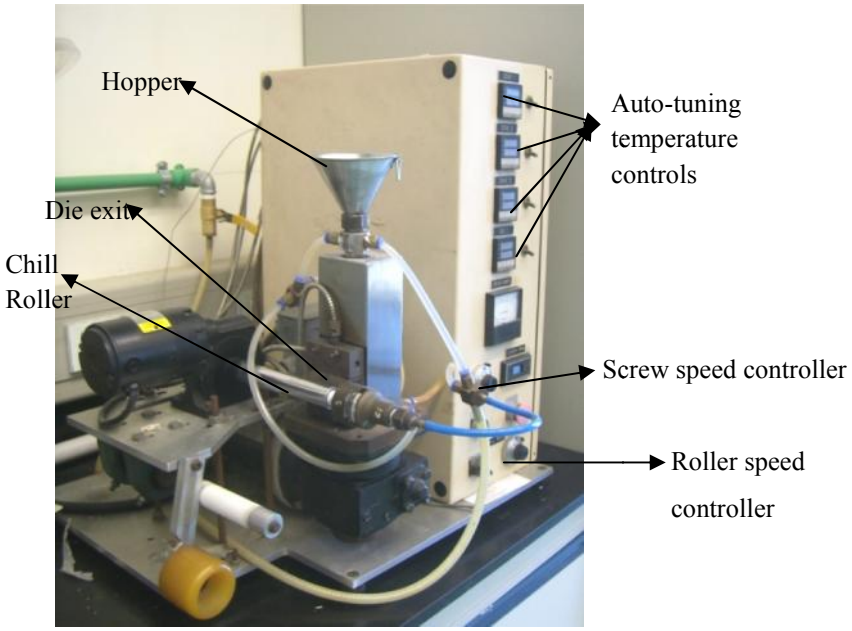

Figure 4.6: Randcastle Micro-extruder

- **Compression Molding**

Figure 4.7 shows the Carver Laboratory Press (Model C) used. Different mold types were used in the compression molding process in order to produce defect-free specimens. First a flash type mold was used which is shown in Figure 4.8. Two flash molds were made, one with 1mm thickness and another with 0.5mm thickness. The molding parameters used for processing using these molds were 180°C at 1.5 tons for 12 min.

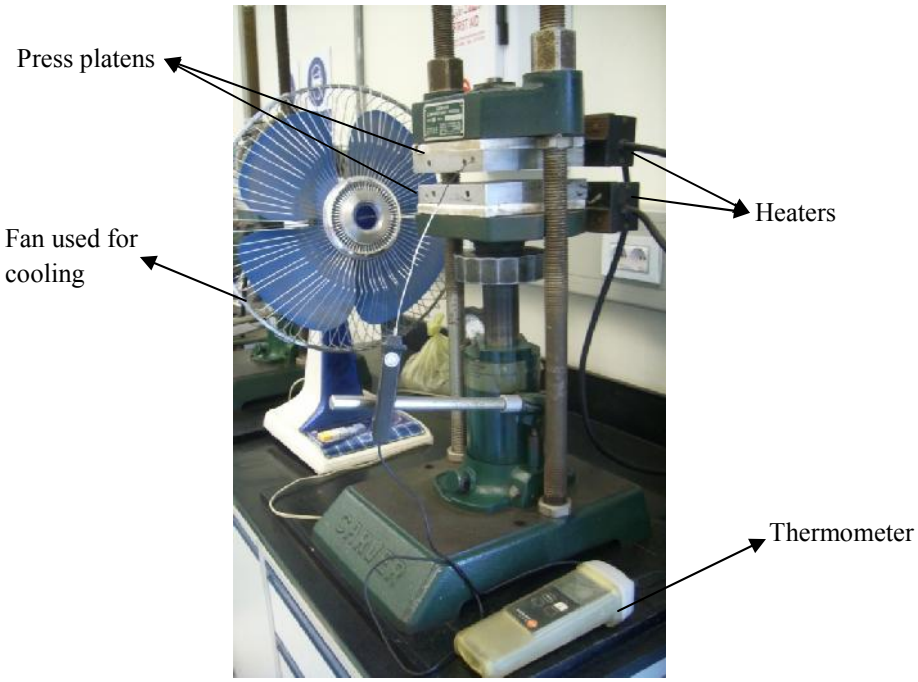

Figure 4.7: Carver Laboratory Press used

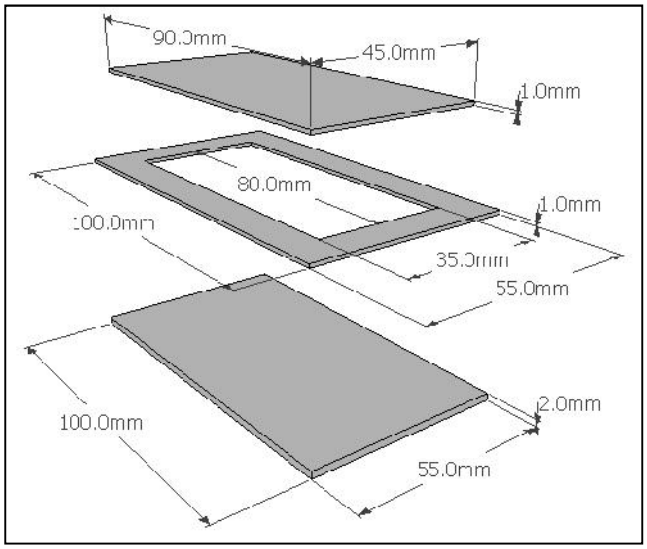

Figure 4.8: Flash type mold

Specimens produced using the two flash type molds contained air pockets so a different type of mold was used, a positive type mold of 0.65mm thickness, presented in Figure 4.9, to improve the quality of specimens. The process parameters were set with the aid of ASTM D4703 [50]. The process was as follows:

- Mixed powder was first degassed, using a vacuum oven (OV-11, JEIO TECH), shown in Figure 4.10, at 80°C for 3 hours to control moisture content

- Powder was preserved in a dessicator until processing started
- Grease is applied on the inner surface of the mold to facilitate specimen removal upon end of processing
- Mold was preheated for 12min at 50°C (±5)
- 15g of mixed powder was added (±0.1)
- Heating took place under constant contact pressure until the molding temperature range is reached
- Molding is carried out at 150°C, 2 tons (±0.1) for 10min
- Forced air was used for cooling applied at a rate of 4°C/min while maintaining pressure till 40°C was reached (this cooling rate was used for all types of molds)

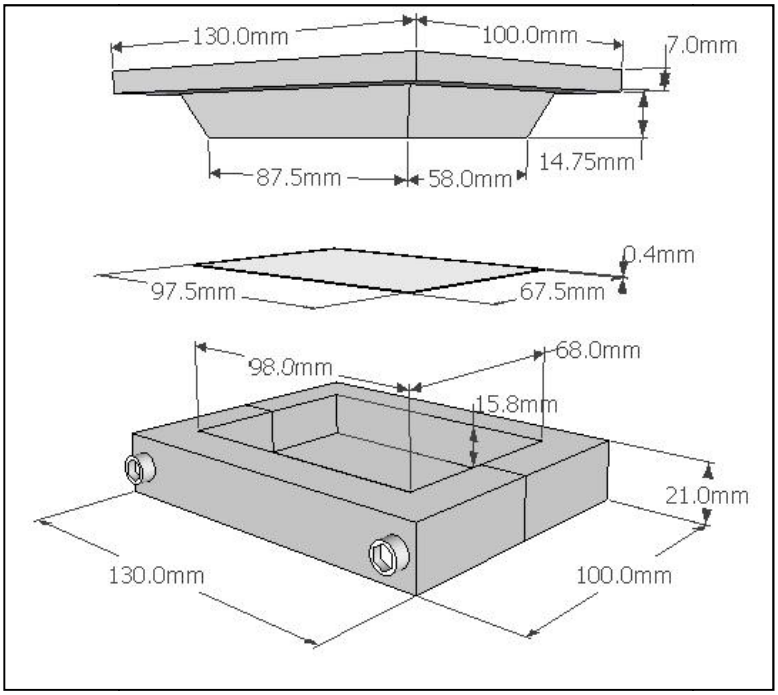

Figure 4.9: Positive type mold

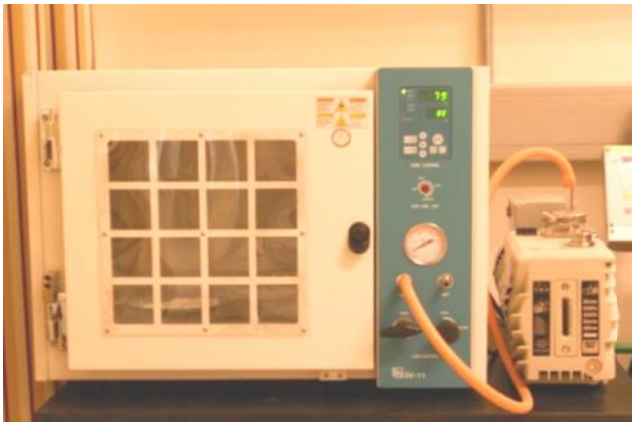

Figure 4.10: Vacuum Oven (OV-11) used for degassing

4.4 Samples preparation

Table 4.1 represents all specimens produced by compression molding.

Table 4.1: Samples produced using compression molding

Mold Type	CNT Type	Mixing type	CNT loadings manufactured
Flash mold (1mm thickness)	Large MWNTs	Ball Milling (as stated in part 4.3.1 above)	0, 1, 2, 3.5, 5, 6.5 & 8 wt%
Flash mold (0.5mm thickness)	Large MWNTs	Ball Milling (as stated in part 4.3.1 above)	0, 1, 2, 3.5, 5, 6.5 & 8 wt%
Positive mold	Large MWNTs	Ball Milling (as stated in part 4.3.1 above)	0, 1, 2, 3.5, 5, 6.5 & 8 wt%
	Elicarb MWNTs	Ball Milling (as stated in part 4.3.1 above)	0, 1, 2, 3.5, 5, 6.5 & 8 wt%

4.4.1 Conditioning prior to testing

ASTM D618 standard [51] was utilized in order to condition specimens manufactured by compression molding, using the positive type mold, prior to testing. Specimens were preconditioned by polishing the surface with sand paper and cleaning it with ethanol to remove any residues on the surface. Then samples were placed on the mesh for 48 hours to adapt to the laboratory environment (23°C (±2), 50% RH) as illustrated in Figure 4.11.

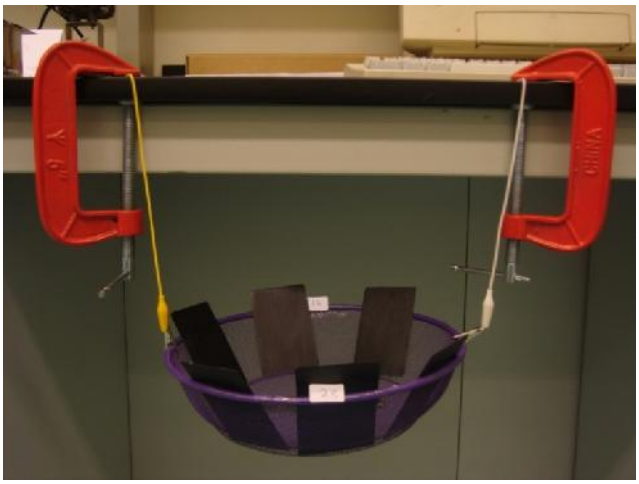

Figure 4.11: Preconditioning samples in the laboratory subsequent to processing

4.4.2 Electrodes painting

Different types of electrodes were examined:

- Aluminum foil with silver paint to adhere it to the sample surface
- Copper sheet with silver paint to adhere it to the sample surface
- Silver paint

For extrusion specimens, one specimen was taken from each produced film sample and adhered to a glass slide for easier handling, and three electrodes were developed on its surface using aluminum foil with the aid of Ag paint as illustrated in Figure 4.12.

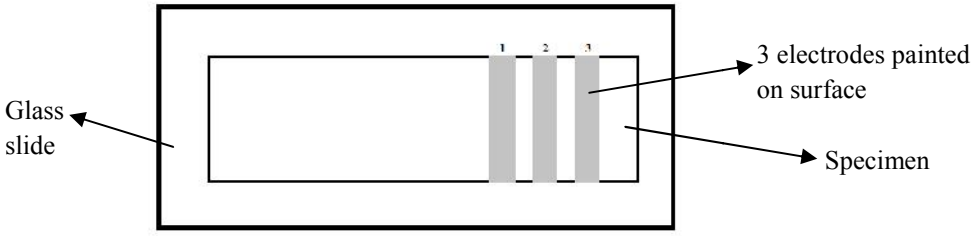

Figure 4.12: Electrodes configuration for extrusion specimen

As for the compression molding samples, after preconditioning took place, three specimens were cut from each produced film sample as described in Figure 4.13. The three specimens of each sample were then adhered on a glass slide using double-faced adhesive tape. Subsequently, silver paint was used to develop two electrodes on the film surface in order to guarantee good electrical conductivity between the film surface and the measurement device. The resistance of the coated electrodes varied between 0 and 60Ω, indicating that contact resistance effect is insignificant relative to the tested specimen films resistance as it usually ranges on the megaohm scale. Figure 4.14, and Figure 4.15 demonstrate specimen adhesion on glass slide after preparation took place, while table 4.2 lists the samples dimensions according to the mold type used.

Table 4.2: Specimens dimensions prepared for electrical resistance measurements

Mold type	Specimens size	Distance between electrodes (mm)	Conditioning
Flash mold	25mm x 7mm	1.5 (±0.5)	N/A
Positive type mold	35mm x 5.5mm	4 (±0.5)	24 hours in laboratory environment (23°C (±2), 50% RH)

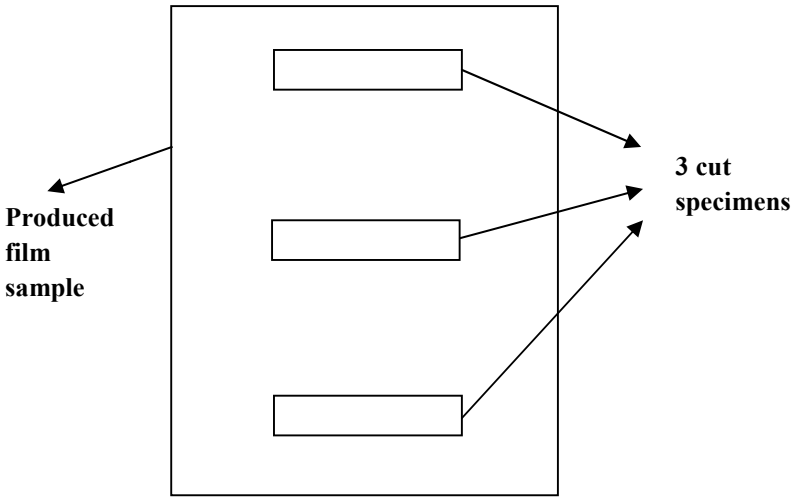

Figure 4.13: Schematic diagram showing the three specimens taken from film sample produced by compression molding

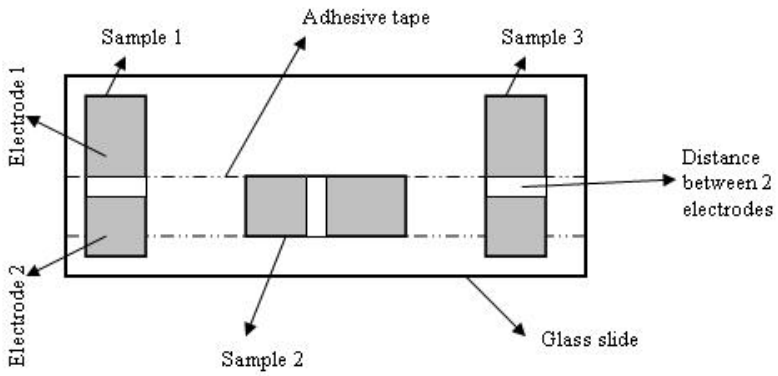

Figure 4.14: Schematic diagram showing compression molding specimens adhered to glass slide after preparation is carried out

Figure 4.15: Specimens produced by flash type mold adhered to glass slide

4.5 Resistance Measurement

Two types of instruments were used to measure resistance according to the range value of the sample macroscopic resistance. Electrical resistance (R) was measured by a digital multi-meter (HP 34401A) for resistance values less than 10^8 Ω

and a high resistance meter (HP-4329A) for greater values, both using two-point probe method as shown in Figure 4.16. Three specimens from each composite sample were tested and an average value was recorded. The value of resistance was recorded after a period of 60 seconds, which is known as the time of electrification, to leave time for the reading to settle.

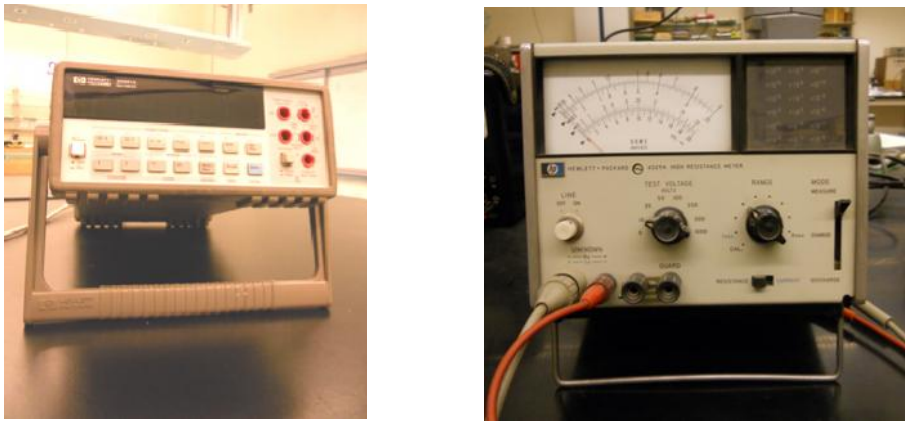

Figure 4.16: Electrical resistance measurement devices used. Left: HP 34401A multimeter; Right: HP-4329A high resistance meter

4.6 Testing setups

4.6.1 Cantilever setup

CNT/LDPE specimens were adhered on the surface of a steel beam of 0.4mm thickness, using steel epoxy adhesive. A unidirectional strain gauge was also adhered on the opposite surface measuring the applied strain using strain-meter (KYOWA type PCD-300A) as strain is assumed to be identical for the composite strain sensor and the strain gauge as both are located at the same place. The cantilever beam setup was used for its simplicity in testing the strain sensor response. A similar approach was used by Kang *et al.* [6]. The testing setup is presented in Figure 4.18 and Figure

4.17 where one end of the beam is fixed to the table using a C-clamp and the other end, the free end, is used to apply the load by attaching a loading box hanging by a string and adding masses of 10, 30, 50, and 100g.

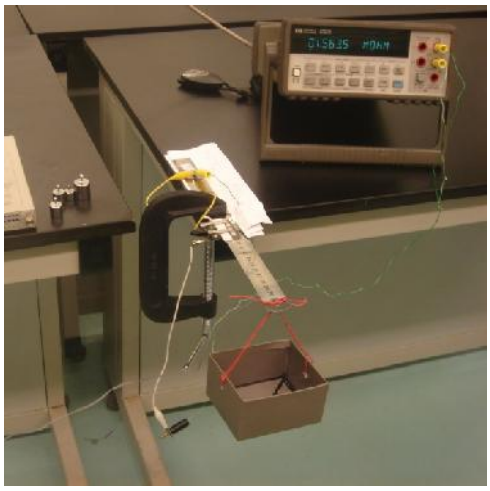

Figure 4.17: Photo of the cantilever setup with the loading box hanging from the free end of the steel beam

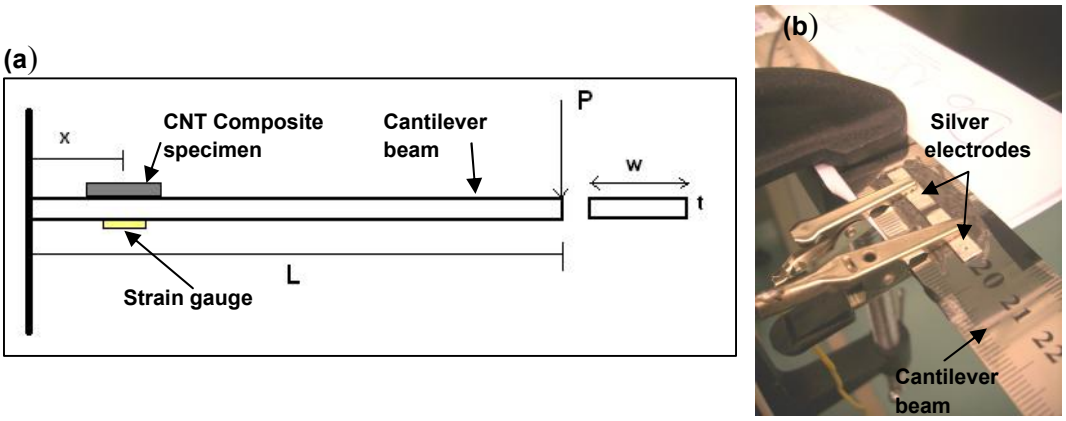

Figure 4.18: Cantilever testing set-up: (a) Diagram describing composite specimen and strain gauge positions and loading (P) direction; (b) Photo of the steel beam with the adhered specimen shown with Ag electrodes painted on its surface

4.6.2 Tensile testing setup

Due to the limitations on the maximum applied load when using cantilever setup as a result of the small thickness of the steel beam, another testing setup was tried. Standard tension aluminum specimens of 0.65mm thickness, shown in Figure

4.19, were gripped in Universal Testing Machine (Instron - Model 3382) after adhering the composite specimen on one face of the aluminum sheet in the middle of the gauge length and the strain gauge on the opposite face. Tension test was applied at a speed of 0.25 mm/min up to a strain value of 5000 με. Figure 4.20 demonstrates the setup used.

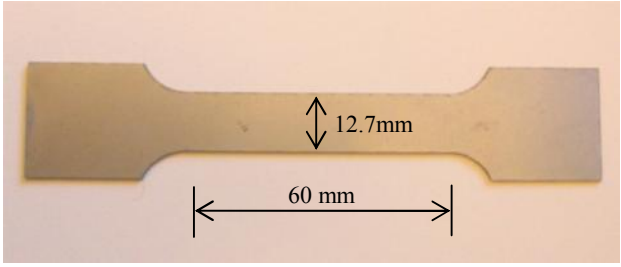

Figure 4.19: Aluminum tension specimen

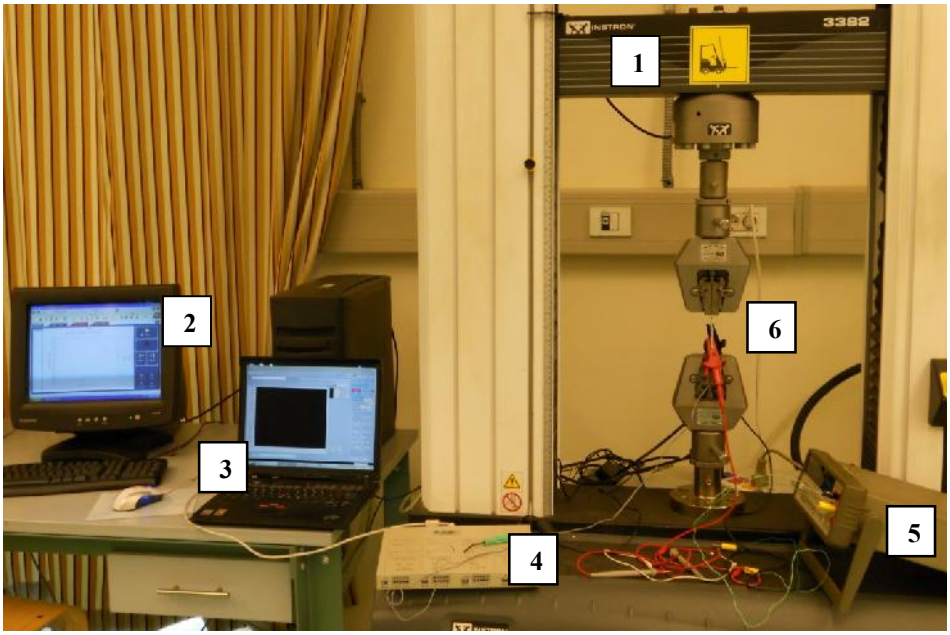

1. Instron Machine
2. Instron controller
3. Computer
4. Strain-meter attached to computer
5. Multimeter
6. Specimen gripped in machine with probes attached

Figure 4.20: Tension testing setup carried out using Instron Machine

4.7 Characterization

4.7.1 DSC

MWNTs/LDPE powder samples as well as LDPE pure polymer powder were analyzed using Perkin-Elmer Differential Scanning Calorimetry (DSC) in order to

examine the melting temperature and degree of crystallization of the composite after the addition of CNTs. Each sample was 7.2 mg (±0.1) encapsulated in an aluminum pan. Temperature range examined from 20 to 150 ºC with a heat flow rate of 10 ºC/min. Samples were first heated until 150 ºC, held at that temperature for 5 min to eliminate any previous thermal history, and then cooled to 20 ºC. Samples were kept at 20 ºC for 1 min and then heating took place again to 150 ºC. Figure 4.21 shows the DSC equipment used.

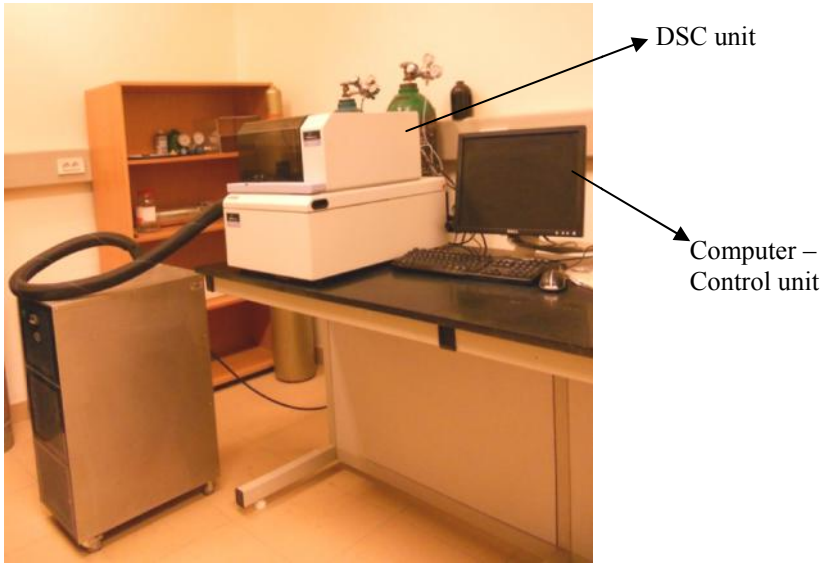

Figure 4.21: diamond DSC - PerkinElmer Inc.

4.7.2 SEM

CNT/LDPE powder samples and film samples were examined using Scanning Electron Microscope (SEM, Leo Supra 55 – Zeiss Inc., Germany) shown in Figure 4.22. Film samples were chilled using liquid nitrogen in order to promote a brittle failure. SEM photos were used to analyze the dispersion of CNTs within the polymer matrix.

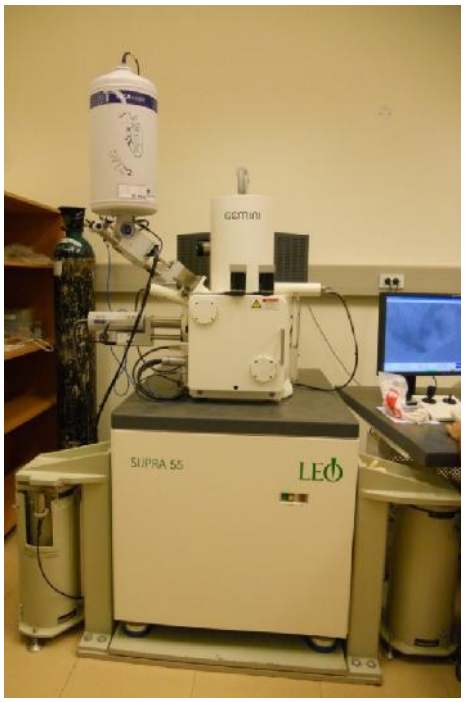

Figure 4.22: SEM (Supra 55, LEO – Zeiss Inc.) used for characterization

CHAPTER 5

RESULTS and DISCUSSION

As stated earlier, several trials were carried out in order to obtain a composite film sample with a good state of CNTs dispersion and electrical properties suitable for strain testing. Hence, different factors were investigated to understand the effect of each on the produced film samples. Herein, the results are divided into sections in which the testing details of each are reported. These main factors are the mixing method, the processing technique, and the effect of CNTs addition on LDPE crystallinity.

5.1 Solid-State Mixing Method

Mixing of CNTs with LDPE powder took place prior to processing in order to disperse CNTs within the LDPE particles. Two solid-state mechanical mixing methods were tried, namely turbula mixing and ball milling. The turbula mixing was carried out at a speed of 46 rpm for 2 hours [26], while the ball milling took place at 400 rpm for 1 hour with the aid of steel balls with BPR of 5:1.

Samples with 8 wt% Large MWNTs were prepared using both techniques and examined using FESEM. 8 wt% samples were selected to compare the two techniques because achieving good dispersion at such a high wt% is not easy. Figure 5.1 and Figure 5.2 show the extent of CNTs dispersion within the LDPE matrix for the turbula mixed and the ball milled powders respectively. Figure 5.3 shows the ball milled powder at higher magnification. It can be seen that the low energy mixing, using the

turbula mixer, was not able to properly mix the powders together. CNTs were not disentangled as agglomerations were observed everywhere throughout the sample, while the high energy mixing, using the ball mill, showed good dispersion of the CNTs within the LDPE particles. The ball milled powder sample showed no sign of CNTs clustering which indicates that CNTs were dispersed throughout the LDPE particles.

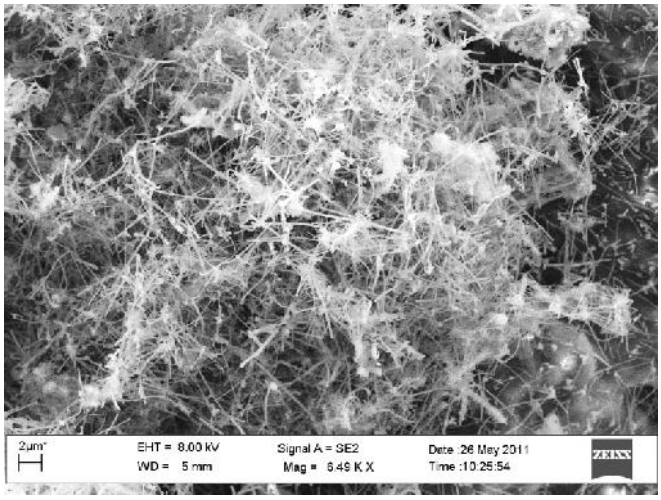

Figure 5.1: Powder sample of 8 wt% Large-tubes MWNTs mixed with LDPE by turbula mixer showing several interconnected clusters of MWNTs

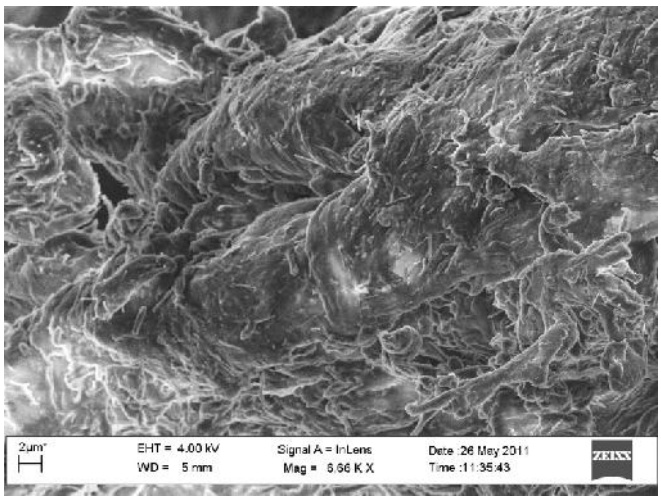

Figure 5.2: Powder sample of 8 wt% Large MWNTs mixed with LDPE by ball mill with no sign of MWNTs agglomerates present

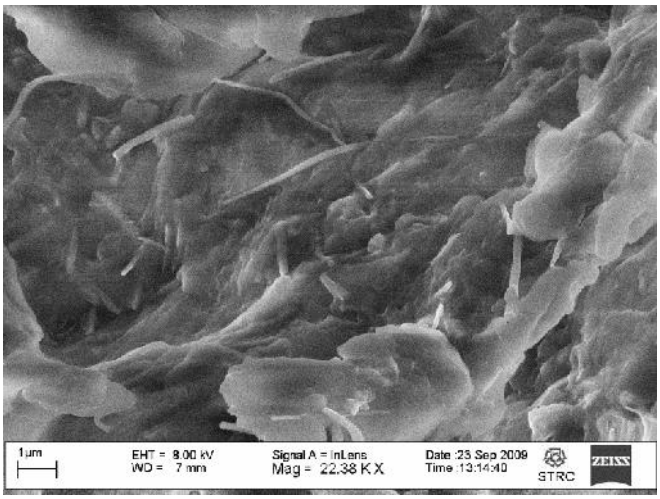

Figure 5.3: Powder sample of 8 wt% Large MWNTs mixed with LDPE by ball mill with no sign of MWNTs agglomerates present (same as in Figure 5.2 at higher magnification)

5.2 Processing Technique

5.2.1 Initial Investigations

Initial MWNT/LDPE composite film specimens were produced by the extrusion process using a single screw micro-extruder. The turbula mixed powders were used in the first processing attempts. The advantage of using extrusion is that the induced shear mixing caused by the screw rotation helps in disentangling the CNTs and in dispersing them within the LDPE matrix hence enhances the mixing.

A trial specimen containing 0.99 wt% Large-tubes MWNT was produced. This initial specimen gave a high electrical resistance value (above 10^{11} Ω) which makes it difficult to use in any further characterization or testing. For this reason, the samples with 8 wt% Large MWNTs were processed to check the effectiveness of the processing method in producing electrically conductive composite films.

5.2.1.1 Extrusion Screw Speed

After various extrusion iterations, the chill roller speed was set at 16 rpm as a continuous film with a smooth surface is obtained with proper thickness. Several trials were carried out at this speed using different screw speeds to obtain a suitable film thickness while maintaining consistent film morphology. Only three screw speeds gave consistently good film specimens with homogenous surfaces. The three screw speeds examined are 73, 107, and 133 rpm. Specimens were cut from each of these three films and their electrical resistances were measured. Specimens electrical resistivity (ρ), measured in Ωcm, was calculated based on resistance measurements using the following equation:

$$\rho = R*A / L \qquad \textbf{(5.1)}$$

Where R is the measured resistance (Ω), A is the specimen cross-sectional area (mm^2), and L is the distance between the 2 electrodes (cm). In Table 5.1 the obtained results are presented.

Table 5.1: Resistance Measurements for Extrusion specimens

Specimen	Screw Speed (rpm)	Thickness (μm)	Resistance (Ω)	Resistivity - ρ (Ωcm)
8wt% MWNTs (turbula mixed)	73	108	3.5×10^{10}	7.42×10^{8}
8 wt% MWNTs (turbula mixed)	107	95	1.5×10^{11}	4.83×10^{9}
8wt% MWNTs (turbula mixed)	133	55	N/A	N/A

As seen in Table 5.1 the electrical resistance of the film processed at a screw speed of 133 rpm could not be obtained due to the difficulty in handling this fine thickness. The film is so delicate that it was hard to paint electrodes on its surface. Samples were further examined by SEM to observe the dispersion of CNTs within the polymer matrix. Samples were fractured after immersing them for 1 minute in liquid Nitrogen. Figure 5.4 to Figure 5.6 show the cross-section of the samples produced at screw speeds of 73, 107, and 133 rpm respectively.

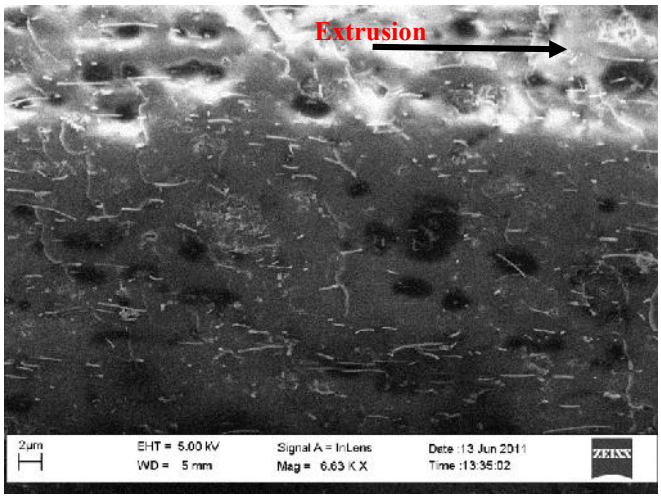

Figure 5.4: Cryo-fractured cross-section of 8 wt% Large-tubes MWNT/LDPE extruded film at screw speed of 73 rpm; photo taken parallel to extrudate film direction

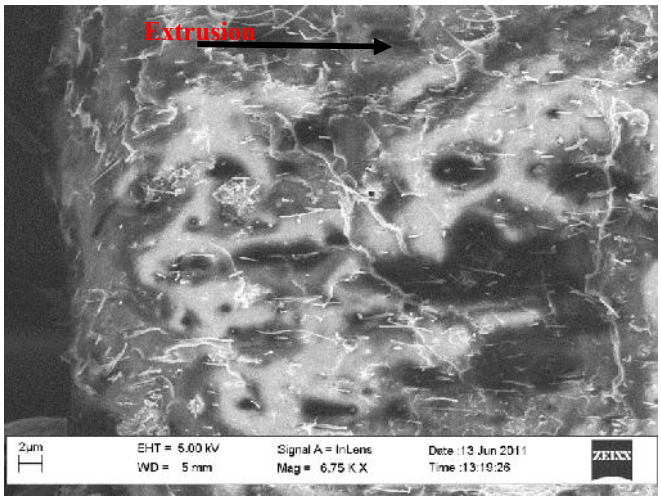

Figure 5.5: Cryo-fractured cross-section of 8 wt% Large-tubes MWNT/LDPE extruded film at screw speed of 107 rpm; photo taken parallel to extrudate film direction

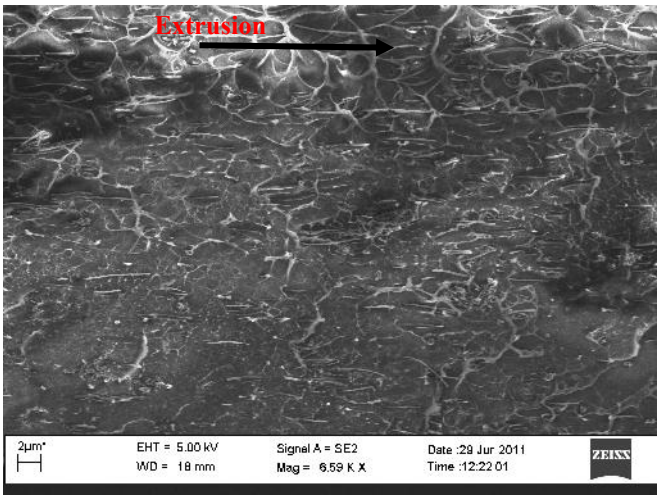

Figure 5.6: Cryo-fractured cross-section of 8 wt% Large-tubes MWNT/LDPE extruded film at screw speed of 133 rpm; photo taken parallel to extrudate film direction

Not much difference in MWNTs dispersion within the LDPE matrix was found between the samples processed at the three screw speeds used. From the electrical resistivity measurements, the film with the lowest screw speed of 73 rpm showed a lower resistivity value of one order of magnitude than the one with screw speed of 107 rpm, while that of the screw speed of 133 rpm was hard to obtain. This variation in resistivity values is mainly attributed to the change in film thickness. Concerning the film surface, the film with the highest screw speed of 133 rpm showed the best consistency, in terms of surface smoothness, followed by the screw speed of 107 rpm then that of the 73 rpm. Thus the screw speed of 107 rpm was selected as it gives the best combination for film thickness, film consistency, and ease of handling.

From the extrusion results obtained so far, it was seen that though the shear mixing induced by the extruder screw helped in dispersing the CNTs throughout the polymer matrix, the electrical resistivity values were too high relative to the large amount of CNTs (8 wt%) added. One of the possible reasons for the low film conductivity is the alignment of the CNTs induced by the geometry of the extruder die causing a reduction in the number of entanglements [4].

5.2.1.2 Mixing Method Effect

After setting the screw speed of the extrusion process, another factor was investigated which is the effect of mixing technique on the produced film specimens. Mixed powders using turbula mixing and ball milling were produced by the extrusion process using the same conditions. Table 5.2 presents the electrical resistivity values obtained for each case. It can be observed that the specimen mixed by ball milling was found to be one order of magnitude lower in resistivity than that of the turbula mixed one which might be a cause of the change in film thickness.

Table 5.2: Electrical resistivity measurements for the two mixing techniques

Specimen label	Mixing Method	Film thickness (µm)	Resistivity – ρ (Ωcm)
8 wt% Turbula	Turbula mixer	95	4.83×10^{9}
8 wt% HEBM	Ball Mill	126	5.52×10^{8}

Figure 5.7 and Figure 5.8 show SEM images of film cross-sections of extruded samples prepared using ball mill mixing and turbula mixing respectively. In Figure 5.7 no clusters of MWNTs were observed, while in Figure 5.8 some MWNTs clustering were observed. This implies that inspite of the shear mixing effect promoted by the extruder, the turbula mixed powders still showed CNTs clusters in the final film specimen. Hence, it is concluded that the ball mill is more effective than the turbula mixing in dispersing the CNTs throughout the LDPE polymer matrix. This observation is in agreement with the work by Esawi *et al.* [26] where it was indicated

that in the case of a single screw extruder the effect of mixing method prior to processing is more influencing than the effect of extrusion shear mixing on CNTs dispersion.

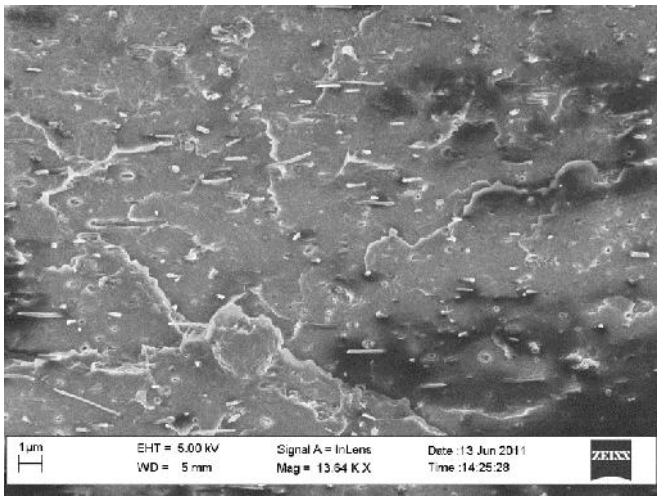

Figure 5.7: Cryo-fractured cross-section of 8wt% Large-tubes MWNT/LDPE, mixed by ball milling, extruded film

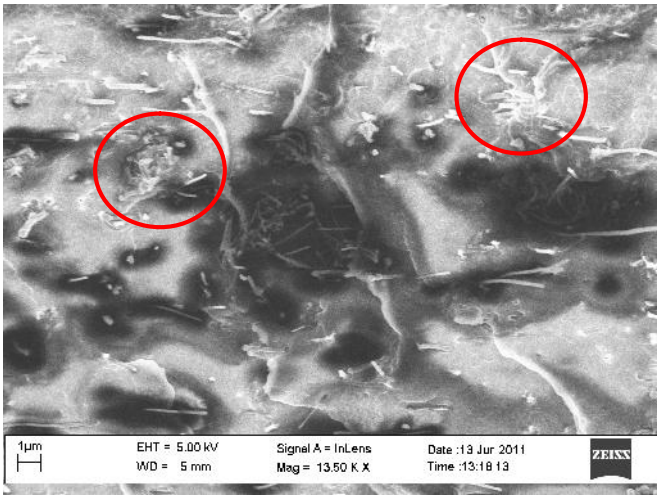

Figure 5.8: Cryo-fractured cross-section of 8wt% Large-tubes MWNT/LDPE, mixed by turbula mixer, extruded film

It was seen during purging runs carried out after each cycle to clean the die that some of the CNTs were still remaining in the extruder indicating that an amount of the CNTs was actually wasted. Moreover, there is a variation in the film thickness that could not be controlled. Also, the fine thickness of the films makes them difficult to handle and in addition it is not possible to obtain a thicker thickness without having

a higher variation in the film thickness. For these reasons, an alternative simpler process was selected for the processing of the CNT/LDPE composite powder which is compression molding to ensure thickness consistency across all prepared specimens as well as minimize CNTs waste.

5.3 Compression Molding Using Flash Type Mold

5.3.1 Ball Milling Mixing Time Factor

For the reasons explained in section 5.2.1.2 above, ball milling was the mixing method selected. However, in the case studied of ball milling powder for 60 minutes, CNTs got disentangled to the extent that a numerous free standing CNTs could be detected which could cause the loss of the CNTs conductive network. This observation was also made by Hu *et al.* [29] who argued that prolonged mixing times lead to overcoming the van der Waals forces between CNTs thus breaking the small CNTs aggregates which in turn reduces the network formation on the macro scale. Yet, it is essential to have a certain level of mixing in order to overcome CNTs bundling.

Accordingly, the mixing time was studied to see its effect on the CNTs dispersion especially that the elimination of the shear mixing step in extrusion could affect the final dispersion of the CNTs in the specimens. The mixing speed and BPR were kept constant at 400 rpm and 5:1 respectively. Three time intervals were examined: 15 min, 30 min, and 60 min. All powders comprised 8 wt% Large-tubes MWNT. Figure 5.9, Figure 5.10, and Figure 5.11 show the dispersion of the CNTs in the LDPE matrix for the 15 min, 30 min, and 60 min intervals respectively. The 15 min mixing interval showed high presence of CNTs agglomerations, which indicates

that the time selected was not sufficient to disentangle the CNTs and well disperse them within the LDPE matrix. As for the 30 min interval, agglomerations were still present but their amount decreased to a great extent than the 15 min interval. At the 60 min interval, no sign of agglomerations was seen and free-standing individual CNTs were observed. This implies that the conductivity of the CNTs network would be reduced to a great extent as distance between neighboring CNTs is wide enough to prevent electron hopping mechanism as noted earlier. Accordingly, the mixing time interval was set to be 30min as it showed the best dispersion out of the 3 cases.

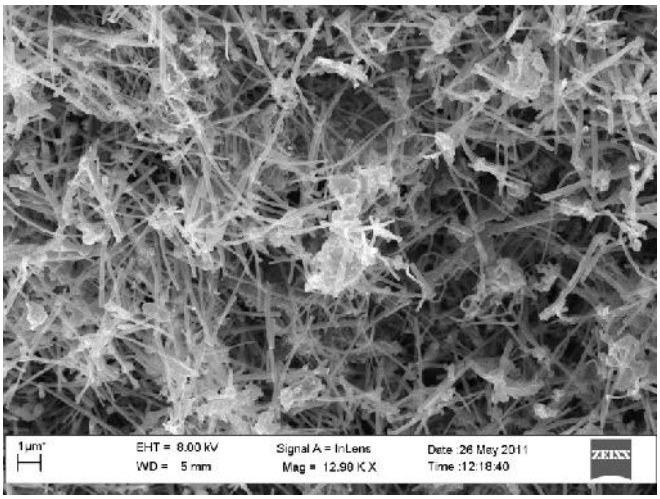

Figure 5.9: powder sample of 8 wt% Large-tubes MWNT/LDPE mixed for 15min by ball milling with heavy presence of CNTs agglomerates

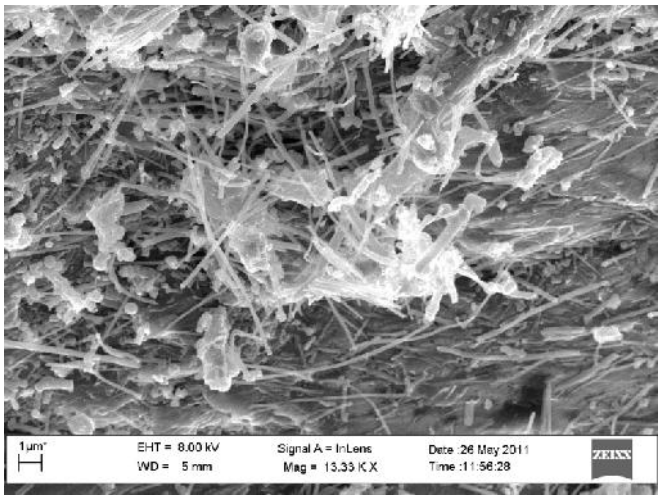

Figure 5.10: powder sample of 8 wt% Large-tubes MWNT/LDPE mixed for 30min by ball milling with MWNTs agglomerates interconnected with polymer particles

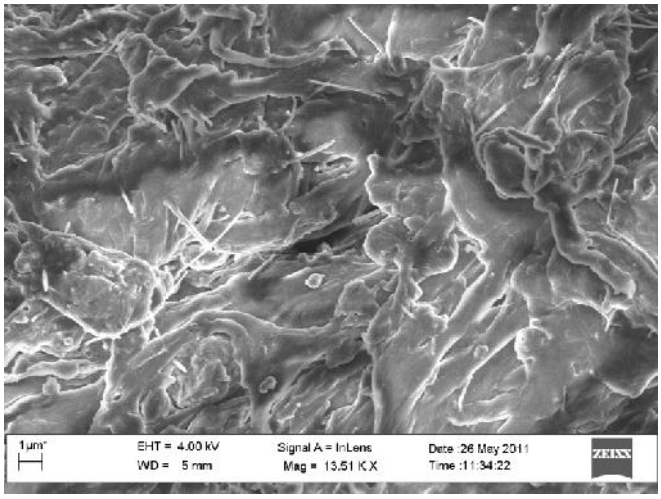

Figure 5.11: powder sample of 8 wt% Large-tubes MWNT/LDPE mixed for 60min by ball milling few scattered free-standing MWNTs present within the polymer matrix with no sign of networking

5.3.1.1 Effect of Mixing Time on Resistivity Measurements

In order to validate the findings of the SEM examinations, the powders comprising 8 wt% Large-tubes MWNT, mixed at 15, 30, and 60 min mixing intervals, were used to produce film samples for electrical conductivity measurements. The samples were processed using compression molding with a flash type mold. The produced samples had a thickness of 1mm. Figure 5.12 shows the average electrical

resistivity value at each time interval with the error bars showing the variability for the three specimens taken from each sample.

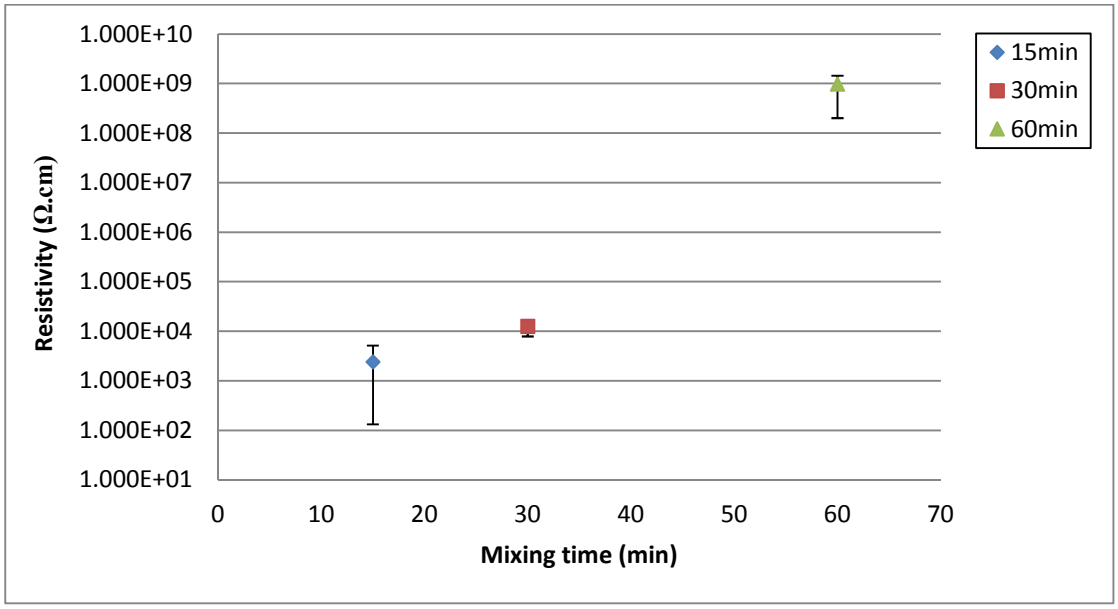

Figure 5.12: Electrical Resistivity measurements for the 15, 30, and 60min mixing intervals

By comparing the 15min and 30min samples, it can be observed that a small difference exists. However, the variability of the electrical resistance measurements for the 15min specimen is large confirming poor dispersion of the CNTs within the polymer matrix. In addition, the severe clustering observed by SEM for the 15min mixed samples is expected to adversely affect the electrical properties of the produced composite film. As for the 30min specimen, a very small variation is noticed which is considered as an acceptable tolerance level for experimentally obtained results. The 60min specimen showed a high resistivity value almost double the value of the 30min specimen, which is reasoned by the loss of the CNTs conductive network throughout the polymer matrix. These results are in accordance with the SEM analysis that showed best mixing time at 30 minutes.

5.3.2 Effect of Film Thickness on Percolation Threshold (Φ_c)

Two sets of samples were produced by compression molding using the same flash type mold. From each sample, three specimens were prepared to be used in measurements in order to obtain an average value for the electrical properties. Each set comprised varying amounts of Large MWNTs of 0, 1, 2, 3.5, 5, 6.5, and 8 wt%. The first set was processed with a 1 mm thickness mold to ensure easy handling of specimens. However, due to this large thickness the specimens did not show good flexibility so a second set was produced using a mold of 0.5 mm thickness.

For the two sets of samples, the 1mm and 0.5mm thickness, it was observed in SEM analysis that the samples contained air bubbles indicating a problem in the processing parameters used. This was observed in all samples where the size of the air bubbles differed from one sample to another. This indicates that the powder mass added was not adequate to ensure proper compaction of the powder. Figure 5.13 shows an example of the air bubbles detected in 8 wt% MWNT samples of 1mm thickness which is similar to what was observed in other samples as well. However, the produced samples showed good electrical conductivity and strain sensitivity as subsequently demonstrated.

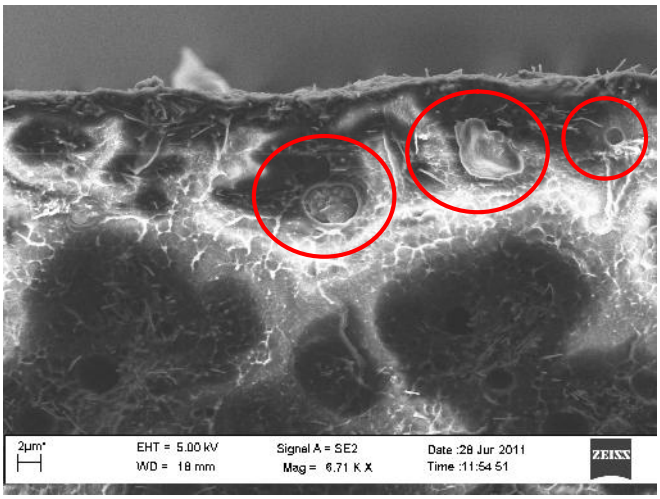

Figure 5.13: Cryo-fractured cross-section of 8wt% Large MWNTs film of 1mm thickness

5.3.2.1 Set of 1mm Thickness Film Samples

The three specimens taken from each film sample were cut to size 25 x 6.5 mm followed by painting silver electrodes on their surface to ensure good electrical contact between film specimen and device probes. Electrical resistance at no load condition was measured after leaving one minute for electrification time. A large reduction in electrical resistivity values upon increasing the CNTs wt% was seen for this set of 1mm thickness as in Figure 5.14. The highest reduction in resistivity was observed in the range of 3.5 to 6.5 wt% which denotes the percolation threshold range. The 5 wt% specimen was then considered as the percolation threshold value. Figure 5.15 shows the equivalent conductivity values for the same set.

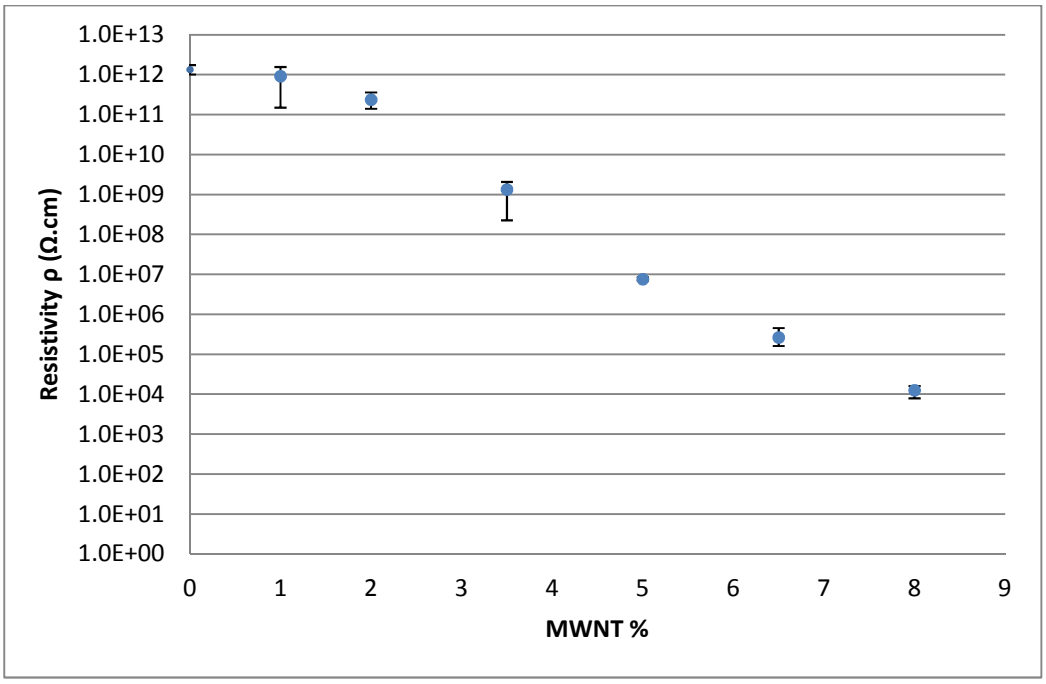

Figure 5.14: Electrical resistivity versus Large-tubes MWNT wt% for 1mm film thickness set

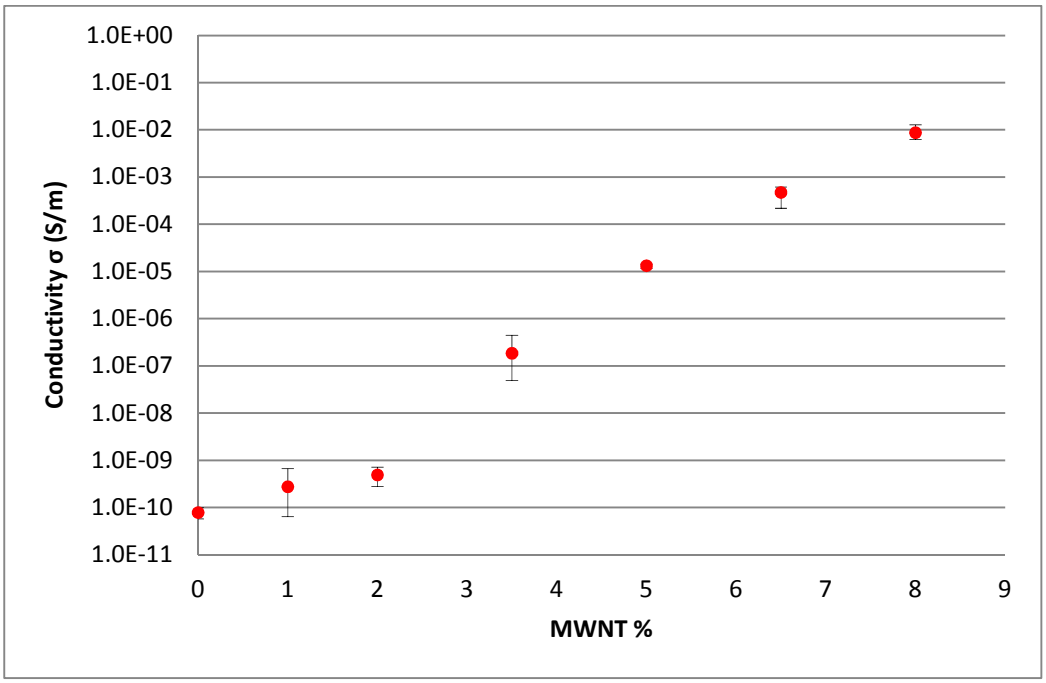

Figure 5.15: Electrical conductivity versus Large-tubes MWNT wt% for 1mm thickness set

5.3.2.2 Set of 0.5mm Thickness Film Samples

The specimen size of this set was changed to 35 x 5 mm in order to obtain larger surface area for better silver electrodes painting. One minute was again left before electrical resistance was recorded. It is noticed that electrical resistivity values increased when compared with the 1mm thickness set as demonstrated in Figure 5.16 and Figure 5.17.

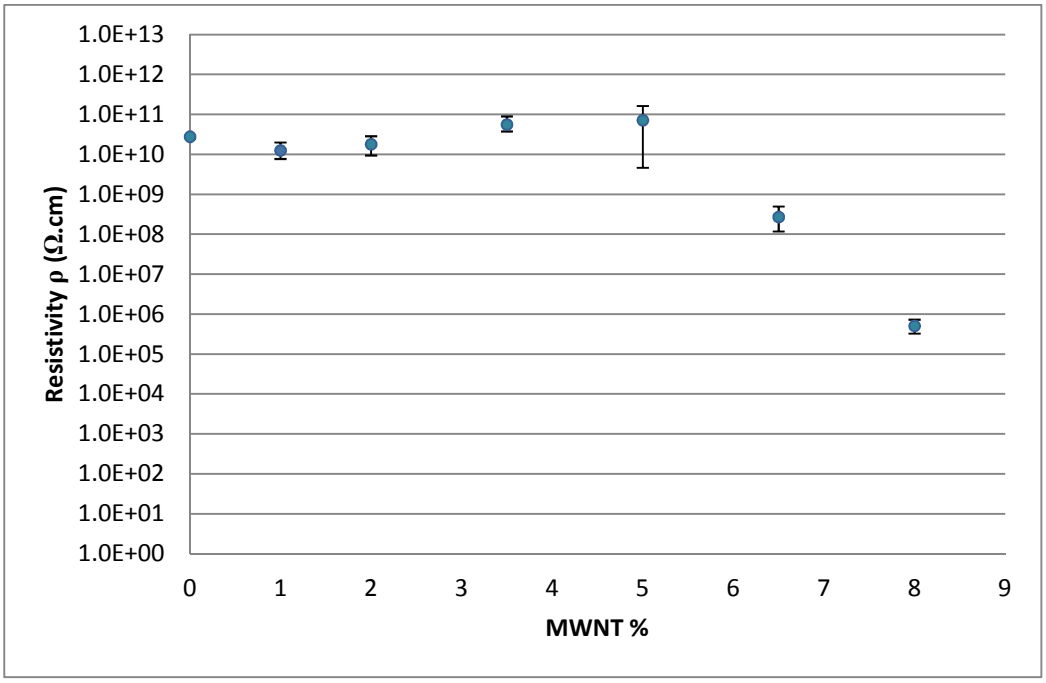

Figure 5.16: Electrical resistivity versus Large-tubes MWNT wt% for 0.5mm film thickness set

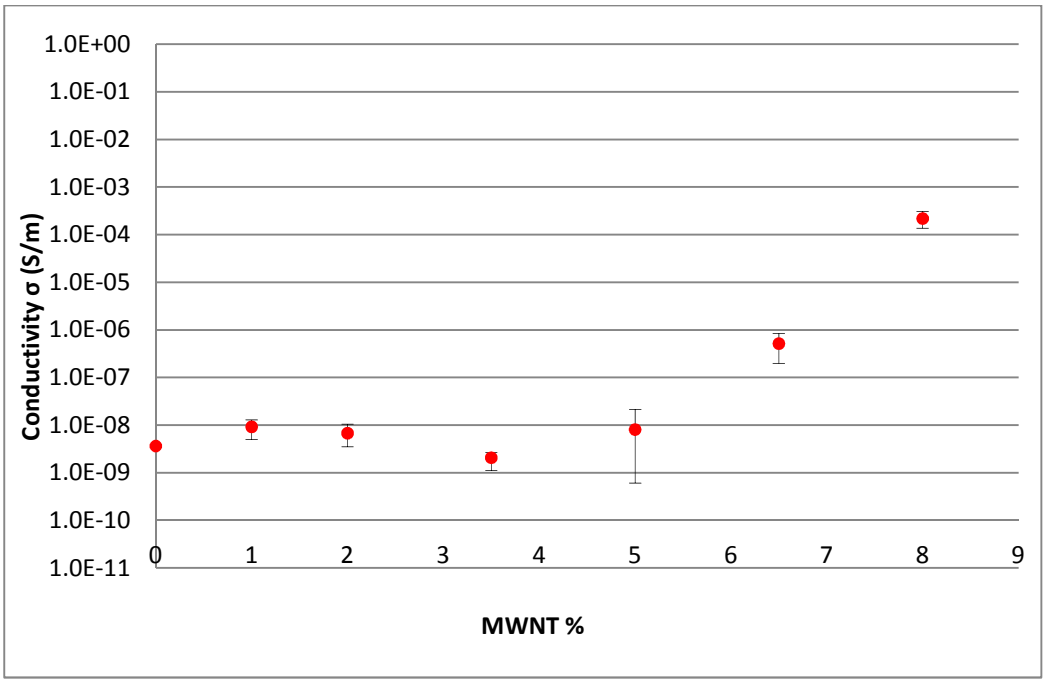

Figure 5.17: Electrical conductivity versus Large-tubes MWNT wt% for 0.5mm thickness set

An investigation was carried out as to make sure that the difference in results between the 1mm & 0.5mm thickness sets was not caused by the change of specimen size. The investigation was done to study the effect of geometric effect of length and width on the specimen resistivity. Six specimens were taken from the 8 wt% sample of 0.5mm thickness. Three of these specimens were cut into (35 x 5 mm), while the other three specimens were cut into (25 x 6.5 mm). As shown in Table 5.3 the specimen dimensions did not have a significant effect on the resistivity values as both values had the same order of magnitude.

Table 5.3: Comparison of specimens different dimensions

Specimen Dimensions ratio	Average Resistance (Ω)	Average Resistivity (Ωcm)
7 (35 x 5) mm	(1.5 – 4) x 10^6	5.07 x 10^5
3.85 (25 x 6.5) mm	(1.3 – 3.22) x 10^6	7.26 x 10^5

One probable reason for this increase in electrical resistivity values when reducing the film thickness is that the decrease in thickness impeded the flow of electrons as the space available for them to move got reduced. The highest reduction in resistivity was observed in the range of 5 to 8 wt% which denotes the percolation threshold range. The 6.5 wt% specimen is hence taken as the percolation threshold value for the 0.5mm thick samples.

5.3.2.3 Resistance Decay

A phenomenon was reported in the literature which is the tendency of the electrical resistance, at no load condition, to decay with respect to time [1, 2, 38]. Loh *et al.* [38] discussed this decay effect of the electrical resistance. They suggested that one contributing factor is the resistive heating caused by the DC current supplied by the multimeter. This heating effect causes increase in bulk film conductance which in turn causes decay in film resistance.

Experiments were done for a group of randomly selected specimens in order to examine the change in resistance with respect to time for a period of 30 minutes. From the 1mm thickness set, the 5 wt% and 8 wt% Large MWNTs specimens were tested as shown in Figure 5.18, and Figure 5.19. In Figure 5.20, the behavior of the 8 wt% Large MWNTs specimen, from the 0.5mm thickness set, is presented.

It can be noted that as the weight percent increased from 5 to 8 wt% for the 1mm thickness specimens, the decay effect decreased indicating that as the CNTs content increases beyond the percolation threshold the composite film conductivity tends to get more stable and less affected by any initial heating effect. Also, there is

no significant difference in the decay effect of the 8 wt% specimen of the 1mm thickness and that of the 8 wt% specimen of the 0.5mm thickness.

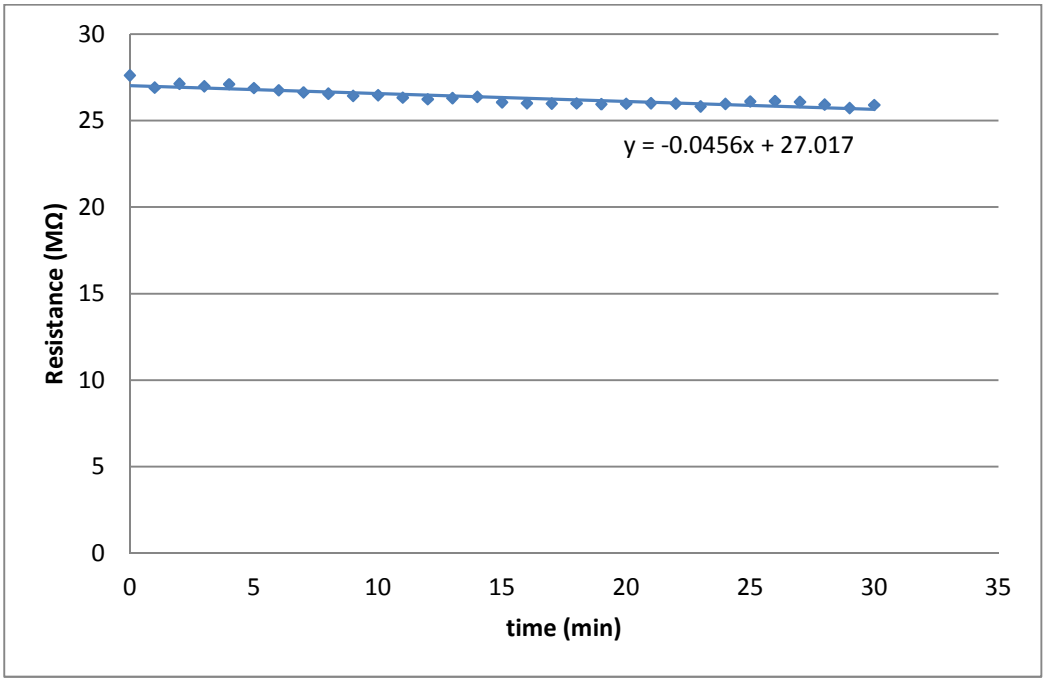

Figure 5.18: The electrical resistance decay for specimen comprising 5 wt% Large MWNTs of 1mm thickness

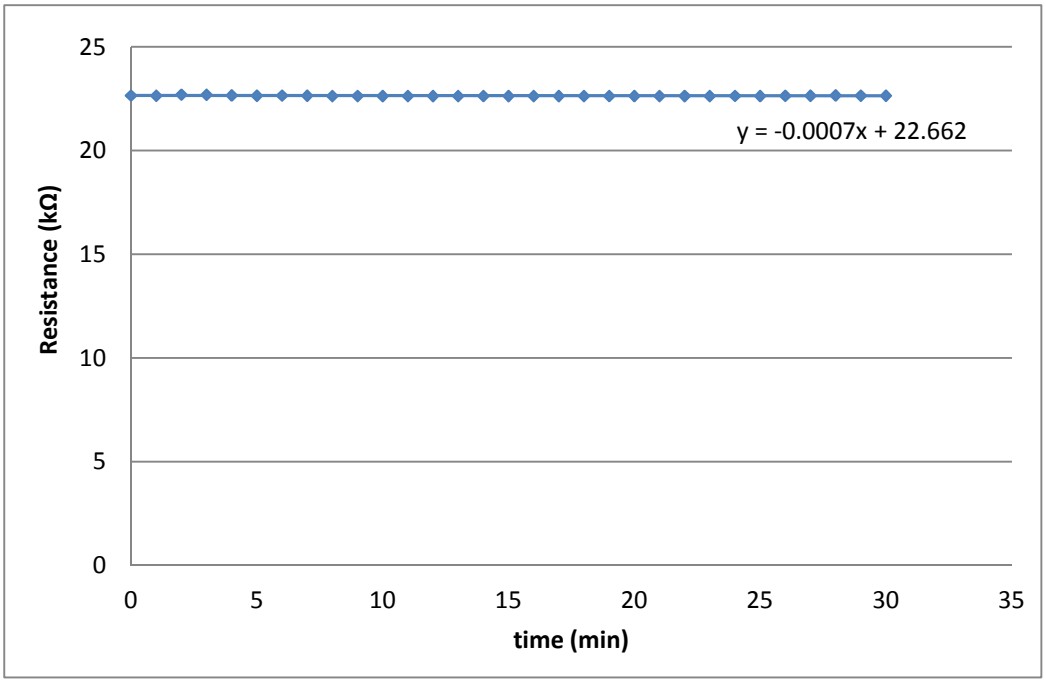

Figure 5.19: The electrical resistance decay for specimen comprising 8 wt% Large MWNTs of 1mm thickness

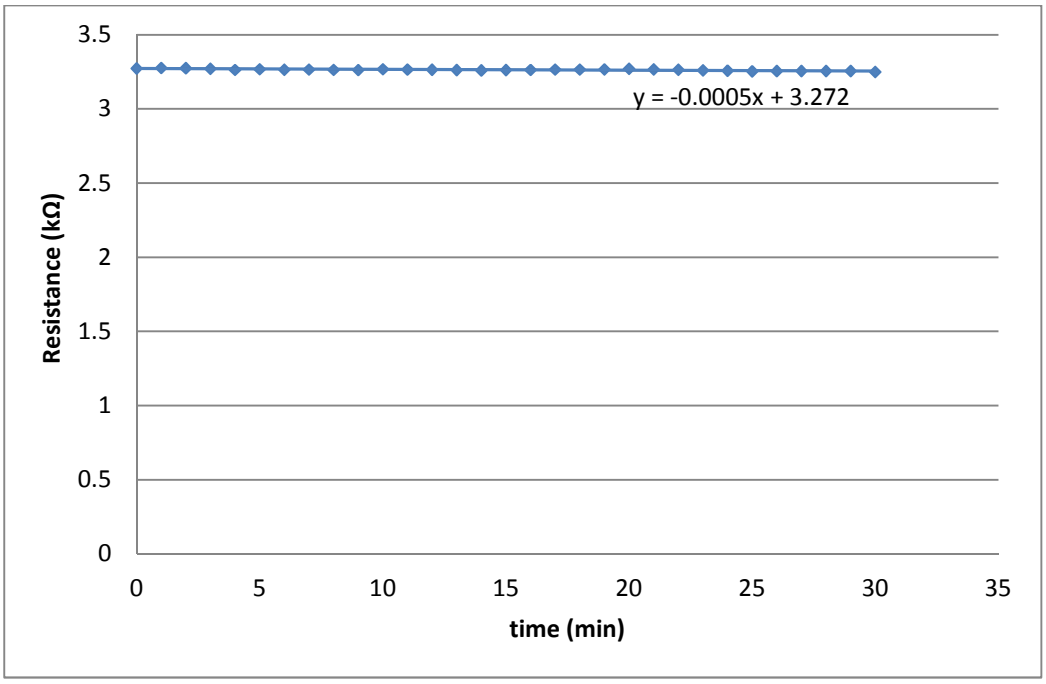

Figure 5.20: The electrical resistance decay for specimen comprising 8 wt% Large MWNTs of 0.5mm thickness

5.3.3 Strain sensitivity measurement

Preliminary testing trials were carried out using the samples of the 1mm thickness. Only samples with CNT content at or higher than percolation threshold were tested for strain sensitivity since lower CNT contents gave electrically resistive samples not suitable for the potential application of strain-sensing. Testing was applied for small strains up to 320 με, using a cantilever setup where a specimen was adhered on the tension side of the steel beam using steel-epoxy adhesive. Low strain values were used to ensure testing is carried out in the elastic range. Dharap *et al.* [5] also tested the response of SWNTs film samples up to a value of 400 με. Figure 5.21 represents the normalized resistance (R*) versus the applied micro-strain for the three samples of 5, 6.5, and 8 wt% of Large MWNTs.

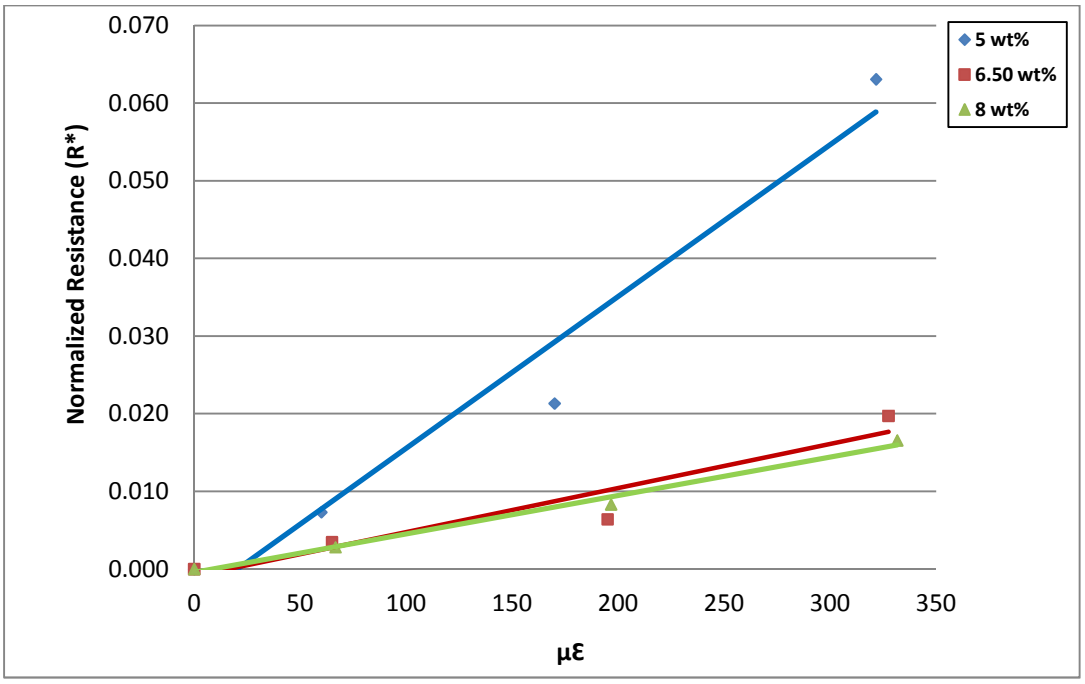

Figure 5.21: Normalized resistance versus Micro-strain for 5, 6.5, and 8 wt% Large-tubes MWNT of 1mm film thickness

A correlation between applied strain and film resistance was obtained as it was observed that resistance increases with applied strain which is in agreement with reported literature [1, 5, 6, 31, 38]. Tensile strain reduces the CNTs network density as it increases the distance between neighboring nanotubes thus lowering film conductivity [1]. Table 5.4 shows the calculated gauge factor, which is the slope of each curve.

Table 5.4: Gauge Factor values at each CNT wt%

CNT wt%	GF
5	200
6.5	60
8	50

The 5 wt% specimen gave the highest gauge factor, when compared with the 6.5 and 8 wt%, which is in accordance with literature as it was stated that the highest

strain sensitivity is obtained at percolation threshold [1]. Moreover, it was stated that increasing concentrations of CNTs can lead to lower film sensitivity [40].

Another observation is the high values of the gauge factors. This is reasoned by the low strain applied on the beam as probably further loading would show a change in the best-fit slope and the linearity. However, due to the fine thickness of the steel beam, further loading could not be applied as the beam underwent severe plastic deformation [52].

As described earlier, the produced samples suffered from some porosity that could be affecting the results. Several trials were later conducted using neat LDPE powder in order to control process parameters to produce specimens with no air bubbles. The use of neat LDPE powder was preferred since the transparency of the produced specimens helped in visual inspection. Although the size and number of the pores decreased upon increasing the mass used, still they were present and randomly distributed all over the specimen. Therefore, a new positive type mold was designed to overcome the difficulty of obtaining pore-free samples with the flash type mold.

5.4 Compression Molding Using Positive Type Mold

As previously mentioned in chapter 4, ASTM D4703 [50] was used in order to set the compression molding process parameters in the case of using positive type mold. The designed mold produced specimens of 0.65mm (±0.05) thickness. This thickness was selected as to have specimens with good flexibility yet bulky enough for ease of handling and preparation for the testing stage.

Two sets of samples were produced using two different types of nanotubes to investigate the effect of CNTs morphology on the composite films conductivity. First set was produced using Large MWNTs, which is the same CNT type used in all previous work. The second set was fabricated using another CNT type named Elicarb MWNTs which has a better quality and higher aspect ratio.

5.4.1 Large MWNTs set

Three samples for each weight percent were manufactured. Three specimens were cut from each sample into 30 x 5.5 mm by using a cutting template and their resistivities at no load condition were measured. Figure 5.22 demonstrates the average resistivity value at each MWNTs weight percent as blue dots with the values of the three samples illustrated in red marks, while Figure 5.23 represents the equivalent conductivity values. It is obvious that the variation in resistivity readings at each weight percent decreased when compared with the previously done sets showing better reproducibility in results except for the 8 wt% one where variation did increase than before. However, it is also detected that the resistance and consequently the resistivity values are higher than before as no percolation behavior was observed in the tested range. It is not odd to have higher percolation threshold for LDPE polymer, Zhao *et al.* [18] reported Φ_c in the range of (10 – 15) wt% for MWNT/LDPE composites fabricated by solution mixing followed by hot pressing.

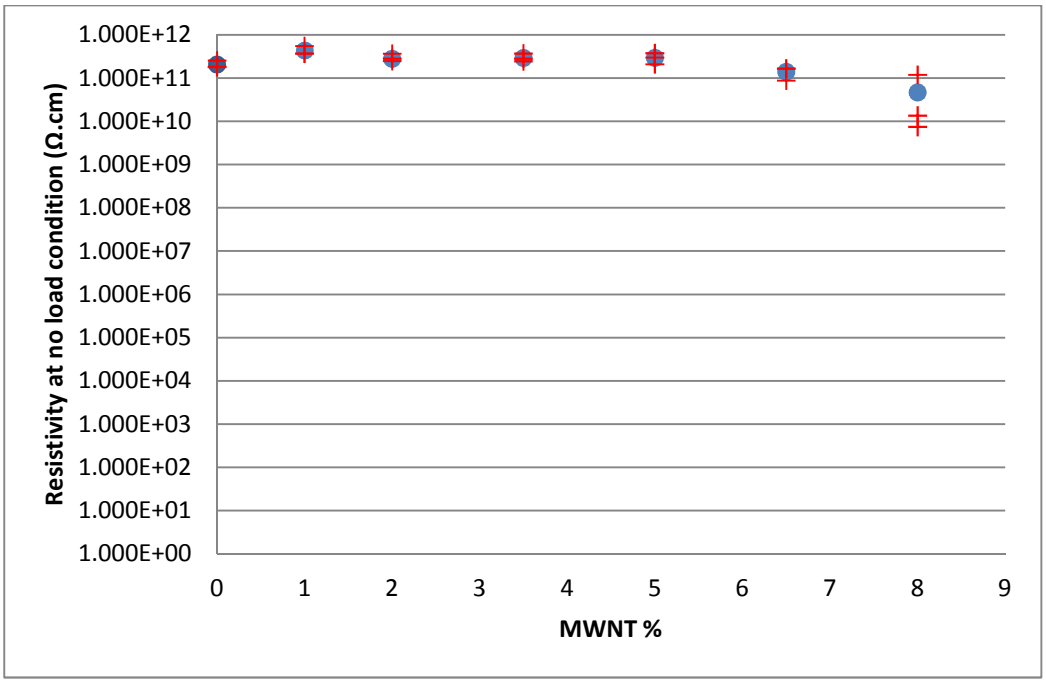

Figure 5.22: Resistivity versus MWNT wt% for Large-tubes MWNT

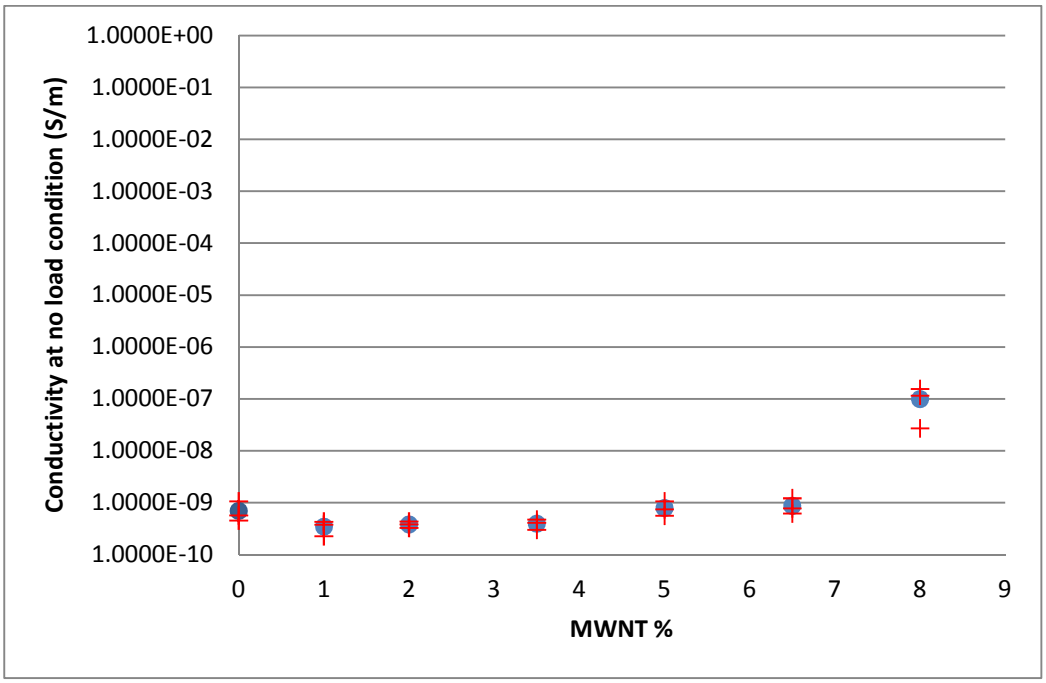

Figure 5.23: Conductivity versus MWNT wt% for Large-tubes MWNT

Samples were inspected by the SEM and no sign of air bubbles was detected as seen in Figure 5.24 and Figure 5.25. It is suspected that this could be one of the contributing factors for having higher resistivity values as the presence of pores in the case of the flash type mold forced the CNTs to be clustered together in the spaces

available thus increasing the network density which in turns lowers the bulk resistance. McNally *et al.* [4] obtained a Φ_c of 7.5 wt% for MWNT/PE composite films, where a special type of medium density polyethylene was used. They explained this high percolation to be possibly due to the polyethylene particles coating the nanotubes thus reducing the nanotube-to-nanotube contact which leads to higher concentration of CNTs needed in order to reach percolation threshold as well as the high resistivity of polyethylene polymer tends to cause high percolations than other polymer composites.

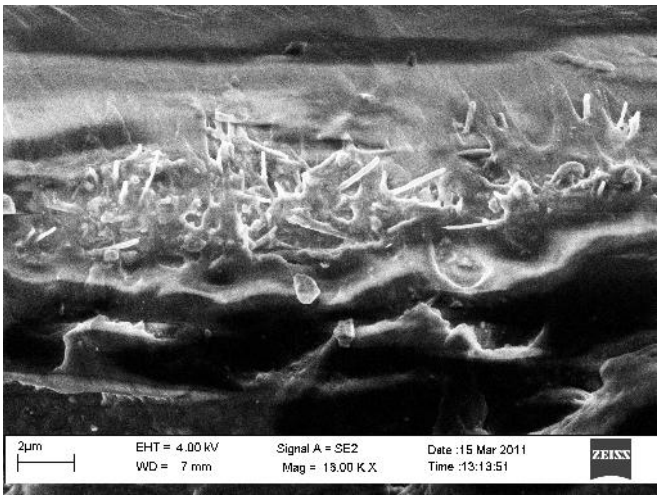

Figure 5.24: Cryo-fractured cross-section of 6.5 wt% Large-tubes MWNT specimen

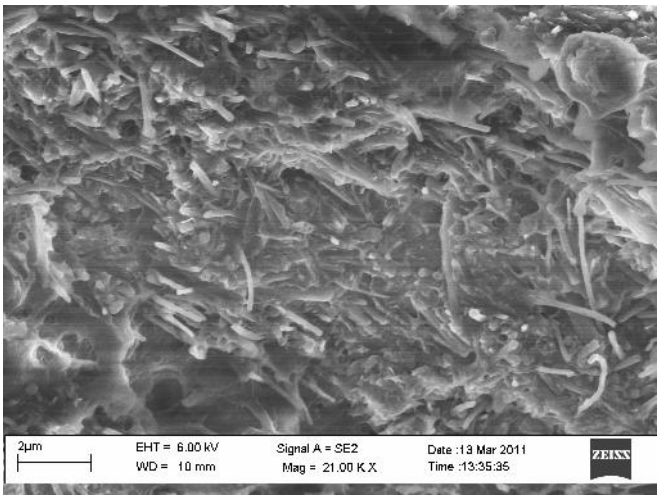

Figure 5.25: Cryo-fractured cross-section of 8 wt% Large-tubes MWNT specimen

For such high resistance values, it would not be possible to test samples to obtain a strain behavior.

5.4.2 Elicarb MWNTs set

Another set of samples was processed using the positive type mold with the same parameters, using Elicarb MWNTs in order to examine the effect of CNTs morphology on the electrical conductivity of samples. Figure 5.26 and Figure 5.27 show the electrical resistivity and conductivity values at each CNT weight percent respectively. The percolation behavior is clear as the resistivity is seen to drop four orders of magnitude between the 3.5 wt% and the 6.5 wt%.

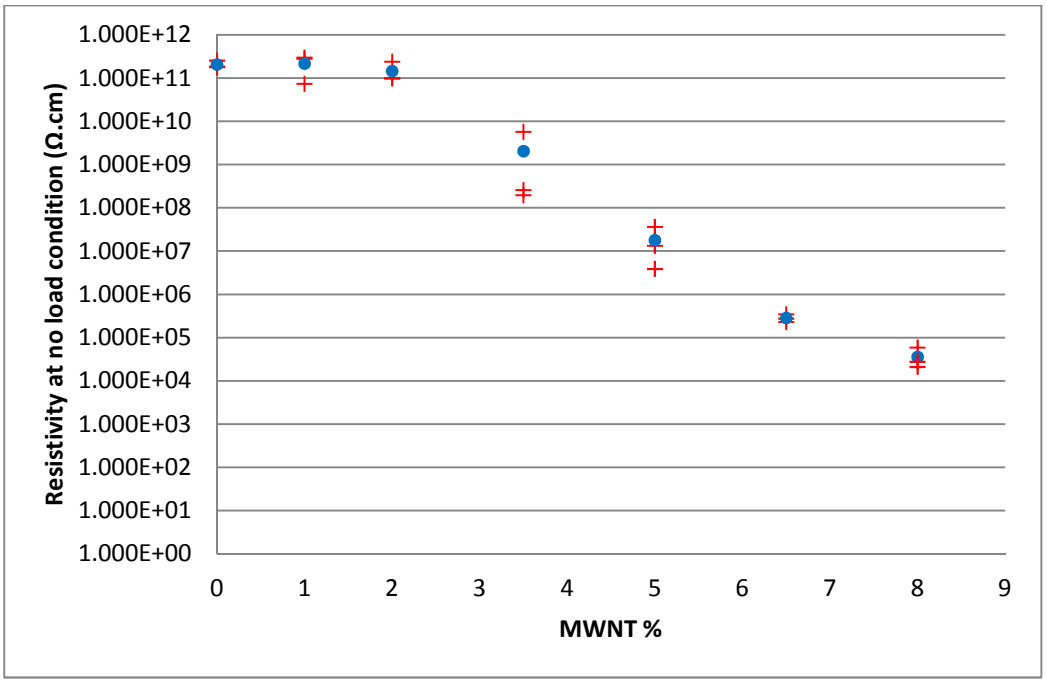

Figure 5.26: Electrical resistivity versus Elicarb MWNT wt%

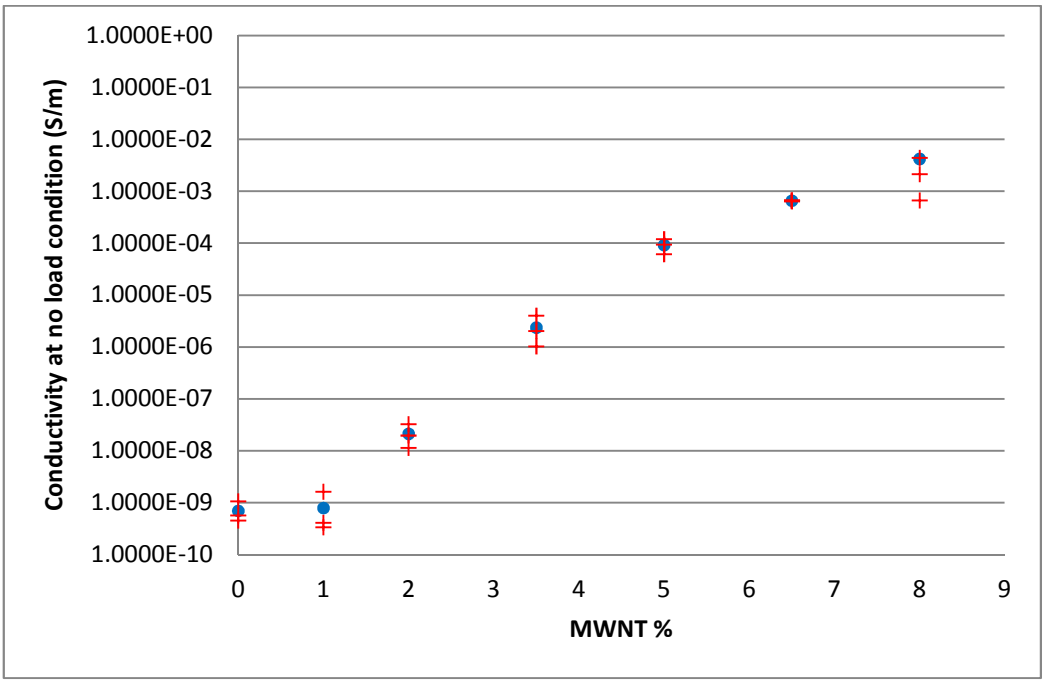

Figure 5.27: Electrical conductivity versus Elicarb MWNT wt%

By comparing the resistivity values of the Elicarb MWNTs samples with the Large MWNTs ones, it is clear that there is a big difference. For instance, by looking at the 5 wt% sample the Large MWNTs showed a resistivity of 2.94 x 10^{11} Ωcm,

while the Elicarb MWNTs gave a value of 1.79 x 10^7 Ωcm. This large difference of four orders of magnitude indicates that the morphology of CNTs used has a great effect on the electrical conductivity and hence the percolation of the produced samples. Moreover, this indicates that as the aspect ratio of CNTs increases the electrical conductivity of CNTs network increases, considering both types have same chirality. Yin *et al.* [39] conducted a comparison between two composite sample sets having the same polymer matrix (epoxy) but with two different morphologies of MWNTs. The study showed that upon application of strain, the underlying working mechanism and piezoresistive properties differed for each MWNT type. For MWNTs that have large average diameter and straight shapes (similar to the morphology of our Large MWNTs), the mechanism of resistance change is based on the tunneling resistance between nanotubes that changes with the change in distance between nanotubes due to the applied strain. On the other hand, the other type of MWNTs that has very small average diameter and curved entangled structure (similar to the morphology of our Elicarb MWNTs), the piezoresistivity of the MWNTs is due to their deformation. It was stated that the second type of MWNTs showed good linear behaviour which renders it to be more suitable for practical sensing applications. Our results therefore support the observation by Yin *et al.* [39].

5.4.2.1 Resistance Decay

Furthermore, the resistance of Elicarb MWNTs samples of 5 wt% and beyond was measured for a time interval of 60 minutes. Figure 5.28, Figure 5.29, and Figure 5.30 demonstrates the resistance decay behavior of the 5 wt%, 6.5wt%, and 8wt% respectively. The 8 wt% showed to be the most stable as the least change in resistance was observed.

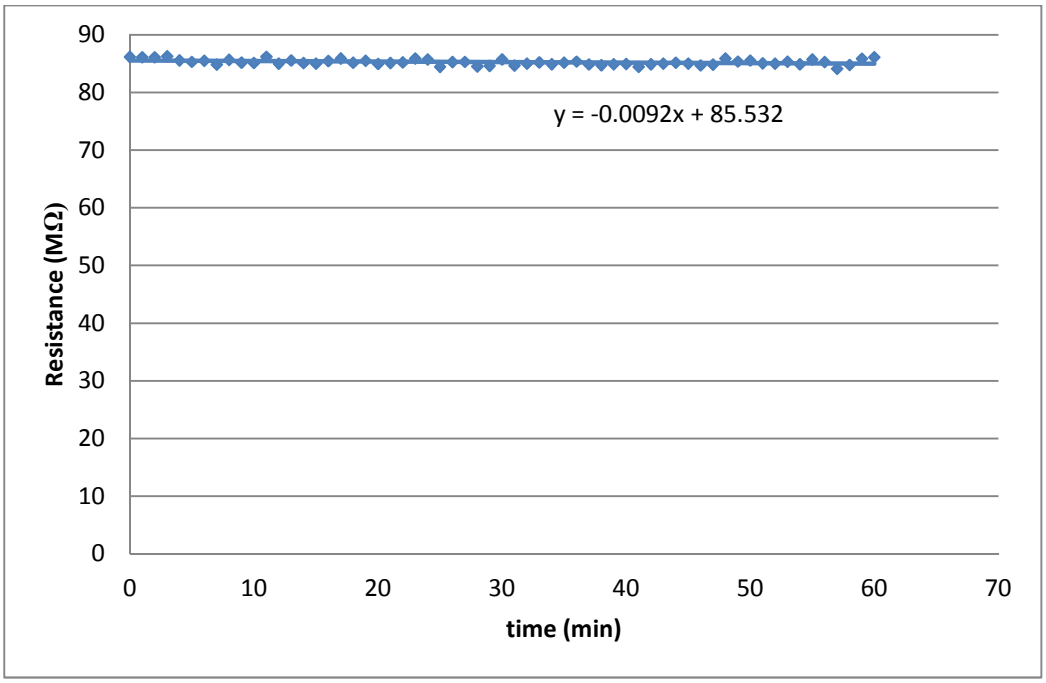

Figure 5.28: Resistance decay curve of 5 wt% Elicarb MWNTs specimen

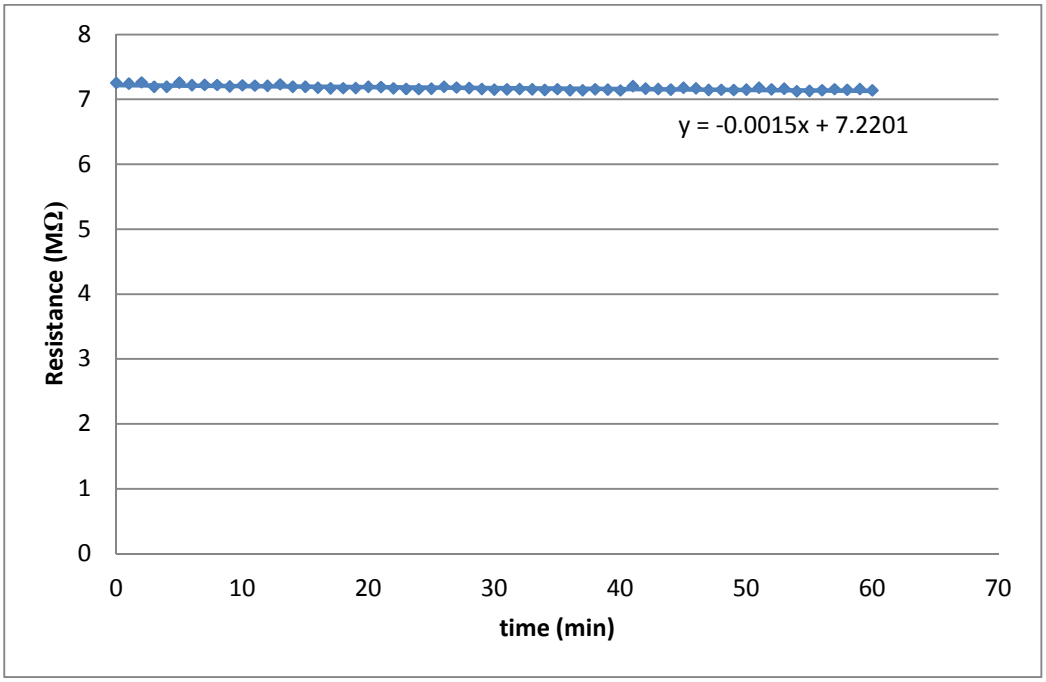

Figure 5.29: Resistance decay curve of 6.5 wt% Elicarb MWNTs specimen

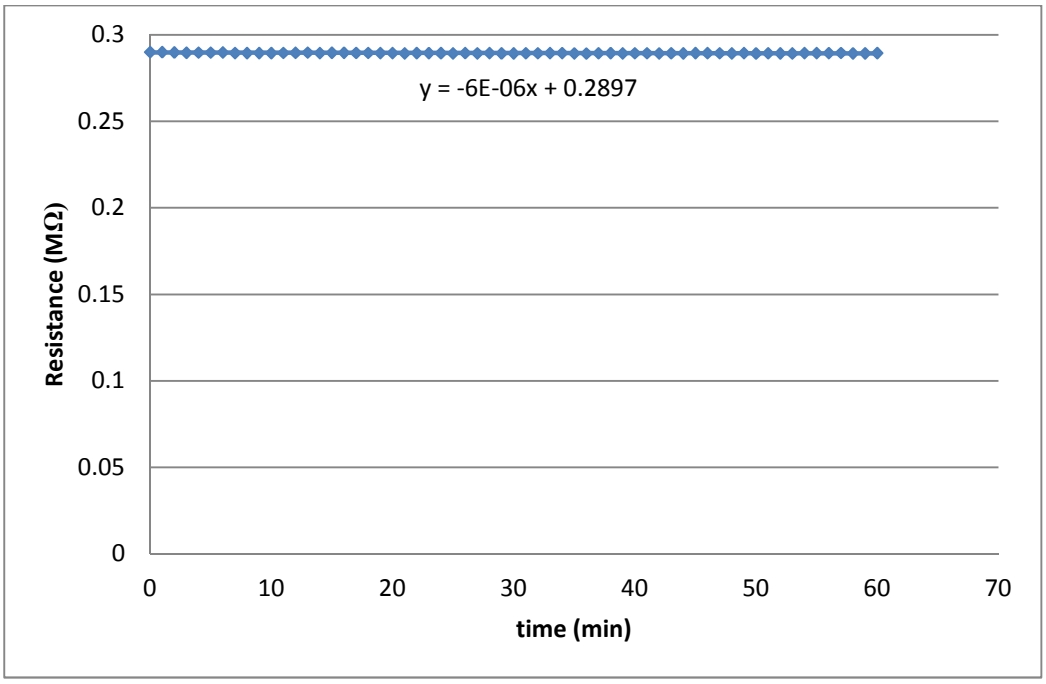

Figure 5.30: Resistance decay curve of 8 wt% Elicarb MWNT specimen

5.4.3 Strain sensitivity measurement

As described in chapter 4, the cantilever setup was limiting due to the restrictive loading capacity therefore, axial tensile loading was carried out using a universal testing machine with a speed of 0.25 mm/min. Li *et al.* [2] used same speed during testing. Specimens were adhered to the aluminum sheet using 2 different types of adhesives. One is steel-epoxy adhesive and the other is called CN adhesive (single component room temperature-curing type consisting of Cyanoacrylate) used for conventional strain gauges. The use of the adhesive is to ensure firm contact between the composite specimen and aluminum beam in order to ensure no slippage thus good strain transfer from beam to composite specimen. The results of the two cases are presented below where 3 specimens were tested at each weight concentration.

5.4.3.1 Steel-Epoxy Adhesive

Specimens of 5, 6.5, and 8 wt% Elicarb MWNT were adhered to aluminum tensile sheets using steel-epoxy adhesive. Figure 5.31 shows the stress-strain curves for all the tested aluminum sheets where strain was measured by metallic foil strain gauge. Strain was applied up to 5000 με which is similar to many reported literature for example like Loh *et al.* [38]. All aluminium sheets showed almost identical stress-strain behavior. Figure 5.32, Figure 5.33, and Figure 5.34 represent the normalized resistance with respect to the applied strain for the 5, 6.5, and 8 wt% specimens respectively. The sensitivity of the composite samples, measured by the slope of the best-fit line, is presented in table 5.5.

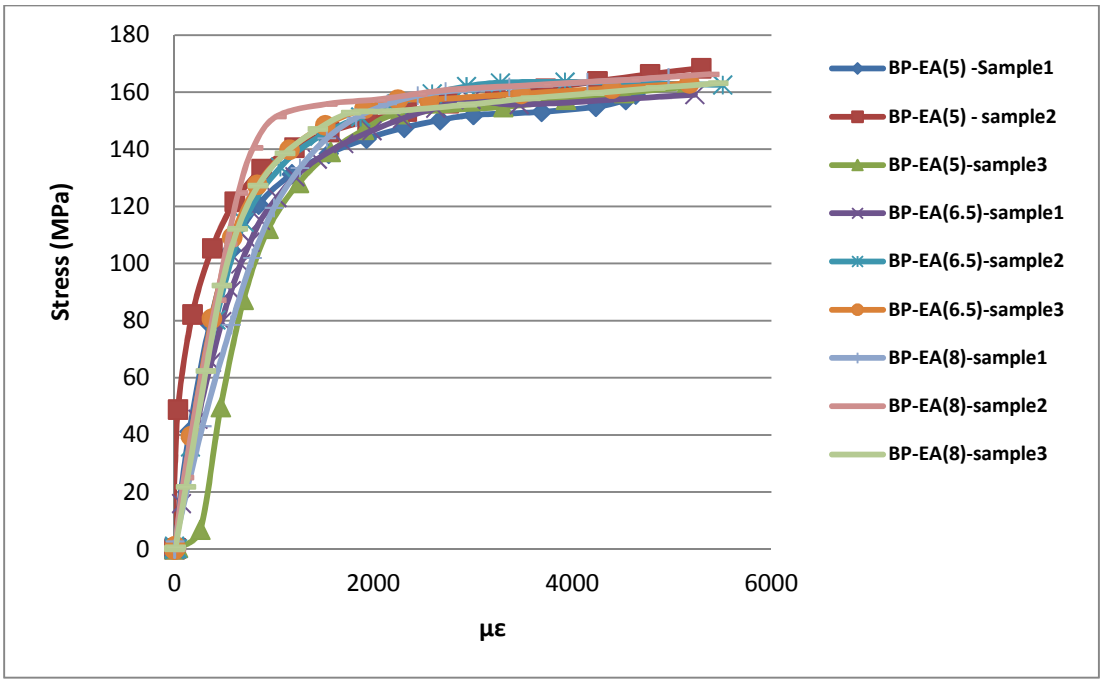

Figure 5.31: Graph showing stress vs strain for the Al tensile sheets upon which the 5, 6.5, and 8 wt% Elicarb MWNT specimens are adhered

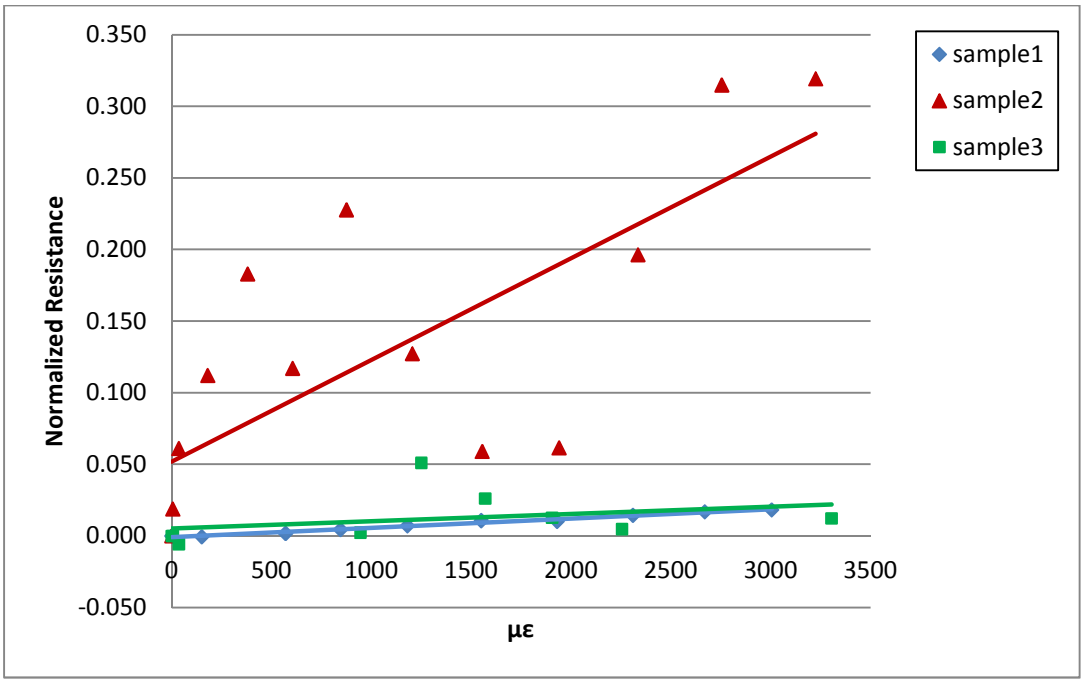

Figure 5.32: Normalized Resistance versus micro-strain for the 5 wt% Elicarb MWNTs samples adhered with steel-epoxy adhesive

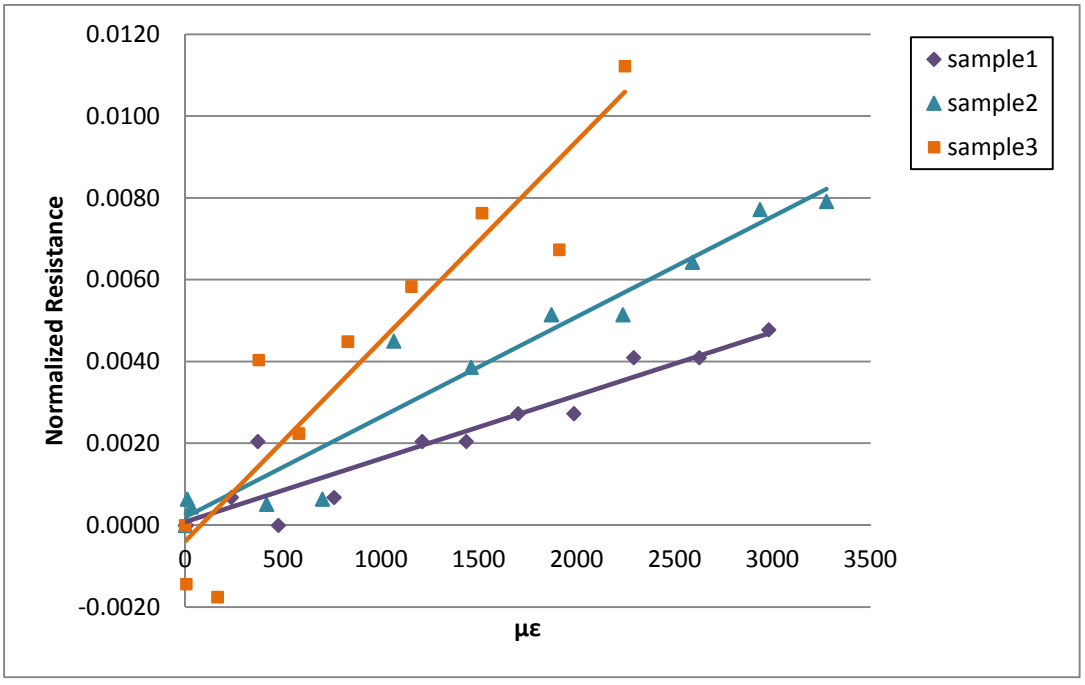

Figure 5.33: Normalized Resistance versus micro-strain for the 6.5 wt% Elicarb MWNTs samples adhered with steel-epoxy adhesive

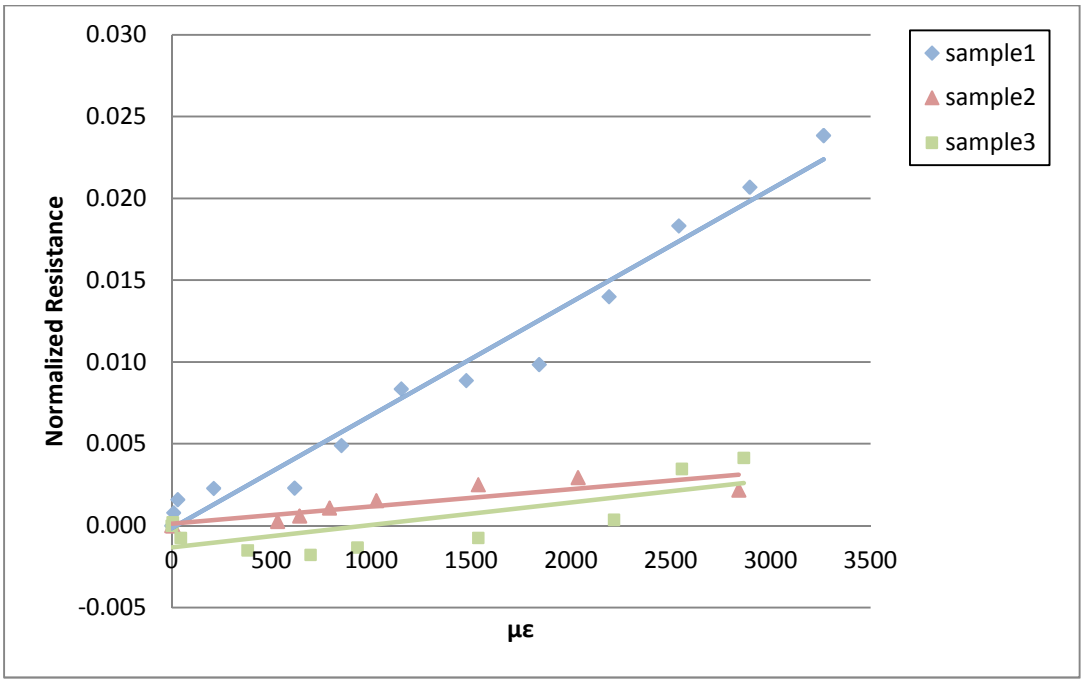

Figure 5.34: Normalized Resistance versus micro-strain for the 8 wt% Elicarb MWNTs samples adhered with steel-epoxy adhesive

Table 5.5: Gauge factor values for samples adhered with steel-epoxy

Composite film samples	Sample #	GF
5 wt% Elicarb MWNT	1	6
	2	70
	3	5
6.5 wt% Elicarb MWNT	1	2
	2	2
	3	5
8 wt% Elicarb MWNT	1	7
	2	1
	3	1

The low gauge factor values show that poor strain transfer took place between the aluminum sheets and the tested specimens. At the end of each test, specimens were checked if they were still adhered to the aluminum sheet and in most cases the specimens together with the steel-epoxy adhesive were detached from the aluminum

sheet surface. Moreover, for each sample variable gauge factor values were obtained again proving low sensing capability. Therefore, testing was redone with another adhesive, which is the same adhesive type used for the conventional strain gauge, called CN.

5.4.3.2 Strain Gauge Adhesive (CN)

Specimens comprising 5, 6.5, and 8 wt% Elicarb MWNTs were adhered to aluminum tensile sheets using the CN adhesive. Again, three specimens were tested for each weight percent and each specimen behavior was recorded separately. In Figure 5.35, Figure 5.36, and Figure 5.37 normalized resistance with respect to the applied strain for the 5, 6.5, and 8 wt% specimens respectively is presented. Measurements were recorded up to 4000 με. The sensitivity of the specimens, measured by the slope of the best-fit line is shown in Table 5.6.

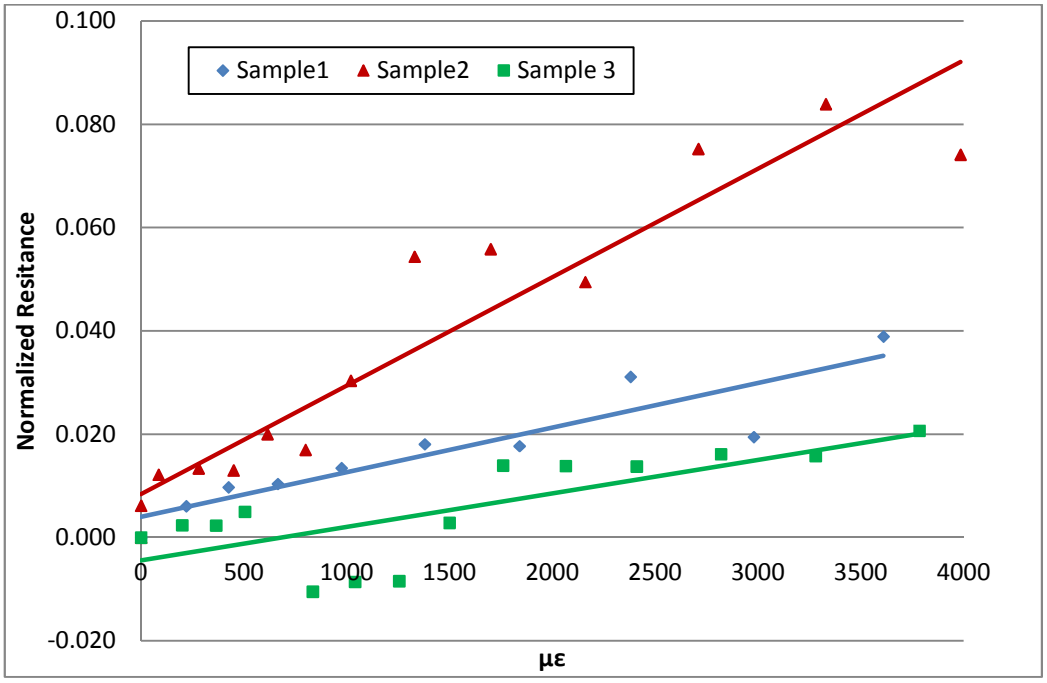

Figure 5.35: Normalized Resistance versus micro-strain for the 5 wt% Elicarb MWNTs samples adhered with CN adhesive

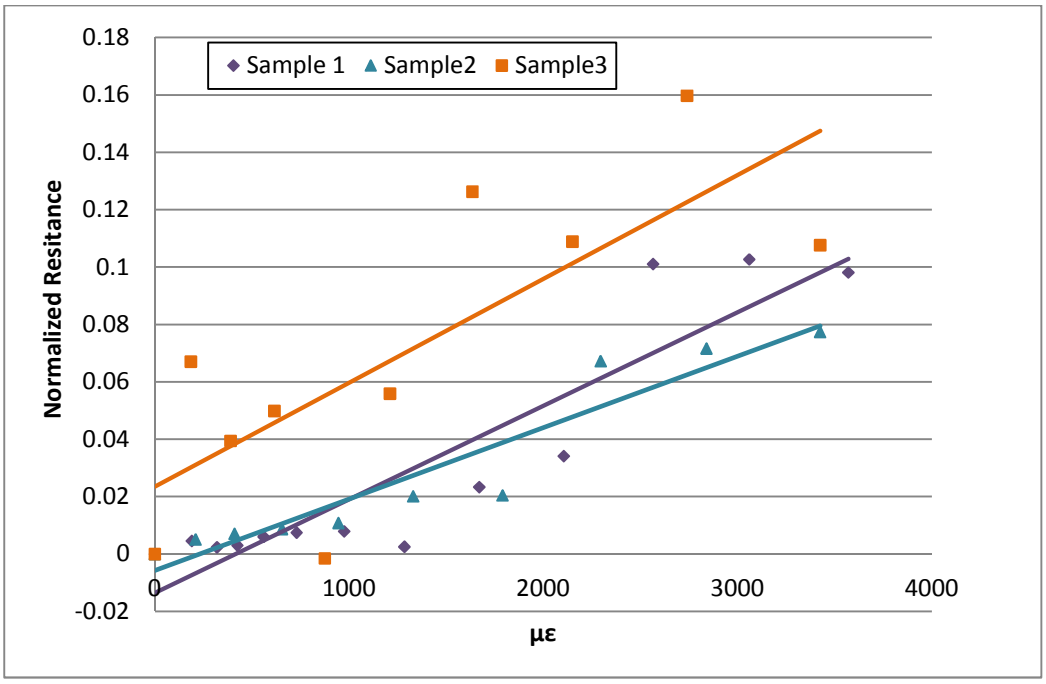

Figure 5.36: Normalized Resistance versus micro-strain for the 6.5 wt% Elicarb MWNTs samples adhered with CN adhesive

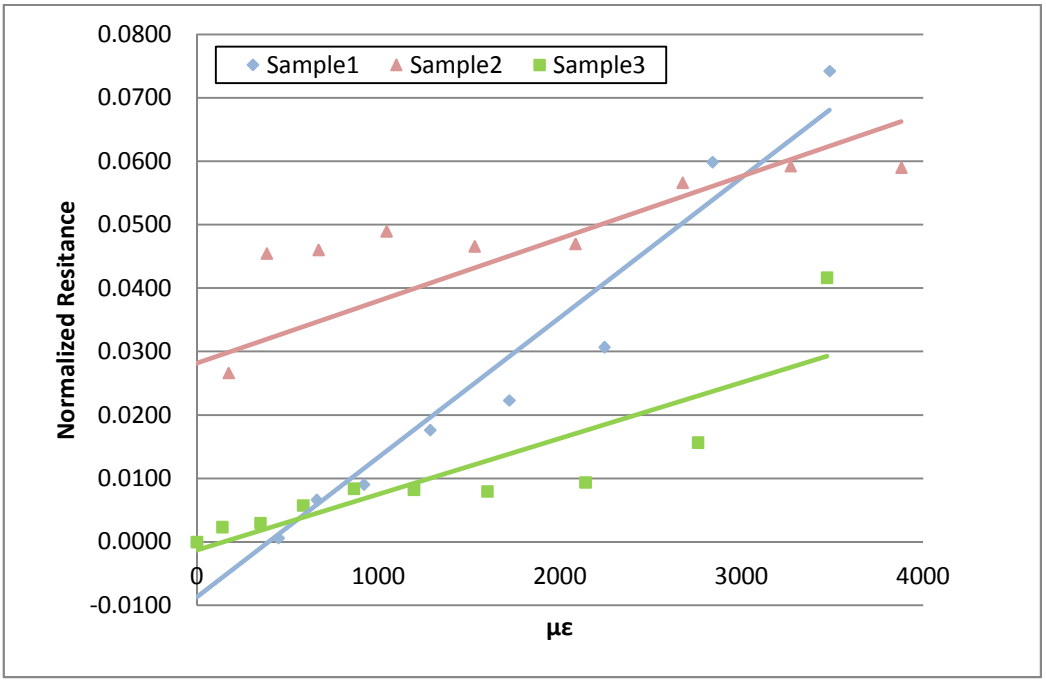

Figure 5.37: Normalized Resistance versus micro-strain for the 8 wt% Elicarb MWNTs samples adhered with CN adhesive

Table 5.6: Gauge factor values for samples adhered with CN

Composite film samples	Sample #	GF
5 wt% Elicarb MWNT	1	9
	2	20
	3	6
6.5 wt% Elicarb MWNT	1	30
	2	20
	3	40
8 wt% Elicarb MWNT	1	20
	2	10
	3	9

By comparing the gauge factors of the samples adhered with steel-epoxy with those adhered with CN adhesive, it is obvious the effect of proper adhesive selection on the sensing capability of the samples is crucial. Gauge factor values increased proving better strain transfer from the aluminum sheet undergoing tension to the adhered MWNT/LDPE composite samples. Gauge factors obtained are much higher than those of the conventional strain gauges. The specimens were still properly adhered to the aluminum sheet surface at the end of test. However, the samples gauge factor at each weight percent did show variation in values. Liu *et al.* [34, 42] results showed similar variations for the same weight percent of MWNTs as the sensors had different resistance values at no load condition thus leading to the obtained variation in gauge factors. They attributed this to the degree of CNTs dispersion within the polymer matrix.

5.4.3.3 Loading Cycles

Further testing was applied as samples were tested for two consecutive cycles to examine their sensing behavior under repeatable loading as described in Figure 5.38. In Figure 5.39, Figure 5.40, and Figure 5.41 the loading curves are demonstrated for the 5, 6.5, and 8 wt% Elicarb MWNTs samples respectively.

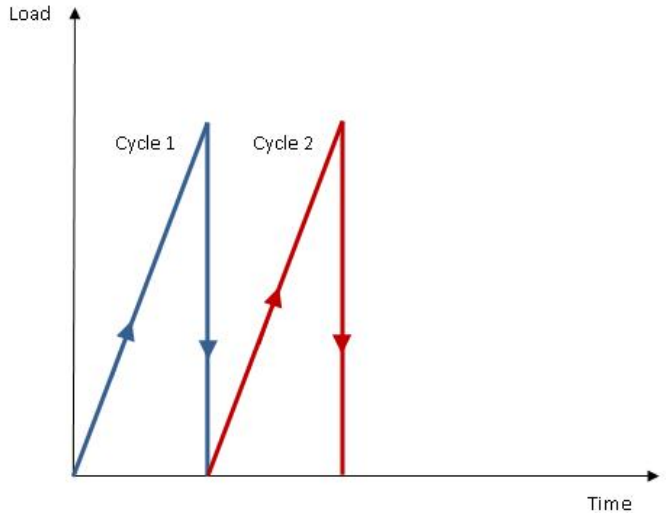

Figure 5.38: Schematic diagram demonstrating loading cycles applied

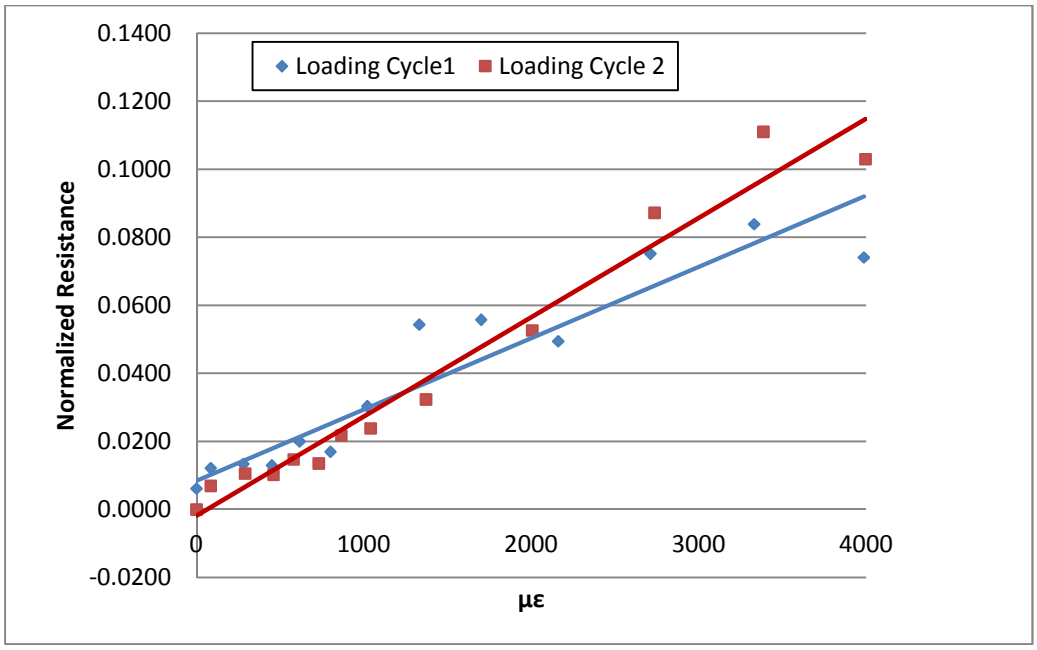

Figure 5.39: Consecutive loading cycles for the same 5 wt% Elicarb MWNTs composite (sample # 1) adhered with CN adhesive

The three samples, 5, 6.5 and 8 wt%, showed similar behavior where it can be observed that composite samples showed a fair sign of reversibility. A drift in the resistance at no load condition after the first loading cycle was detected which caused a change in the sensitivity of the composite samples, thus a change in the gauge factor, which is the main reason behind the imperfect reversible behavior. The presence of a drift in resistance upon repeatable loading for nanocomposites is still a challenge [53].

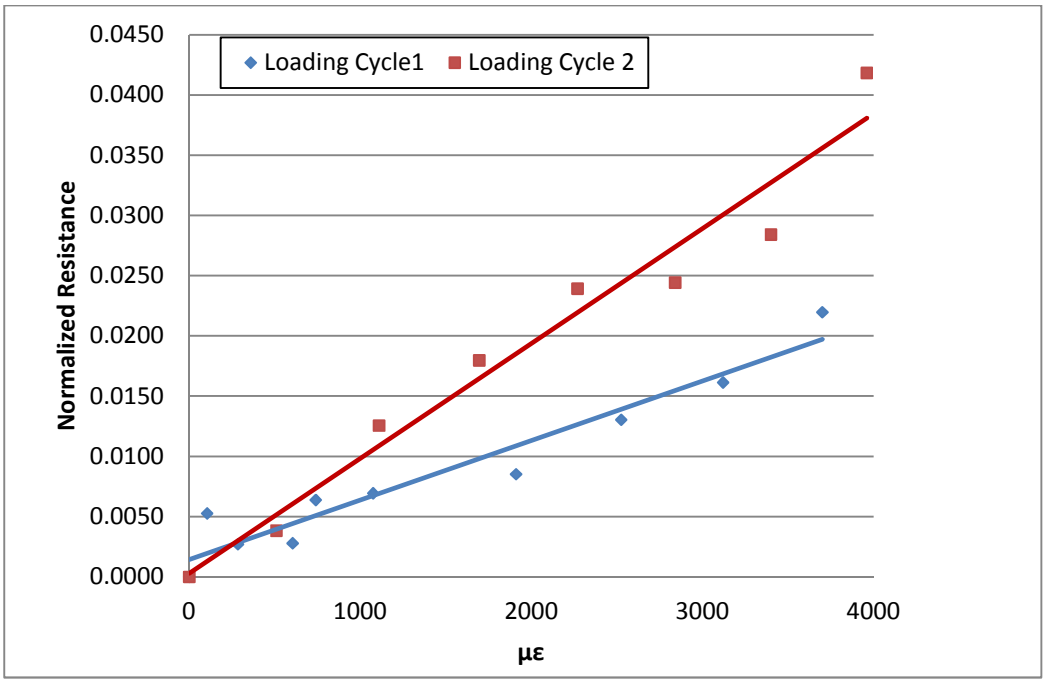

Figure 5.40: Consecutive loading cycles for the same 6.5 wt% Elicarb MWNTs composte (sample # 3) adhered with CN adhesive

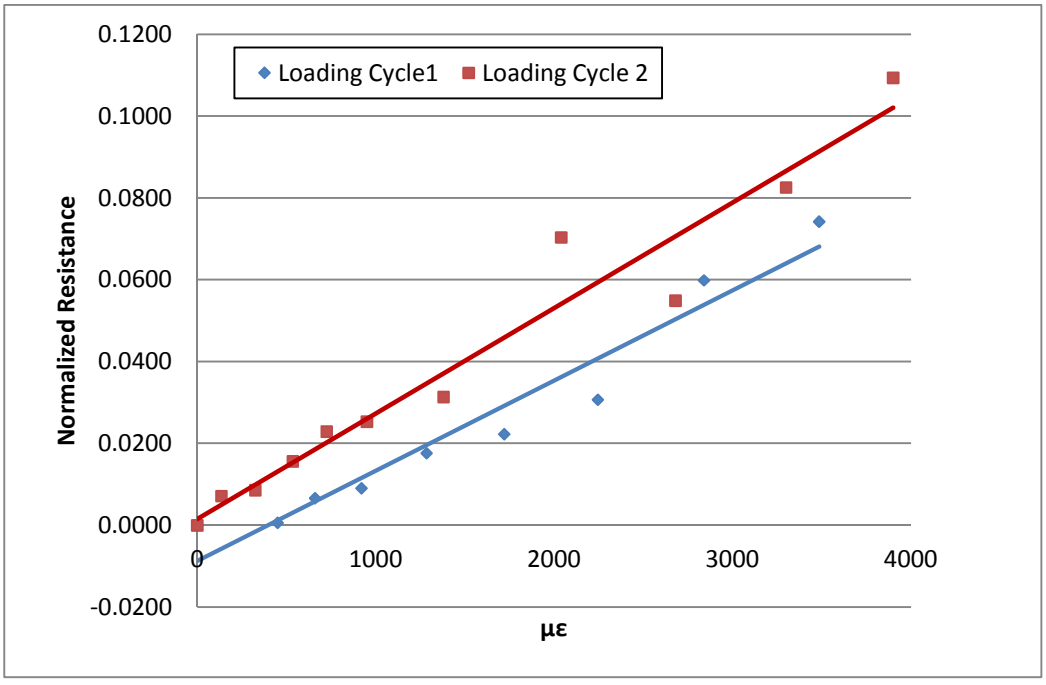

Figure 5.41: Consecutive loading cycles for the same 8 wt% Elicarb MWNTs composite (sample # 1) adhered with CN adhesive

5.5 Effect of Adding MWNTs on LDPE Crystallinity

DSC characterization of pure low-density polyethylene and of the composite powders was carried out in order to understand the effect of CNTs addition on the LDPE melting temperature and degree of crystallinity which are expected to also affect the electrical properties as mentioned in section 3.5. Three weight percentages were examined, for both the Large MWNTs and the Elicarb MWNTs, which are the 1, 5, and 8 wt%. Three samples were tested for each weight percent as well as for the pure polymer and average values were recorded. Table 5.7 shows the resulting averages of the melting temperature (T_m), the degree of crystallinity (X_c), the crystallization peak temperature (T_p), and the degree of supercooling ($T_m - T_p$). In addition, Figure 5.42 and Figure 5.43 show the DSC curves for the low-density polyethylene polymer with Large MWNTs and the Elicarb MWNTs samples respectively. The degree of crystallinity (X_c) is calculated as follows:

$$X_c = \frac{\Delta H_f}{\Delta H_f^o (1 - \varphi)} \qquad \textbf{(5.2)}$$

Where ΔH_f is the enthalpy of melting (J/g), ΔH_f^o is the theoretical enthalpy for a 100% crystalline low-density polyethylene (209 J/g), and (1 - φ) is the weight fraction of polymer [47].

The melting temperature of the LDPE did not show much variation upon the addition of the nanotubes – whether Large-tubes or Elicarb MWNTs. This is in agreement with McNally *et al.* [4] observations who used PE (linear medium density type).

Table 5.7: DSC results showing the melting temperature and the degree of crystallinity for the tested samples

Sample	T_m (°C)	X_c (%)	T_p (°C)	$T_m - T_p$ (°C)
LDPE	105.97	28.989	92.97	13
1 wt% Large MWNTs	106.12	32.162	92.88	13.24
5 wt% Large MWNTs	107.59	28.045	93.5	14.09
8 wt% Large MWNTs	106.32	38.140	92.75	13.57
1 wt% Elicarb MWNTs	105.92	28.739	92.83	13.09
5 wt% Elicarb MWNTs	106.21	27.997	92.44	13.77
8 wt% Elicarb MWNTs	106.89	28.588	92.59	14.3

As for the degree of crystallization, it was examined using two measures which are the degree of crystallinity as well as the degree of supercooling. It can be deduced that the MWNTs did not affect the crystallization of LDPE as no significant increase was observed. The only apparent increase in X_c was obtained for the 8 wt% Large MWNTs where an increase of almost 10% was detected. Yet the degree of supercooling did not show any equivalent increase. This could be due to the fact that LDPE has a very low crystallinity

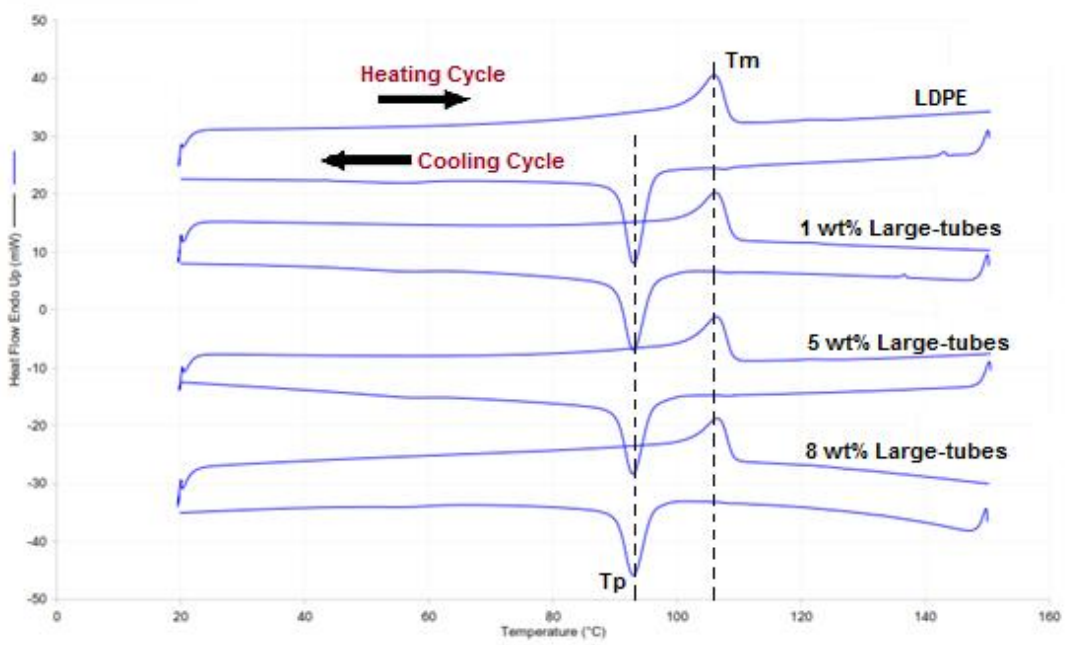

Figure 5.42: DSC curves for LDPE sample labeled polymer, and Large MWNTs samples comprising 1, 5, and 8 wt%

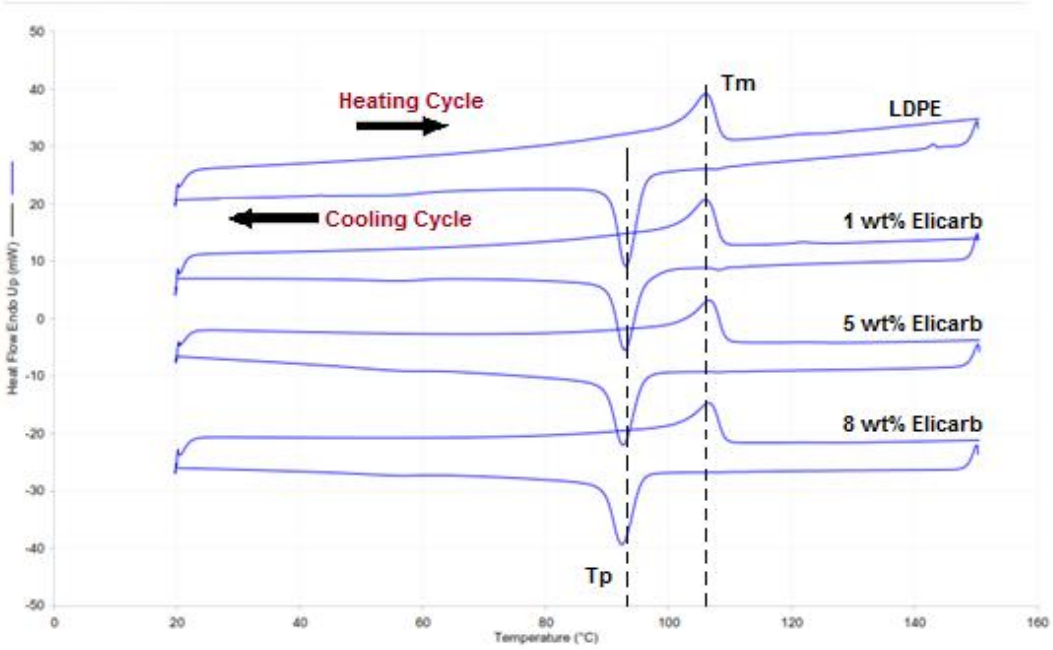

Figure 5.43: DSC curves for LDPE sample labeled polymer, Elicarb MWNTs samples comprising 1, 5, and 8 wt%

CHAPTER 6

CONCLUSIONS and RECOMMENDATIONS

6.1 Conclusions

By reviewing the results obtained in this experimental study, some concluding remarks can be pointed out.

- With regards to the mixing of the MWNTs with the LDPE polymer, ball milling was shown to be more effective than turbula mixing as it promoted better MWNTs dispersion.
- Concerning the ball milling time factor, 30 minutes of milling showed adequate level of nanotubes dispersion when compared with the 15 and the 60 minutes milling.
- The mixing process, prior to processing, was found to have a greater influence on the nanotubes dispersion than the shear mixing induced in the extrusion process.
- Positive type mold gave pore-free samples.
- Percolation threshold depends on the film thickness as well as MWNTs wt% and MWNTs morphology.
- For Elicarb MWNTs, a percolation threshold in the range of 3.5 to 6.5 wt% was found for the 0.65mm samples produced by the positive type mold.

- MWNT/LDPE composite films showed a correlation between the change in resistance and the applied strain.

- The composite film thickness and its electrical conductivity were found to be proportional.

- The CNTs morphology and aspect ratio were found to have an important effect on the bulk composite conductivity. The higher aspect ratio MWNTs gave better conductive behavior. At 5 wt% concentration, Elicarb MWNTs composite film showed lower resistivity of 4 orders of magnitude than the Large MWNTs composite film.

- Strain sensitivity is highest for composite samples near the percolation threshold.

- Upon applying repeatable load on the MWNT/LDPE samples, a drift was observed to affect the repeatability of the sensing behavior.

- As for the effect of adding carbon nanotubes on affecting the LDPE polymer crystallinity and melting temperature, no significant changes were observed for either type of the used MWNTs.

6.2 Recommendations

The field of nanotube/polymer composites for strain sensing applications is still in its early stages. Future work would be focusing on examining the effect of using the solution fabrication method which according to the literature gives better dispersion on composite samples strain sensing to compare it with that of the solid-

state mixing method. Moreover, it would be beneficial to study the effect of CNTs dispersion on the composite sensing capability.

Further investigation should be carried out on the resistance decay phenomenon experienced in composites to be able to eliminate its effects completely. Also, a more in-depth analysis should be carried out to explain the degree of crystallization results obtained from the DSC investigation. In addition, a cost-benefit analysis would be needed to assess the possibility of industrially manufacturing such sensors.

REFERENCES

[1] Pham G T, Park Y-B, Liang Z, Zhang C, and Wang B. Processing and modeling of conductive thermoplastic/carbon nanotube films for strain sensing. *Journal of Composites: Part B* 2008. **39**: p. 209–216.

[2] Li X, Levy C, and Elaadil L. Multiwalled carbon nanotube film for strain sensing. *Journal of Nanotechnology* 2008. **19**.

[3] Esawi A M K and Farag M M. Carbon nanotube reinforced composites: Potential and current challenges. *Journal of Materials and Design* 2007. **28**: p. 2394–2401.

[4] McNally T , Potschke P, Halley P, Murphy M, Martin D, Bell S E J, Brennan G P, Bein D, Lemoine P, and Quinn J P. Polyethylene multiwalled carbon nanotube composites. *Journal of Polymer*, 2005. **46**: p. 8222–8232.

[5] Dharap P, Li Z, Nagarajaiah S, and B.E. V. Nanotube film based on single-wall carbon nanotubes for strain sensing. *Journal of Nanotechnology*, 2004. **15**: p. 379–382

[6] Kang I, Schulz M J, Kim J H, Shanov V, and Shi D. A carbon nanotube strain sensor for structural health monitoring. *Journal of Smart Materials and Structures*, 2006. **15**: p. 737–748

[7] Murray W M and Miller W R, *The Bonded Electrical Resistance Strain Gage: An Introduction*. 1992: Oxford University Press.

[8] Zagreb, U.o. *Strain Gauge image*. (14/1/2012) [cited; Available from: http://www.phy.pmf.unizg.hr/~nnovosel/etuf/nastavni_materijali.php.

[9] Gorrasi G, Sarno M, Bartolomeo A D, Sannino D, Ciambelli P, and Vittoria V. Incorporation of Carbon Nanotubes into Polyethylene by High Energy Ball Milling: Morphology and Physical Properties. *Journal of Polymer Science: Part B: Polymer Physics*, 2007. **45**: p. 597– 606.

[10] Park M, Kim H, and Youngblood J. Strain-dependent electrical resistance of multi-walled carbon nanotube/polymer composite films. *Journal of Nanotechnology*, 2008. **19**.

[11] Du J-H, Bai J, and Cheng H-M The present status and key problems of carbon nanotube based polymer composites *Journal of eXPRESS Polymer Letters*, 2007. **1** p. 253–273.

[12] Valentino O, Sarno M, Rainone N G, Nobile M R, Ciambelli P, Neitzert H C, and Simon G P. Influence of the polymer structure and nanotube concentration on the conductivity and rheological properties of polyethylene/CNT composites. *Journal of Physica E*, 2008. **40**: p. 2440–2445.

[13] Barus S, Zanetti M, Bracco P, Musso S, Chiodoni A, and Tagliaferro A. Influence of MWCNT morphology on dispersion and thermal properties of polyethylene nanocomposites. *Journal of Polymer Degradation and Stability*, 2010. **95**: p. 756-762.

[14] Spitalsky Z, Tasis D, Papagelis K, and Galiotis C. Carbon nanotube–polymer composites: Chemistry, processing, mechanical and electrical properties. *Journal of Progress in Polymer Science*, 2010. **35**: p. 357–401.

[15] Schulz M J, Kelkar A D, and Sundaresan M J, *Nanoengineering of Structural, Functional and Smart Materials*. 2005: CRC Press.

[16] Wikipedia. *Carbon nanotube*. [cited (14/1/2012)]; Available from: http://en.wikipedia.org/wiki/Carbon_nanotube.

[17] Therapeutiques, I.e.C. *Functionalised carbon nanotubes as therapeutic vectors*. (14/1/2012) [cited; Available from: http://www-ibmc.u-strasbg.fr/ict/vectorisation/nanotubes_eng.shtml.

[18] Zhao D, Lei Q, Qin C, and Bai X. Melt process and performance of multi-walled carbon nanotubes reinforced LDPE composites. *Journal of Pigment & Resin Technology*, 2006. **35**: p. 341–345.

[19] Na X, Qingjie J, Chongguang Z, Chenglong W, and Yuanyuan L. Study on dispersion and electrical property of multi-walled carbon nanotubes/low-density polyethylene nanocomposites. *Journal of Materials and Design*, 2010. **31**: p. 1676–1683.

[20] Bauhofer W and Kovacs J Z. A review and analysis of electrical percolation in carbon nanotube polymer composites. *Journal of Composites Science and Technology*, 2009. **69**: p. 1486–1498.

[21] Tsinghua University and H.H.P. Industry. *"Kite-Mechanism" to Produce Carbon Nanotube Loudspeakers*. [cited (17/1/2012)]; Available from: http://nanopatentsandinnovations.blogspot.com/2010/02/tsinghua-university-and-hon-hai.html.

[22] Verploegen E, Wang B, Bennett R, Hart A J, and R.E. Cohen. *Quantitative Characterization of the Morphology of Multiwall Carbon Nanotube Films by Small-Angle X-ray Scattering*. 2007 [cited (17/1/2012)]; Available from: http://www.nsls.bnl.gov/newsroom/science/2007/09-Cohen.htm.

[23] Cowie J M G and Arrighi V, *Polymers: chemistry and physics of modern materials*. Third Edition ed. 2008: CRC Press.

[24] WAB. *Mixer/ Turbula*. 2012 [cited (14/1/2012)]; Available from: http://www.wab.ch/en/mischer/turbula.html.

[25] *One type of machiney with three different name,ball mill*. 2012 [cited (14/1/2012)]; Available from: http://www.cnbestmill.com/xinwenzixun/6046.html.

[26] Esawi A M K, Salem H G, Hussein H M, and Ramadan A R. Effect of Processing Technique on the Dispersion of Carbon Nanotubes Within Polypropylene Carbon Nanotube-Composites and Its Effect on Their Mechanical Properties. *Journal of Polymer Composites*, 2010. **31**: p. 772–780.

[27] *Hot-Melt Extrusion: Novelty In Pharmaceutical Manufacturing*. 2012 [cited (14/1/2012)]; Available from: http://www.pharmapolis.net/featured-articles/new-technologies/132-hot-melt-extrusion-technology?start=2.

[28] *Polymer Rheology - Viscosity Behavior and Flow Types*. [cited (14/1/2012)]; Available from: http://www.che.lsu.edu/faculty/dooley/rheology/rheo1.htm.

[29] Hu N, Masuda Z, Yamamoto G, Fukunaga H, Hashida T, and Qiu J. Effect of fabrication process on electrical properties of polymer/multi-wall carbon nanotube nanocomposites. *Journal of Composites: Part A* 2008. **39**: p. 893–903.

[30] Sun J-S, Gokturk H S, and Kalyon D M. Volume and surface resistivity of low-density polyethylene filled with stainless steel fibres. *Journal of Material Science*, 1993. **28**: p. 364-366.

[31] Hu N, Karube Y, Yan C, Masuda Z, and Fukunaga H. Tunneling effect in a polymer/carbon nanotube nanocomposite strain sensor. *Journal of Acta Materialia* 2008. **56**: p. 2929–2936.

[32] Nan C-W, Shen Y, and Ma J. Physical Properties of Composites Near Percolation. *Annual Review of Materials Research*, 2010. **40**: p. 131-151.

[33] Zhang Q, Rastogi S, Chen D, Lippits D, and Lemstra P J. Low percolation threshold in single-walled carbon nanotube/high density polyethylene composites prepared by melt processing technique. *Journal of Carbon*, 2006. **44**: p. 778–785.

[34] Liu Y, Chakrabartty S, Gkinosatis D S, Mohanty A K, and Lajnef N. Multi-walled Carbon nanotubes/ Poly(L-lactide) strain sensor for biomechanical implants. in *Biomedical Circuits and Systems Conference, 2007. BIOCAS 2007. IEEE* 2007. Montreal: IEEE.

[35] Knite M, Tupureina V, Fuith A, Zavickis J, and T. V. Polyisoprene—multi-wall carbon nanoube composites for sensing strain. *Journal of Materials Science and Engineering C* 2007. **27**: p. 1125-1128.

[36] Yu X and Kwon E. A carbon nanotube/cement composite with piezoresistive properties. *Journal of Smart Materials and Structures*, 2009. **18**.

[37] Kang I, Abdul-Khaleque M, Yoo Y, Yoon P J, Kim S-Y, and Lim K T. Preparation and properties of ethylene propylene diene rubber/multi walled carbon nanotube composites for strain sensitive materials. *Journal of Composites: Part A*, 2011. **42**: p. 623- 630.

[38] Loh K J, Kim J, Lynch J P, Kam N W S, and Kotov N A. Multifunctional layer-by-layer carbon nanotube–polyelectrolyte thin films for strain and corrosion sensing. *Journal of Smart Materials and Structures*, 2007. **16**: p. 429–438

[39] Yin G, Hu N, Karube Y, Liu Y, Li Y, and Fukunaga H. A carbon nanotube/polymer strain sensor with linear and anti-symmetric piezoresistivty. *Journal of Composite Materials* 2011. **45**: p. 1315-1323.

[40] Vemuru S M, Wahi R, Nagarajaiha S, and Ajayan P M. Strain sensing using a multiwalled carbon nanotube film. *Journal of strain Analysis*, 2009. **44**: p. 555-562.

[41] Kwok N and Hahn H T. Resistance Heating for Self-healing Composites. *Journal of Composite Materials*, 2007. **41**: p. 1635-1654.

[42] Liu C-X and Choi J-W. Strain-Dependent Resistance of PDMS and Carbon Nanotubes Composite Microstructures. *IEEE transactions on Nanotechnology*, 2010. **9**: p. 590-595.

[43] Hu N, Karube Y, Arai M, Watanabe T, Yan C, Li Y, Liu Y, and Fakunaga H. Investigation on sensitivity of a polymer/carbon nanotube composite strain sensor. *Journal of Carbon*, 2010. **48**: p. 680-687.

[44] S, K. Percolation and Conduction. *Journal of Reviews of Modern Physics*, 1973. **45**(4): p. 574-588.

[45] Hu N, Masuda Z, Yan C, Yamamoto G, Fukunaga H, and Hashida T. The electrical properties of polymer nanocomposites with carbon nanotube fillers. *Journal of Nanotechnology*, 2008. **19** p. 1 – 10.

[46] Jeon K, Warnock S, Ruiz-Orta C, Kismarahardja A, Brooks J, and A.R. G. Role of Matrix Crystallinity in Carbon Nanotube Dispersion and Electrical Conductivity of iPP-Based Nanocomposites. *Journal of Polymer Science Part B: Polymer Physics*, 2010. **48**: p. 2084–2096.

[47] Razavi-Nouri M, Ghorbanzadeh-Ahangari M, Fereidoon A, and Jahanshahi M. Effect of carbon nanotubes content on crystallization kinetics and morphology of polypropylene. *Journal of Polymer Testing*, 2009. **28**: p. 46-52.

[48] *Materials and Electrochemical Research Corporation* [cited (14/1/2012)]; Available from: http://www.mercorp.com/

[49] *Performance and speciality chemicals* [cited (14/1/2012)]; Available from: http://www.thomas-swan.co.uk/.

[50] D4703, A., *Standard Practice for Compression Molding Thermoplastic Materials into Test Specimens, Plaques, or Sheets*, A. International, Editor. 2010. p. 12.

[51] D618, A., *Standard Practice for Conditioning Plastics for Testing*, A. International, Editor. 2010, ASTM International. p. 4.

[52] Abdel Chafy R R, Arafa M H, and Esawi A M K, *Fabrication of Carbon Nanotube/Low Density Polyethylene Composites for Strain Sensing* in *ICMAST 2011*, J.o.K.E. Materials, Editor. 2012, Trans Tech Publications: Greece. p. 33-36.

[53] Yamada T, Hayamizu Y, Yamamoto Y, Yomogida Y, Izadi-Najafabadi A, Futaba D N, and Hata K. A stretchable carbon nanotube strain sensor for human-motion detection. *Journal of Nature Nanotechnology*, 2011. **6**: p. 296-301.